PARAMETERIZATION OF MODELING SUBSURFACE HYDROCARBON CONTAMINATION AND BIOSURFACTANT ENHANCED REMEDIATION PROCESSES

by

© Zelin Li

A Thesis Submitted to the School of Graduate Studies

in partial fulfillment of the degree of

Master of Engineering

Department of Civil Engineering

Faculty of Engineering and Applied Science

Memorial University of Newfoundland

May, 2016

St John's, Newfoundland

ABSTRACT

Subsurface hydrocarbon contamination caused by accidental spills or operational leakages of petroleum products is a global environmental concern. In order to cost-effectively and eco-friendly recover the contaminated sites, biosurfactant enhanced aquifer remediation (BSEAR) technologies have become a popular subject in both research and practice. However, the inherent uncertainties and complexities of the subsurface systems make it challenging in numerical simulation of the hydrocarbon transport and fate as well as remediation processes. Efforts in developing more efficient and robust parameterization approaches for such modeling purpose, therefore, are highly desired.

This research aims to help fill the gap by developing a novel hybrid stochastic – design of experiment aided parameterization (HSDP) method for modeling BSEAR processes. The method was developed and tested based on an integrated physical and numerical modeling system comprised of a set of intermediate scale flow cells (ISFCs) and a numerical simulator named BioF&T 3D. Generally, the HSDP method was performed by: 1) building the design of experiment (DOE) models based on screened parameters and defined responses, which could reflect the goodness of fit between observed and simulated data; 2) identifying the and interactions among parameters and their significance; 3) optimizing the DOE predicted responses; 4) introducing stochastic data within reduced intervals based on the optimized parameters; 5) running Monte Carlo simulation to find the optimal responses with the corresponding combinations of parameters. The flow cell tests proved that the HSDP method could improve both

efficiency and robustness of modeling parameterization and significantly reduce the computational demand without compromising the effectiveness in quantifying parameter interactions and uncertainties.

Furthermore, a specific lab synthetized surfactin was applied in this study. The effect of dissolution enhancement was observed from parallel flow cell experiments especially during the first 12 hours following the initial hydrocarbon release. The HSDP method was demonstrated to be capable of advancing BioF&T 3D, which lacks the capacity of simulating surfactant. By incorporating the HSDP method, the BSEAR processes were effectively simulated with a satisfactory overall goodness of fit (R^2 = 0.76, 0.81, 0.83, and 0.81 for benzene, toluene, ethylbenzene, and xylene, respectively). The enhanced dissolution effect was also reflected in the modeling parameterization by increasing the first 12 hours hydrocarbon loading ratio (12LR) compared to non-biosurfactant processes.

This research developed a new parameterization method HSDP, which is capable of revealing interactions of parameters, as well as quantifying their uncertainties, in a robust and efficient manner. Also, using this method, this study initiated the attempts to advance simpler numerical models in simulating complicated BSEAR processes, which is particularly attractive for the potential applications in practice.

AKNOWLEDGEMENTS

First and foremost, I would like to express my cordial gratitude to my supervisor, Dr. Bing Chen, for thoughtfully guiding and motivating me through this extremely valuable researching experience. I am profoundly inspired by his immense knowledge, critical thinking, and rigorous attitude as a scholar. Also, I deeply admire him for his vision, passion, and dedication, from which I will benefit for a life time.

I would like to extend my appreciation to Dr. Baiyu Zhang and Dr. Tahir Husain for their constructive academic advices and encouragement. I also would like to thank Dr. Leonard Lye for taking me into the mentorship program and kindly helping me prepare for the future professional career.

I gratefully acknowledge the Faculty of Engineering and Applied Science, Memorial University of Newfoundland, the Natural Sciences and Engineering Research Council of Canada (NSERC), and Canada Foundation for Innovation (CFI) for their financial support. I would also like to thank my colleagues from the Northern Region Persistent Organic Pollution Control (NRPOP) Lab for their kind assistance with priceless friendship. They include Dr. Pu Li, Dr. Liang Jing, Dr. Yinchen Ma, Hongjing Wu, Xudong Ye, Qinhong Cai, Zhiwen Zhu, He Zhang, Bo Liu, Tong Cao, Jisi Zheng, Fuqiang Fan, Kedong Zhang, and many others.

Last but not least, I am grateful for the support and unconditional love from my family in China. Special thanks also go to my girlfriend, Pengqi Wang, whose love and understanding have brought me many joys and continuously stimulated me to tenaciously peruse my dream during the journey of my master studies.

TABLE OF CONTENTS

ABSTRACT I
AKNOWLEDGEMENTS III
TABLE OF CONTENTS IV
LIST OF TABLES VII
LIST OF FIGURES VIII
LIST OF ABBREVIATIONS AND SYMBOLS X
CHAPTER 1: INTRODUCTION 3
1.1 Background 3
1.2 Statement of Problems 6
1.3 Objectives 10
1.4 Structure of the Thesis 11
CHAPTER 2: LITERATURE REVIEW 14
2.1 Background 14
2.2 Simulation of Subsurface Contamination and Remediation 18
2.2.1 Physical simulation 18
2.2.2 Numerical simulation 22
2.2.3 Coupled physical and numerical simulation 26
2.3 Parameterization of Numerical Models 29
2.3.1 Sensitivity analysis 29
2.3.2 Uncertainty analysis 32
2.3.3 Calibration and verification 35
2.3.4 Design of experimental aided parameterization 36
2.4 Summary 38
CHAPTER 3: AN INTEGRATED PHYSICAL AND NUMERICAL MODELING APPROACH 40
3.1 Background 40
3.2 Physical Model 41
3.2.1 An intermediate scale flow cell system 41

3.2.2 Experimental design and sample analysis 46
3.3 Numerical Simulator 46
3.3.1 Structure and Compositions 46
3.3.2 Governing equations 47
3.3.3 Solution method 50
3.4 Summary 50
CHAPTER 4: A HYBRID STOCHASTIC-DESIGN OF EXPERIMENT AIDED PARAMETERIZATION METHOD 52
4.1 Background 52
4.2 Methodology 52
4.3 Case Study 57
4.3.1 Data acquisition 57
4.3.2 Parameterization 62
4.3.3 Verification 79
4.4 Summary 89
CHAPTER 5: SIMULATION OF BIOSURFACTANT ENHANCED AQUIFER REMEDIATION PROCESSES 90
5.1 Background 90
5.2 Methodology 92
5.2.1 Materials and Experimental Setups 92
5.2.2 Parameterization 94
5.3 Result and Discussion 95
5.3.1 Flow cell experiment 95
5.3.2 Parameterization 98
5.3.3 Comparison of BS and NOBS processes 120
5.3.4 Verification 126
5.4 Summary 135
CHAPTER 6: CONCLUSIONS AND RECOMMENDATIONS 137
6.1 Summary 137
6.2 Research Achievements 138
6.3 Recommendations for Future Research 139

REFERENCES 141

LIST OF TABLES

Table 2.1 Summary of aquifer remediation approaches 16
Table 3.1 Soil particle size distribution..... 45
Table 4.1 Observed BTEX concentrations..... 59
Table 4.2 Selected parameters for the DOE models 61
Table 4.3 ANOVA results of minimum run resolution V design 65
Table 4.4 Summary of predicted and actual responses after optimization of the DOE models 72
Table 4.5 Summary of the final parameterization results without / with Monte Carlo simulations 75
Table 4.6 BioF&T 3D model inputs for verification 80
Table 5.1 Monitored BTEX concentration from parallel flow cell experiments 96
Table 5.2 Screened parameters and their ranges for the DOE models..... 100
Table 5.3 ANOVA results of central composite design..... 109
Table 5.4 Summary of predicted and actual responses after optimization of the DOE models 110
Table 5.5 Summary of the final parameterization results without / with Monte Carlo simulations 116
Table 5.6 R^2 values of all the sampling ports at different time stages 118
Table 5.7 R^2 values during the entire sampling period from different sampling ports 119
Table 5.8 Comparisons of parameters values for BS / NOBS processes after the final parameterization..... 125

LIST OF FIGURES

Figure 1.1 Roadmap to the research 13
Figure 3.1 Outlook of the ISFC 43
Figure 3.2 Sketch of the ISFC setup 44
Figure 4.1 Framework of the proposed hybrid stochastic - DOE aided parameterization method 55
Figure 4.2 Half-normal probability plots 64
Figure 4.3 3D surface graph of factors A and C interactions for benzene 66
Figure 4.4 3D surface graph of factors A and C interactions for toluene 67
Figure 4.5 3D surface graph of factors B and C interactions for toluene 68
Figure 4.6 3D surface graph of factors C and D interactions for ethylbenzene 69
Figure 4.7 3D surface graph of factors C and D interactions for xylene 70
Figure 4.8 Effects of Porosity uncertainties on RMSD 76
Figure 4.9 Effects of AKD uncertainties on RMSD 77
Figure 4.10 Effects of GAMA uncertainties on RMSD 78
Figure 4.11 Simulated benzene concentration (in ppb) contours at the X-Z plane (in cm) at different time stages after initial diesel injection 81
Figure 4.12 Simulated toluene concentration (in ppb) contours at the X-Z plane (in cm) at different time stages after initial diesel injection 82
Figure 4.13 Simulated ethylbenzene concentration (in ppb) contours at the X-Z plane (in cm) at different time stages after initial diesel injection 83
Figure 4.14 Simulated xylene concentration (in ppb) contours at the X-Z plane (in cm) at different time stages after initial diesel injection 84
Figure 4.15 BTEX verification results for sampling port #2 85
Figure 4.16 BTEX verification results for sampling port #3 86
Figure 4.17 BTEX verification results for sampling port #4 87
Figure 4.18 BTEX verification results for sampling port #6 88
Figure 5.1 Flow cell experiments with biosurfactant injection 93
Figure 5.2 Analyzed BTEX concentrations in the effluents 97

Figure 5.3 3D surface graph of factors C and D interactions for benzene..... 103
Figure 5.4 3D surface graph of factors C and D interactions for toluene..... 104
Figure 5.5 3D surface graph of factors A and C interactions for ethylbenzene..... 105
Figure 5.6 3D surface graph of factors C and D interactions for ethylbenzene..... 106
Figure 5.7 3D surface graph of factors C and D interactions for xylene..... 107
Figure 5.8 Effects of 12LR uncertainties on RMSD.....113
Figure 5.9 Effects of AKD uncertainties on RMSD 114
Figure 5.10 Effects of GAMA uncertainties on RMSD.....115
Figure 5.11 Effects comparison of BS and NOBS after the parameterization at sampling port #1 121
Figure 5.12 Effects comparison of BS and NOBS after the parameterization at sampling port #2 122
Figure 5.13 Effects comparison of BS and NOBS after the parameterization at sampling port #3 123
Figure 5.14 Effects comparison of BS and NOBS after the parameterization at sampling port #6 124
Figure 5.15 BTEX verification results for sampling port #1 127
Figure 5.16 BTEX verification results for sampling port #2 128
Figure 5.17 BTEX verification results for sampling port #3 129
Figure 5.18 BTEX verification results for sampling port #6 130
Figure 5.19 Simulated benzene concentration (in ppb) contours at the X-Z plane (in cm) at different time stages after initial diesel injection 131
Figure 5.20 Simulated toluene concentration (in ppb) contours at the X-Z plane (in cm) at different time stages after initial diesel injection..... 132
Figure 5.21 Simulated ethylbenzene concentration (in ppb) contours at the X-Z plane (in cm) at different time stages after initial diesel injection..... 133
Figure 5.22 Simulated xylene concentration (in ppb) contours at the X-Z plane (in cm) at different time stages after initial diesel injection..... 134

LIST OF ABBREVIATIONS AND SYMBOLS

AKD	Distribution coefficient.
ANN	Artificial neural networks.
ANOVA	Analysis of variance.
ASP	Alkaline-surfactant-polymer.
BEB	Biosurfactant enhanced bioremediation.
BS	Biosurfactant enhanced soil flushing.
BSEAR	Biosurfactant enhanced aquifer remediation.
BTEX	Benzene-toluene-ethylbenzene-xylene.
CCD	Central composite design.
CMC	Critical micelle concentration.
DCAY	First order decay coefficient.
DIFA	Diffusion coefficient in air.
DIFW	Diffusion coefficient in water.
DNAPL	Dense non-aqueous phase liquid.
DOE	Design of experiment.
FSMS	Factorial-design-based stochastic modeling system.
GAMA	Henry's constant.
GC	Gas chromatography.
HPAI	Highly pressurized air injection.
HRF	Horizontal radial flow.
HSDP	Hybrid stochastic-design of experiment aided parameterization.
HSSM	Hydrocarbon spill screening model.
ISCO	In-situ chemical oxidation.
ISFC	Intermediate-scale flow cell.
LNAPL	Light non-aqueous phase liquid.
MNN	Modular neural networks.
MPRS	Multipurpose reservoir simulator.
MS	Mass spectrum.
MTBE	Methyl tert-butyl ether.

MT3DMS	Modular three-dimensional multi-species transport model.
NAPL	Non-aqueous phase liquid.
NRPOP	Northern Region Persistent Organic Pollution Control
NOBS	Soil flushing without introducing biosurfactant.
OFAT	One-factor-at-a-time.
PAH	Polycyclic aromatic hydrocarbon.
PCB	Polychlorinated biphenyl.
PCE	Tetrachloroethylene.
PDFs	Probability distribution functions.
QMC	Quasi-Monte Carlo.
RMSD	Root mean square deviation.
RSM	Response surface method
RT3D	Reactive transport in 3 dimensions.
SDS	Sodium dodecyl sulfate.
SEAR	Surfactant enhanced aquifer remediation.
UHBS	Biosurfactants synthetized at the University of Houston.
USTs	Underground storage tanks.
UTCHEM	University of Texas chemical compositional simulator.
VOCs	Volatile organic compounds.
12LR	First 12 hours loading ratio.

x	spatial coordinates.
i	unit vector.
j	unit vector.
K_{ij}	saturated hydraulic conductivity tensor.
k_{rw}	relative permeability.
ψ	pressure head.
ψ_0	initial pressure head.
ψ_p	fixed pressure head.
t	time.
u_j	unit vector pointing in the vertical direction upward.
n_i	unit vector normal to the boundary.
S_w	water saturation.
$\bar{S}_w$	effective water saturation.
S_s	specific storage.
Φ	porosity.
q_s	source/sink volumetric rate per unit volume of the porous medium.
q_i	Darcy velocity.
q_{wD}	volumetric rate of dispersive flux.
q_{wT}	total solute mass fluxes.
S_m	irreducible water saturation.
α	Van Genuchten parameter.
n	Van Genuchten parameter.
m	n related porous medium parameter.
θ_m	fraction of the soil filled with mobile water.
θ_{im}	fraction of the soil filled with immobile water.
C_{ws}	concentration of species in the injected/withdrawn fluid.
C_{wm}	concentration of species in the mobile water.
C_{wim}	concentration of species in the immobile water.
C_{w0}	initial concentration of species in the immobile water.

C_{wt}	concentration of species in the immobile water at time t.
D_{ij}	hydrodynamic dispersion tensor.
H_w	contaminant loading due to dissolution of NAPL from the source to the mobile phase.
H_{iw}	contaminant loading caused by groundwater infiltration through the NAPL plume under equilibrium state.
H_{gw}	contaminant loading by groundwater flowing under the NAPL plume.
X	mass transfer coefficient.
k_d	partitioning coefficient of species incorporating linear adsorption.
λ_{wm}	decay loss from mobile liquid phase.
λ_{wim}	decay loss from immobile liquid phase.
f	fraction of the sorption sites which is directly contacted with the mobile liquid.
ρ	soil bulk density.
b	denotes for benzene.
t	demotes for toluene.
e	denotes for ethylbenzene.
x	denotes for xylene.
R^2	coefficient of determination.
$\hat{y}_i$	the i th simulated data.
y_i	the i th observed data.
$\bar{y}$	the mean value of the observed data.
N	number of groups of observed/simulated data.

CHAPTER 1: INTRODUCTION

1.1 Background

Soil and groundwater contamination is one of the most intractable environmental problems around the globe. The contaminated sites threaten human health, and might lead to a variety of unforeseen negative impacts, risks and liabilities to the environments (Li et al., 2003; Huang et al., 2006b; Swartjes et al., 2012; Yang et al., 2012). These concerns are especially pertinent in Canada, where petroleum production and consumption activities are intensive, and oil leakages from transportation pipelines and underground storage tanks (USTs) are ubiquitous (Zhang et al., 2012). According to the most recent data from Treasury Board of Canada Secretariat (2015), 5,786 out of 20,216 federal contaminated sites require remedial actions, and 729 sites are considered as high priority for action.

Major categories of contaminants such as polychlorinated biphenyl (PCB), tetrachloroethylene (PCE), methyl tert-butyl ether (MTBE), polycyclic aromatic hydrocarbon (PAH), as well as benzene-toluene-ethylbenzene-xylene (BTEX) are among the most common hazardous compounds found in contaminated sites. Varying in solubility and density, light non-aqueous phase liquid (LNAPL) and dense non-aqueous phase liquid (DNAPL) migrate differently in nature, which favors different removal mechanisms (Alvarez and Illman, 2005). Many remediation technologies have been made viable during the past few decades, such as soil flushing, pump and treat, and bioremediation. However, it has been a significant challenge to efficiently remove the

targeted contaminants in practice, especially considering that non-aqueous phase hydrocarbon contaminants tend to adhere to the surfaces of soil particles and are usually low in water solubility.

In order to overcome this obstacle, surfactants have recently become a promising option in soil and groundwater remediation practices (Pacwa-Płociniczak et al., 2011; Mao et al., 2014). It can be introduced as additives in different operational systems to enhance the performance of remediation technologies (Jácome and Van Geel, 2013; Guo et al., 2014). As a group of amphiphilic compounds, surfactants contain both hydrophilic and hydrophobic parts. When surfactants are applied to a soil-water-hydrocarbon heterogeneous system, their particular molecular structures allows them to gradually replace the interfacial solvent like water at an increasing concentration, resulting in a decreased surface tension, which can consequently accelerate the dissolution of the non-aqueous hydrocarbon contaminants. When the concentration of surfactants reaches a certain threshold termed Critical Micelle Concentration (CMC), micelles begin to form and desorption of contaminants is remarkably promoted with increased solubility for mechanical removal (e.g., soil flushing and subsequent separation), and simultaneously make it easier for biodegradation (Paria, 2008; Mao et al., 2014). The kinetics, performance, and side effects of surfactants have been at length studied, and it was suggested that toxicity can be a critical concern when a certain type of surfactant is selected for enhanced site remediation (Volkering et al., 1997; Franzetti et al., 2006; Rebello et al., 2014; Li et al., 2015a). At the current stage, most commercially available surfactants are synthetized by chemical processes. Empirical studies demonstrated that non-naturally produced surfactants are generally toxic and mostly difficult to be degraded

by micro-organisms, which makes biosurfactants a promising alternative for potential applications (Zhang et al., 2011; Cai et al., 2014).

Biosurfactants are compounds that exhibit similar functions as chemically synthetized surfactants in reducing the surface and interfacial tension of liquids, but originated from naturally existing living organisms, such as microbes, plants, animals, and even human beings, which are associated with low toxicity and high biodegradability (Christofi and Ivshina, 2002; Paria, 2008; Mao et al., 2014). Compared to chemical surfactants, biosurfactants are still at a relatively early stage. Production, testing, and deployment of biosurfactants are receiving extensive attentions lately by researchers. Many studies have been focused on screening, isolation, and characterization of microbes that are capable of producing surfactants. The sources of bacteria and their substrates are various, and generally the production of biosurfactants is costly with low yields (Banat et al., 2010; Banat et al., 2011; Dhail and Jasuja, 2012; Pereira et al., 2013; Vijaya et al., 2014). Biosurfactants are normally classified based on the chemical composition and microbial origin. The major classes of biosurfactants include glycolipid, rhamnolipids, sophorolipids, lipopeptides, lipoproteins, phospholipids, fatty acids, and polymeric surfactants (Rahman and Gakpe, 2008; Pacwa-Płociniczak et al., 2011; Shoeb et al., 2013; Rautela and Cameotra, 2014). However, due to the limited commercial options available, there is often a lack of uniform standards and specifications for biosurfactants regarding their properties and details of production processes, which implies that performance evaluations of different types of biosurfactants have to be conducted on a case by case basis (Santa Anna et al., 2007; Marchant and Banat, 2012; Damasceno et al., 2014; Lotfabad et al., 2015).

1.2 Statement of Problems

In previous studies, lab scale column experiments were extensively involved to evaluate the performances of various types of biosurfactants. The quantity of required biosurfactants was relatively low, but it inevitably compromised the reflection of multi-dimensional transportations and heterogeneities in practices (Gudiña et al., 2012; Khodadadi et al., 2012; Joshi and Desai, 2013; da Rosa et al., 2015). On the other hand, large pilot-scale experiments or field-scale testing often require significant amount of biosurfacants, long sampling durations and complex physical systems for data acquisitions, which are costly and difficult to control. As a consequence, not many researching projects have been attempted (Maqsood, 2004; Huang et al., 2006b; Yu et al., 2010). As a trade-off option, Song and Seagren (2008) designed and applied an intermediate-scale flow cell (ISFC), which was able to interpret relatively large-scale physical, chemical, and biological processes, while keeping the complexities of the modeling system under controlled laboratory conditions. However, there is a lack of existing applications of flow cells in subsurface contamination and remediation experiments, and biosurfactants were rarely involved (Harvell, 2012; Tick et al., 2015).

Moreover, it is vital to achieve a better understanding of the fate of contaminants in aquifer, particularly with the presence of surfactants, and further to assess the potential impacts on the contaminated sites for the optimization of the remediation strategies. In this regard, numerical model has generally been accepted as an effective tool to fulfill these expectations and as such has been continuously studied (Huang, 2004; Maqsood, 2004; Bear and Cheng, 2010; Yeh, 2015). During recent decades, many numerical models have been developed and applied in simulating the subsurface flow and

contaminants transportation within porous media. Primarily based on Darcy's law and mass transferring kinetics, most of the up to date numerical models have been enabled to simulate multi-dimensional, multi-stages, multi-phases, and multi-components scenarios which can reflect real world conditions using finite-element or finite-difference approximations (Crawford, 1999; Mulligan and Yong, 2004; Bear and Cheng, 2010; Agah et al., 2013).

Numerical models are expected to accurately reflect the real world situations. However, there is often a lack of fit existing due to the intrinsic system heterogeneities and imprecisely defined parameter uncertainties, which makes it essential to calibrate the numerical models before applying them for predictions. The traditional method of model calibration is essentially a trial and error process which uses iterations to adjust the relevant parameters until the simulated outputs are sufficiently close to the experimental data. This method is still popular and has been embedded in commercial modeling tools for automatic calibration (Solomatine et al., 1999; Sonnenborg et al., 2003; Mugunthan et al., 2005; Razavi and Tolson, 2012). Despite a good level of fit with observed data can be expected by using the trial-and-error calibration method, it should not be ignored that some major limitations such as extensive computational requirements, low physical plausibility, and over-parameterization often exist, which might lead to the ignorance of the potentially significant variables (Neuman, 1973; Daliakopoulos et al., 2005; Van Griensven et al., 2006; Whittaker et al., 2010; Okamoto and Akella, 2012). Hence, it is essential to conduct uncertainty and sensitivity analysis for parameterization of the models, and further to minimize the discrepancies between simulated and observed data. Many standard methods are generally available in this regard (Sin et al., 2011; He et al.,

2012; Shen et al., 2012; Zhuo et al., 2013; Houska et al., 2014; Tang et al., 2015). For uncertainty analysis, Monte Carlo simulations are one of the most common stochastic methods involving random sampling with certain types of distributions, and it has been widely applied in environmental systems by propagating the parameter uncertainties and reflecting their impacts on the model output (Helton, 1993; Huang and Loucks, 2000; Jing et al., 2013a; Jing et al., 2013b; Li et al., 2014). One-factor-at-a-time (OFAT) is one of the traditional sensitivity analysis methods. This method simply adjusts one parameter at a time while keeping other parameters fixed. Its applications have been found in multiple studies conducted on various models (Lenhart et al., 2002; Holvoet et al., 2005; Jing and Chen, 2011). However, it is challenging to find a method which is not only capable of revealing the interactions between parameters, but also efficient in computational capacity (Saltelli, 1999; Montgomery, 2008; Peeters et al., 2014).

To address this issue, design of experiment (DOE) provides an alternative for parameterization of numerical models. DOE is a well-known statistical methodology, which can unveil the interrelationships between parameters and the corresponding responses by conducting controlled experiments (Park, 2007). By using DOE methods, it is possible to simultaneously study several parameters and their interactions (Czitrom, 1999; Veličković et al., 2013; Sarikaya and Güllü, 2015). Despite that many recent studies have also involved DOE in various types of simulations and optimizations, relationships between responses and stochastically distributed parameters are seldom integrated. In addition, DOE aided parameterization method has rarely been used in groundwater and subsurface modeling, in which uncertainties commonly exist and

knowledge concerning complicated interactions between each parameter is far from adequate.

It is particularly appealing to use the DOE aided parameterization method when complicated surfactant enhanced aquifer remediation (SEAR) processes are simulated. Existing studies of SEAR processes based on multidimensional physical and numerical modeling systems are limited; particularly for biosurfactant enhanced aquifer remediation (BSEAR) processes (Brown et al., 1994; Huang et al., 2003; Liu, 2005; Huang et al., 2006b; Yu et al., 2010). For instance, a specific SEAR simulator named UTCHEM (University of Texas Chemical Compositional Simulator) was mainly used in previous studies to numerically describe the multiphase and multicomponent contaminants transportations under the presence of surfactant (Delshad et al., 1996; Zhang et al., 2005; Qin et al., 2007; Jin et al., 2014). The complex kinetic equations reflecting non-equilibrium flow and mass transfer processes, however, make it a heavy computational burden to specifically identify all the surfactant properties or to introduce stochastic parameters for sensitivity analysis and model calibration (He et al., 2008; Luo and Lu, 2014). It is particularly challenging for practices considering types of biosurfactants and conditions for their application may vary from case to case, which might pose significant uncertainties associated with the limited data available. Therefore, it is highly desired to study the possibility of using a simplified modeling approach for practices, so that the simulation of BSEAR processes can be more efficiently and robustly conducted at a comparable level of accuracy. As an example, BioF&T 3D is a mature simulator developed by Katyal (1997a) to solve multiphase and multicomponent biodegradation, flow, and transport in porous media, and it has been used in multiple previous studies

(Suk et al., 2000; Lee et al., 2001; Liu et al., 2004; Qin et al., 2008b; Kumar, 2012). Compared to UTCHEM, BioF&T 3D is simpler but not originally built with surfactant modules. Therefore, surfactant related parameters have not been identified in BioF&T 3D for SEAR simulations. In order to help fill this technical gap, it would be critical to investigate on the following two questions:

1) Is it possible to develop an effective and efficient parameterization method to assess uncertainties and sensitivities associated with the parameters, such that simpler numerical models can be advanced to simulate complicated BSEAR processes, particularly under practical situations?

2) If possible, which parameters are considered significant with the presence of biosurfactant? How are they adjusted compared to none biosurfactant scenarios? What are the physical explanations of these adjustments?

1.3 Objectives

To answer above questions, this research aims to build an integrated physical and numerical modeling approach, based on which a new parameterization method is developed to examine modeling uncertainties and improve simulation performance in an effective and efficient manner. The new parameterization method is further used to advance simpler numerical models to simulate BSEAR processes with the physical explanations of the corresponding adjustments of parameters. The research tasks entail: 1) to conduct ISFC soil washing experiments to physically simulate subsurface hydrocarbon contaminates transportations with and without the additions of biosurfactants; 2) to develop a new parameterization method that can quantify the

significance of modeling parameters with their interactions, and the influence from their uncertainties; 3) to employ the developed parameterization method and generate a verified combination of parameters that can advance simpler numerical models in simulating BSEAR processes; 4) to evaluate the performance of the biosurfactant applied in this study, and further to investigate how the modeling parameters should be adjusted to simulate BSEAR processes.

1.4 Structure of the Thesis

This thesis is composed of 6 chapters. The structure of the thesis is illustrated in Figure 1.1. Chapter 2 reviews the previous studies in physically and numerically describing subsurface contaminants transportation and remediation, especially for BSEAR processes. Existing parameterization methods for numerical models, including uncertainty analysis, sensitivity analysis, model calibration and verification, as well as DOE aided parameterization methods, are also reviewed in this chapter. Chapter 3 presents an integrated physical and numerical modeling approach, which is established by coupling flow cell experiments with BioF&T 3D. The experimental setups, governing equations and the corresponding solution methodologies are also introduced. Chapter 4 proposes a hybrid stochastic-design of experiment aided parameterization (HSDP) method, which is demonstrated with a case study to simulate a soil flushing process based on the ISFC. Chapter 5 advances and parameterizes BioF&T 3D to simulate BSEAR processes using the HSDP method. A type of lab synthetized surfactin is introduced into one of the ISFC units as an enhancement of soil flushing. Its performance is evaluated by

comparing to a parallel flow cell experiment for non-biosurfactant scenarios. Finally, Chapter 6 draws conclusions along with suggestions for future work.

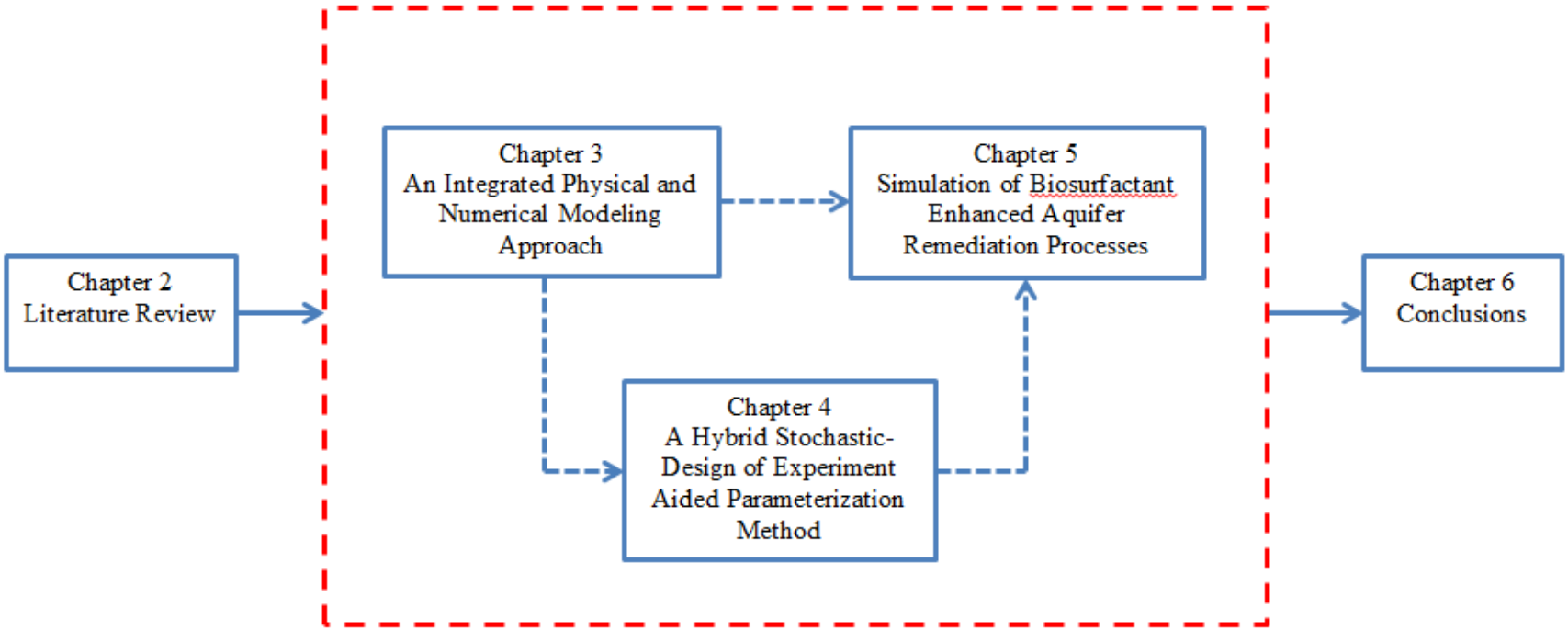

Figure 1.1 Roadmap to the research

CHAPTER 2: LITERATURE REVIEW

2.1 Background

Subsurface non-aqueous phase liquid (NAPL) contamination from spill and leakage of petroleum products has become a major environmental concern. It may result in long term adverse health impacts due to its persistence in nature (Braddock and McCarthy, 1996; Li et al., 2003; Yang et al., 2012; Jácome and Van Geel, 2015). To remediate the contaminated sites under different situations, many technical countermeasures have been developed, as summarized in Table 3.1. In order to achieve a better understanding of the fate of contaminants in aquifer, thus to support decision makings regarding remediation practices, many studies have been conducted during the past decades.

Many numerical models have been developed to mathematically describe the subsurface processes. Physical models, on the other hand, have also played a significant role in providing observed data for calibration and verification of numerical models. It is of importance to get a general image of different types of numerical and physical models, as well as how they are integrated in the previous studies, especially relating to biosurfactant enhanced aquifer remediation (BSEAR) processes (Yu et al., 2011; Harendra and Vipulanandan, 2012).

In order to improve the performance of numerical models, it is essential to conduct parameterization processes, including sensitivity and uncertainty analysis, as well as to calibrate and verify the numerical models for practical applications in predictions. Many methods have been developed in the previous studies, and each method has its own

advantages and limitations. Therefore, it is highly desired to review these different methods, especially how they were conducted within the complicated subsurface modeling systems.

In this chapter, different physical and numerical models, as well as their integrations will be reviewed especially focusing on studies of BSEAR processes. Parameterization methods for subsurface modeling, including previous attempts on sensitivity analysis, uncertainty analysis, model calibration and verification, will also be reviewed. As a relatively new parameterization methodology recently utilized in different types of numerical models, Design of experiment (DOE) will also be reviewed regarding its principles and corresponding applications.

Table 2.1 Summary of aquifer remediation approaches

Technology	Description	Strengths	Limitations
Soil vapor extraction	Creating vacuum by extracting subsurface air laden with contaminant vapors through pre-laid extraction wells or pipes, normally in series with vapor treatment technologies.	+Minimum disturbance to site operations; +Cost efficient for large volume; +Mobile and flexible.	-Greatly impeded by weathering effects; -Only effective for VOCs; -Requires high permeable and homogeneous soil profile.
Bioremediation	Using microorganisms to break down and digest the contaminants. It can be conducted naturally (natural attenuation) or enhanced by adjusting operating conditions and adding nutrients and microbes (biostimulation and bioaugmentation).	+low cost; +Fundamental removal for organic contaminants; +Does not dewater the aquifer; +Minimum disturbance to site operations; +Public acceptances.	-Requiring extensive monitoring; -Long remediation duration under natural conditions; -Risk for accumulation of toxic biodegradation products.
Air sparging	Air is injected into water-saturated soils, often in conjunction with vacuum extraction systems for stripped VOCs removal. It also stimulates biodegradation by transferring oxygen into groundwater.	+Minimal disturbance to site operations; +Cost efficient for large volume; +Mobile and flexible system; +No requirements on removal, treatment, storage or discharge for groundwater.	-Not recommended for confined aquifers; -Requires high permeable and homogeneous soil profile; -Risk for inducing VOCs migration with insufficient vacuum extraction capacity.
Soil fracturing	Normally a pretreatment process, high pressure air (pneumatic) and water (hydraulic) are injected, creating factures in dense soils to enhance the mass transfer of contaminants.	+Adaptive with a wide range of remediation technologies; +Improve the effectiveness of in-situ remediation by increasing the permeability.	-Not viable in areas of high seismic activity and possible underground utilities; -Might create new pathways for contaminants migration.
Soil flushing	Involving the injection or infiltration	+Can be applied either in-situ or	-Flushing solution might not be

	process using the flushing solution, normally water or water with additives, to dissolve and extract contaminants for above ground treatment.	off-situ, flexible in scales and locations; +Wide applicability for different types of contaminants;	efficient for mixtures of contaminants; -May cause secondary pollution. -Requires high permeable and homogeneous soil profile.
Pump and treat	Pumping groundwater up to the surface for contaminants separation and removal.	+A proven mature technologies; +Wide applicability to different types of contaminants;	-High cost; -Long operating duration; -Rebound effects might occur when groundwater level recovers.
Phytoremediation	Using plants to remediate contaminated sites by direct uptake (phytotransformation) and degradation in rhizosphere (Rhizosphere bioremediation).	+low cost; +Easy implementation and maintenance; +Aesthetical value; +Can effectively prevent migration of contaminants by direct uptake.	-Long remediation duration; -Dependence on climate and hydrologic conditions ; -Only applicable to shallow aquifers.
Stabilization and solidification	Involves no removal or degradation, but to limit the mobility of contaminants by chemical and physical processes.	+Low cost; +Wide applicability to different types of contaminants and soils; +Simple operations	-No fundamental removal; -Emissions might occur during processing VOCs; -May hinder future site usage.
In situ reactive walls	Installing impermeable barriers, such as slurry walls, to control and direct contaminated groundwater plumes through impacted porous reactive medias for adsorption and removal.	+Capable of integrating other remediation technologies; +Effective in plume isolation and control; +Replaceable reactive gates;	-Leakage might happen; -Accumulated waste can compromise the function of the wall.

References: (Alvarez and Illman, 2005; Bhandari et al., 2007; Higgins and Olson, 2009; Hu et al., 2010; Nilsson et al., 2011; Atteia et al., 2013; Camenzuli et al., 2013; Gillespie and Philp, 2013; Gomes et al., 2013; Ashraf et al., 2015; Wang et al., 2015)

2.2 Simulation of Subsurface Contamination and Remediation

2.2.1 Physical simulation

As a significant part of aquifer contamination and remediation studies, physical model not only can approximate real site conditions and generate measurements of specific parameters, but also can directly reflect the behavior and fate of non-aqueous phase liquid (NAPL) contaminants in porous media, thus to provide general insights regarding effectiveness and efficiency of remediation options to practitioners (Peurrung et al., 2013; Renard and Allard, 2013). In the past few decades, experiments at different scales have been widely conducted to physically simulate subsurface contamination as well as various types of remediation processes.

As a type of the most commonly applied physical models, lab-scale column experiments are simply structured with controlled experimental conditions, requiring relatively low media volume and short sampling duration, which makes it easier in reproducibility (Suthar et al., 2008; Pfletschinger et al., 2012; Maszkowska et al., 2013; Rezanezhad et al., 2014). Many recent studies included column experiments, for example, Schubert et al. (2007) conducted lab-scale measurements of radon partitioning coefficients between water and organic liquids in NAPL-contaminated sand columns, which led to a general implication of using radon as an indicator to quantitatively estimate aquifer NAPL contaminations. Bouchard et al. (2008) employed a 1.2 m long column filled with alluvial sand and performed measurements of Volatile Organic Compounds (VOCs) concentrations and compound-specific isotope ratios. The findings of the study could greatly contribute to the source depletion monitoring and biodegradation assessing. Russo et al. (2010) conducted miscible-displacement experiments using 7 cm long by 2.1 cm diameter stainless-steel columns to examine the occurrence of asymptotic elution tailing when

organic compounds are transported within porous media. The results of the study suggested that the retardation effect associated with the organic-carbon contents of the porous media was the major reason associated with this phenomenon. Estrada et al. (2015) investigated the surfactant/foam technique for NAPL aquifer remediation based on 40 cm long by 4.4 cm inner diameter sand columns. Using resistance factor as an indicator of the presence of weak or strong foam, the experimental results revealed that the impacts on permeability reduction from surfactant/foam were minor, which further confirmed the applicability of the technology in field practices.

Column experiments are particularly popular in testing the performance of biosurfactant in SEAR processes. Bai et al. (1997) investigated rhamnolipid biosurfactant produced by Pseudomonas aeruginosa for its potential to remove residual hexadecane using sand columns. The results showed that the removal coefficient was much higher for column packed with larger diameter sand, and 500 mg/l was the optimal biosurfactant concentration of those tested (40, 300, 500, 800, and 1500 mg/l) over the duration of experiments. It was also suggested that mobilization, including displacement and dispersion, was the primary mechanism for the removal of residual hexadecane. Rhamnolipid also exhibited best performance compared to two synthetic surfactants, sodium dodecyl sulfate (SDS) and Tween 80, regarding removal efficiency as well as interfacial tension lowering effects. Similar column experiments were also found in studies regarding the remediation of heavy metal-contaminated soil, in which the injections of rhamnolipid biosurfactant in the form of foam and liquid solution were involved (Mulligan and Wang, 2006; Wang and Mulligan, 2009). Targeting different aquifer contaminants, soil columns were also widely employed in many other recent studies for biosurfacant performance

evaluations (Stumpp et al., 2011; Liu et al., 2012; Bayer et al., 2013; Haryanto and Chang, 2014; Bolobajev et al., 2015; Chang et al., 2015; Zhang, 2015).

Compared to lab-scale column experiments, measurements from pilot-scale soil reactors or even real sites are favorable options when a study of more complicated subsurface processes is desired, especially under multi-dimensional and heterogeneous circumstances. For example, a three-dimensional pilot-scale physical model was built by loading a 3.6 m × 1.2 m × 1.4 m reactor with four soil layers, and discretized into 180 grid cells (0.15 m × 0.15 m × 0.35 m). 12 L gasoline was injected into the bottom of the second soil layer to simulate a point source NAPL leakage, and aqueous samples were collected from 25 pre-installed monitoring wells at a certain time intervals and analyzed (Huang et al., 2006b). The pilot-scale physical model was also demonstrated in studies focusing on different subsurface processes facilitated by various types of in-situ remediation systems including natural attenuation and enhanced bioremediation, in which reasonable temporal/spatial migrations of hydrocarbon compounds were observed (Maqsood, 2004; Huang et al., 2006a; He et al., 2008; Qin et al., 2008a; Zhang et al., 2012). Similarly, Cápiro et al. (2008) applied a pilot-scale aquifer tank (3.7 m × 1.8 m × 1.2 m) and evaluated the potential impacts on bacteria associated with degradation of hydrocarbon contaminants by monitoring the microbial community following a release of neat ethanol onto a residual hydrocarbon source. Akbari and Ghoshal (2014) conducted pilot-scale biopiles experiments based on the 1 m × 0.7 m × 0.35 m stainless steel tanks to mimic bioremediation from a sub-Arctic site, and assessed the rates and extents of biodegradation of aged petroleum hydrocarbons.

In terms of SEAR processes, a pilot-scale demonstration was undertaken to recover PCE from a sandy glacial outwash aquifer at the Bachman Road site in Oscoda, Michigan (Abriola et al., 2005; Ramsburg et al., 2005). The establishment of physical models included site

characterization, system design and operation, as well as tracer test design. Tween 80 was applied in surfactant flushing over a period of 10 days, and an estimation of 19 L PCE and 95% injected surfactant were recovered. PCE concentrations within the treated zone were reduced by as much as two orders of magnitude from pre-SEAR levels without rebound 450 days after the operations ceased. Similarly, Svab et al. (2009) built a pilot-scale physical model consisted of a steel column (3 m in length, 1.5 m in diameter) and a liquid circulation system. A type of anionic surfactant Spolapon AOS 146 solution was circulated with the system to treat the PCB contaminated soil. Um et al. (2013) conducted a feasibility test of in-situ soil flushing base on a pilot-scale xylene contaminated test site (5 m × 5 m × 3 m). Tween 80 solution at low concentration was applied to enhance the remediation processes.

Considering that it is still a challenge for the massive production of biosurfacants, existing studies related to field -scale or pilot-scale demonstrations are rare. Tick et al. (2003) employed a 3 m × 4 m enclosed cell to demonstrate the remediation of PCE-contaminated aquifer using cyclodextrin, which was a type of commercial solubility-enhancement agent produced from the degradation of starch by bacteria. Integrated with a pump-and-treat operational system, a much greater mass removal rate of PCE was observed using cyclodextrin as a flushing agent compared to water flushing without additives. Yu et al. (2010) loaded a pilot-scale soil reactor (3.6 m × 1.2 m × 1.4 m) and built a three dimensional physical modeling system to simulate a rhamnolipid based biosurfactant-enhanced bioremediation (BEB) process for a gasoline contaminated site. Lee et al. (2011) performed a pilot scale test for in-situ biosurfactant flushing coupled with a highly pressurized air injection (HPAI) processes to remediate a bunker oil contaminated site (17 m × 12 m × 4 m).

Intermediate scale flow cells (ISFCs) provided another alternative for physical simulations of subsurface processes. Compared to lab-scale columns and pilot-scale soil reactors, ISFCs were normally applied to interpret two dimensional subsurface processes under controlled laboratory conditions. An earlier example was found in the study of Kueper et al. (1989), where a 60 cm × 80 cm × 0.6 cm parallel-plate laboratory cell was filled with sand to perform the tetrachloroethylene-water displacement experiments, which was able to qualitatively reflect the effects of porous media heterogeneity on the movement of a dense, chlorinated solvent. More recent implementations of ISFCs in modeling subsurface processes were found in the studies of Song and Seagren (2008) and Song et al. (2014), who developed a quantitative framework based on a set of dimensionless numbers in defining the limiting factors of the in-situ bioremediations. Also, in the studies of Chokejaroenrat et al. (2013) and Kananizadeh et al. (2015), a flow cell unit with internal dimensions of 21.6 cm × 12.7 cm × 5.1 cm was applied to investigate the improved efficiency of in situ chemical oxidation (ISCO) for groundwater treatment by injecting xanthan to modify the viscosity of remedial fluids. Gu et al. (2015) presented a new closed specimen cell (154 mm wide, 254 mm long, and 90 mm deep) to simulate the electrochemical remediation processes and accurately monitor the most important parameters. However, applications of ISFCs in studying SEAR processes, especially involving biosurfactants, have rarely been reported.

2.2.2 Numerical simulation

Taking accumulative knowledge from physical simulation at different scales, numerical models have generally been recognized as important as physical models to depict the fate of contaminants in the aquifer, and further to guide decision makings on remediation strategies accordingly under various scenarios using mathematical approaches (Kobus et al., 2012; Gerhard

et al., 2014). Particularly since the 1970s, two factors have greatly stimulated the developing of subsurface simulations: 1) in terms of demand, increasingly stringent remediation standards require a better understanding of the fate of contaminants in the aquifer; and 2) in terms of supply, the rapid development of information technologies make it possible for implementing more advanced numerical solution techniques together with the evolutionary data processing and graphic display capabilities (Zheng and Bennett, 2002; Konikow, 2011).

The fundamentals of simulating groundwater flow and contaminant transport are essentially comprised of two partial differential equations. The first one is the flow equation that describes the connection between hydraulic heads and system stresses such as pumping, initial conditions, and boundary conditions (Cooper, 1966; Pinder and Bredehoeft, 1968). The second one is the transport equation that describes the migration of contaminants mainly including decaying, advection, and dispersion (Reddell and Sunada, 1970; Bear, 1972; Konikow and Grove, 1977). These two governing equations are coupled and solved from three aspects: 1) the velocity vector component obtained through Darcy's law; 2) the hydrodynamic dispersion tensor as a function of molecular diffusion and groundwater velocity; and 3) the fluid source/sink term (Bachmat and Bear, 1964; Bredehoeft and Pinder, 1973; Dagan, 1979; Whitaker, 1986; Souto and Moyne, 1997). The framework as well as the corresponding equations has generally been accepted as the rule of thumb in simulating aquifer contamination and remediation processes (Gorelick, 1990; Miller et al., 1998; Zheng and Bennett, 2002; Borsi and Fasano, 2009).

In terms of modeling subsurface processes where surfactants are applied, existing studies have attempted to present the major kinetics and integrate the corresponding governing equations with the primary framework. Early efforts could be found in the works of Wilson (1989) and Wayt and Wilson (1989), who considered adsorption of surfactant and solubilization of

contaminants in a two dimensional SEAR process. Abriola et al. (1993) further investigated the enhanced solubilization process subject to non-equilibrium mass transfer between NAPL and an aqueous surfactant solution. White and Oostrom (1998) coupled four nonlinear mass balance conservation equations (i.e. water, NAPL-phase organic, aqueous-phase organic, and aqueous-phase surfactant) in simulating the main processes associated with SEAR processes.

Based on the earlier developed theoretical fundaments, a number of multidimensional and multiphase numerical simulators have been made available by introducing finite difference or finite element methods during the past few decades (Widdowson et al., 1988; Kaluarachchi and Parker, 1989, 1990; Katyal and Parker, 1992; Delshad et al., 1996; Clement et al., 1998). For example, Katyal (1997b) presented a software named BIOSLURP, which can delineate the plumes and estimate the volume of subsurface NAPL in a 2D domain. Written in FORTRAN programming language, MODFLOW is one of the mature software packages including processes observation, sensitivity and parameter estimation, aid calibration and model evaluation. It has been consistently upgraded and extensively applied in simulate subsurface flow and transport, even associated with external stresses such as wells, recharges, drains, and rivers (Langevin et al., 2003; Harbaugh, 2005).

Brown et al. (1994) and Delshad et al. (1996) developed UTCHEM by incorporating phase equilibrium relationships such as phase viscosities, densities, and interfacial tensions. Capillary pressure and relative permeability can also be adjusted accordingly, which makes it one of the most attractive and irreplaceable alternatives in the latest studies especially in simulating SEAR processes (Prasanphanich et al., 2012; Luo et al., 2013; Bu et al., 2014). However, the complex kinetics regarding non-equilibrium flow and mass transfer between multiple components dramatically increase the computational costs for model parameterization by requiring the

specific properties of surfactant (He et al., 2008; Luo and Lu, 2014). It is particularly true considering the types of biosurfactants and their application methods may vary from case to case, which can bring significant inconvenience to practical applications.

Despite that existing simulators designated for BSEAR are rare; it is common to find potential substitutive models that are capable of simulating the fate of subsurface NAPL contaminants when surfactant is not presented. As an example, a type of more simplified modeling software named BioF&T 3D was developed by Katyal (1997a). Requiring no surfactant specified inputs, BioF&T 3D models contain much fewer parameters compared to the ones built using UTCHEM. Involving three different kinetics of biodegradation, it allows the multistage simulation of flow and phase transport for up to five contamination species in variably saturated porous media. It also allows real world modeling, which is not available in many similar software packages (Kumar, 2002). Primarily designed for NAPL simulations, BioF&T 3D was also widely used in multiple previous studies to simulate biologically reactive multispecies transport in sanitary landfill (Suk et al., 2000), soil pile bioremediation (Mesania and Jennings, 2000), landfill leachate circulation (Lee et al., 2001), petroleum contaminants transport in the subsurface (Liu et al., 2004), and natural attenuation of contaminated soils (Mulligan and Yong, 2004). According to the study of MDH Engineered Solutions Corporation, (2005), BioF&T 3D surpassed UTCHEM in the overall performance, and exhibited superiority particularly in mesh flexibility, data requirements, computational requirements, and ease of use.

General reviews including many other alternatives of numerical simulators can be found in the works of Crawford (1999), Mulligan and Yong (2004), Šimůnek and Bradford (2008), and Kumar (2012).

In the more recent studies, numerical simulations of subsurface processes mainly focused on model application, integration, and improvement based on previous attempts. For example, Liu (2005) and Qin et al. (2007) applied UTCHEM to simulate a SEAR process at heterogeneous DNAPL contaminated sites. Also, Qin et al. (2008a) improved the model by introducing parameter uncertainties using Monte Carlo simulations. Gomez et al. (2008) studied benzene plume elongation mechanisms based on the Reactive Transport in 3 Dimensions (RT3D) model by including subtract interactions, which was not previously considered, as well as microbial population shifts. Mohammadi et al. (2009) looked into the Alkaline-Surfactant-Polymer (ASP) module of UTCHEM, and studied the phase behavior associated with chemical reactions, alkali consumption, and soap generation effects during ASP flooding. Farajzadeh et al. (2012) integrated a multipurpose reservoir simulator (MPRS) with PHREEQC model to develop a robust and flexible tool in modeling ASP floods. The validation of the approach was further confirmed by benchmarking the results with UTCHEM. Yang et al. (2012) applied BIOPLUME III to simulate natural attenuation, pump-and-treat, enhanced natural attenuation, as well as the combined remedial processes under fuzzy sets model parameters, based on which evaluation of different remedial options were performed.

2.2.3 Coupled physical and numerical simulation

Neither physical models nor numerical models alone could explicitly and evidently represent the complicated solute behaviors in the aquifer (Voss, 2011). Physical models often serve as data sources for the calibration and validation of numerical models. Vice versa, numerical models can also support the design and sampling schedules of physical models (Maqsood, 2004; Smith et al., 2012). Hence, it is critical to integrate physical and numerical

models in simulations of subsurface systems. Some recent studies coupling different types of physical and numerical models were reviewed as follows.

Di Julio and Shallenberger (2002) designed and fabricated a horizontal radial flow (HRF) test cell to measure the flow rate and pressure of a simulated pilot-scale bioslurping remediation system, and further to validate the derived two dimensional numerical model. Reasonable agreement between the theory and experimental data was achieved.

Jean et al. (2002) accessed the biodegradation of benzene, toluene, and xylene by a bacterial culture through lab experiments and numerical simulations. The physical model was built by loading a stainless-steel tank (108 cm × 24.5 cm × 24.5 cm) with medium-size sand and silt sand to create two artificial layers as semi-confined aquifer. Twelve wells were installed to sample the contaminated groundwater for analysis. The numerical model used in this study incorporated advection, hydrodynamic dispersion, adsorption, and biodegradation. Three biodegradation models, namely first order, zero order, and Monod degradation kinetics were evaluated. By comparing experimental and numerical results, it was suggested that Monod degradation kinetics gave the best reflection of biodegradation processes in this study.

Kim and Corapcioglu (2003) developed a vertically averaged two-dimensional model to investigate the subsurface contamination of LNAPL caused by dissolution and volatilization effects. Simulation and sensitivity analysis were conducted based on pure benzene. The kinetic models were then applied to a case study regarding subsurface contamination by jet fuel. The results of the study indicated that volatilization was the main effect for LNAPL migration in the aquifer, and most of the hydrocarbons remained as a free LNAPL phase even for as long as 20 years after the spill, which would result in the contamination of both groundwater and a large volume of soil.

Base on the study of Jean et al. (2002), Agah et al. (2013) expanded the simulation of processes controlling distribution and natural attenuation of benzene, toluene, and xylene into two dimensions. In addition to the fundamental subsurface transport mechanisms, the numerical model applied in this study also considered linear and nonlinear adsorption processes under static as well as dynamic conditions. The model equations were numerically solved by a commercial simulator named PHOENICS. The model verification data were achieved from original data from Jean et al. (2002). Taking oxygen and biomass distributions into account, it was confirmed that Monod approach provided the best agreement with the experimental data.

Falciglia and Vagliasindi (2015) investigated a microwave heating remediation of diesel polluted soils by combining contaminant removal kinetics models with a bench-scale apparatus. The influences of power treatment, treatment time, and soil texture on the soil temperature profiles, on the diesel residual, and on the treatment efficiency were evaluated. A good fit was also achieved between the experimental data and the kinetic model.

Particularly, some recent efforts, though not many, have been put into studies involving biosurfacants. For example, Kuyukina et al. (2005) integrated soil column experiments with a one-dimensional filtration model to study the enhanced effects of crude oil desorption and mobilization by using biosurfactant. The results of the study showed that the crude oil removing ability of the Rhodococcus biosurfactant was 1.4 - 2.3 times greater than that of Tween 60. A strong positive correlation was also found between the oil-contaminated soil penetrating ability and the oil removal performances of surfactants.

Yu et al. (2010) developed an integrated mathematical modeling system to simulate Biosurfactant enhanced bioremediation (BEB) processes using rhamnolipid solution. The numerical model included modules of multiphase, multicomponent flow and transport, biological

degradation, and biosurfactant enhanced remediation. The numerical model was solved by UTCHEM and validated by comparing its output with the observed data from a pilot scale physical model, and the results showed reasonable agreement, which suggested that the developed model was effective in simulating the coupled effects of biodegradation and biosurfactant enhancement.

Harendra and Vipulanandan (2012) examined the sorption and transport mechanisms of surfactant in clayed soil by coupling column experiments and a two-region transport convective-diffusive model. Two types of surfactant SDS and UHBS, which was the abbreviation of Biosurfactants Synthetized at the University of Houston, were studied. Transport parameters such as the dispersion coefficient and the retardation factor of both of the surfactant solutions in clayed soils were determined, and the modeled breakthrough curves well matched the experimental measurements.

Bezza and Nkhalambayausi-Chirwa (2015) investigated the effects of lipopeptide in enhancing PAH desorption and mobilization in a spiked soil system built based on batch experiments. A first-order two-compartment model was developed to simulate desorption processes when different lipopeptide concentrations were introduced. Desorption rates were also consequently calculated under the experimental conditions.

2.3 Parameterization of Numerical Models

2.3.1 Sensitivity analysis

Sensitivity analysis is an essential step for numerical simulations in examining how the outputs respond to the variation of parameters within the models. It is critical in testing the robustness of the model, understanding the relationships between input and output variables, as

well as simplifying the model by screening the insensitive parameters of the model, which can reduce the calculation burden for model calibration (Zheng and Bennett, 2002; Saltelli et al., 2004). Different methods for sensitivity analysis have been developed in the previous studies, and their applicability varies from case to case (Gan et al., 2014).

One-factor-at-a-time (OFAT) is one of the traditional sensitivity analysis methods. This method simply adjusts one parameter at a time while keeping other parameters fixed, and to evaluate the effects of this individual parameter on the outputs of the targeted model. OFAT is still popular in many recent studies due to its simple concepts and easiness to perform (Lenhart et al., 2002; Holvoet et al., 2005; Jing and Chen, 2011). However, without taking into account the simultaneous variation of parameters, OFAT is incapable of revealing the interactions between different parameters, which might lead to the ignorance of the potentially significant variables to the models (Saltelli, 1999; Montgomery, 2008; Peeters et al., 2014).

Considering the interaction effects of multiple parameters in a nonlinear mathematical models, Sobol' (1990) developed a variance-based sensitivity analysis method by introducing the Sobol' sensitivity indices. This model independent method is able to quantify the amount of variance to the model output caused by the variance of each single parameter or multiple parameters collectively. The Sobol' method has been studied and applied in different modeling processes during the past few decades. However, the intensive computational requirement makes it less attractive in general applications (Campolongo and Saltelli, 1997; Sobol, 2001; Jacques et al., 2006; Nossent et al., 2011; Luo and Lu, 2014).

Regression analysis is another approach commonly used in the context of sensitivity analysis. It is conducted by fitting a linear regression equation between the model response and relevant variables, in which the standardized regression coefficients can directly reflect the

significances of the input parameters (Welsch, 1980; Liang and Zeger, 1993; Chatterjee and Hadi, 2009). This method can also be associated with the models built based on the concept of Artificial Neural Networks (ANN), which is inspired by the complex systems involving interconnected neurons within human brain to simultaneously process multiple input factors. The assigned neural net weight matrix can thus represent the sensitivities of each parameter in a direct way Garson (1991). Many studies in modeling different processes have implemented the regression method for sensitivity analysis, especially using ANN (Kermani and Ebadi, 2012; Nourani and Fard, 2012; Jing et al., 2014). However, in order to be qualified for ANN modeling, the number of observed data has to be large enough for a proper modeling training process. Moreover, the "black box" nature of ANN also makes it debatable and controversial as a generally accepted method (Olden and Jackson, 2002; Olden et al., 2004; Witek-Krowiak et al., 2014).

In addition to the methods mentioned above, other approaches for sensitivity analysis are also available and can be classified based on different criteria, as summarized in many published reviews (Hamby, 1994; Saltelli et al., 2004; Tian, 2013; Borgonovo and Plischke, 2015).

As a complex system with complicated processes, subsurface contaminant transport modeling is especially in demand of proper methods for sensitivity analysis. Different methods have been attempted in the recent studies. For example, Clement et al. (2000) used a perturbation method based on OFAT (by either increasing or decreasing the relevant parameters by 50%) to assess the sensitivity of the natural attenuation model at field scale applications. Targeting the boundaries of TCE plumes, it was noticed that transmissivity was the most sensitive factor as opposed to source release rates, which was the least significant factor. Almasri and Kaluarachchi (2005) simulated the nitrate distribution in groundwater by using Modular Neural Networks

(MNN). Different MNN architectures were attempted to achieve regression equations involving different combination of parameters, thus to evaluate their sensitivity towards the performance of the MNN model. Similarly, Al-Mahallawi et al. (2012) elaborated a predictive model of assessing the groundwater nitrate contamination based on ANN. After training and verification, sensitivity analysis was conducted to rank six explanatory variables, namely well depth, screen length, nitrogen load, houses density, infiltration rate, as well as discharge. Luo and Lu (2014) adopted the Sobol' method based on surrogate models, which can closely mimic the behavior of the original model but with lower computational requirements, to assess the relative importance of each variable contributing to the SEAR efficiency of TCE contaminated aquifer. Xu et al. (2015) deployed the OFAT method in identifying the factors that influence the fate of gasoline spills in soil and groundwater. Based on the numerical model combing Hydrocarbon Spill Screening Model (HSSM) in vadose zone and modified Modular three-dimensional multi-species transport model (MT3DMS) in saturated zone, the gasoline leakage rates and the water saturation in the vadose zone were adjusted for six different levels one at a time, with the corresponding time recorded when the peak of gasoline reaches the groundwater table.

2.3.2 Uncertainty analysis

Numerical simulations are often complicated by the prevailingly existing uncertainties of the physical systems. Especially for models involved in environmental studies, uncertainty analysis usually plays the role as to identify the reliability of model predictions by accounting for uncertainties from various sources in model input and design, thus to determine the confidence intervals of the simulation output (Isukapalli, 1999; Bennett et al., 2013).

The sources for uncertainties can be mainly classified into three groups, namely natural uncertainty, model uncertainty, as well as parametric uncertainty. Natural uncertainty is inherent

in environmental systems but can be characterized through ensemble averages. Model uncertainty is mainly originated from the structure of mathematical models and is an important criterion in evaluating the quality of numerical models. Parametric uncertainty is mainly associated with the estimates of parametric values required by the numerical models. This type of uncertainties commonly exists due to misclassification, estimation through a small sample, and estimation through non-representative samples (Isukapalli, 1999). Therefore, uncertainty analysis often prioritize parametric uncertainties when mature simulation models are applied. Especially for parameterization studies in modeling complex systems, increasing effort has been focused on quantifying the influence form parametric uncertainties, particularly in tandem with sensitivity analysis and model calibrations (Saltelli et al., 2006).

Interval, fuzzy, and stochastic are three major categories of conventional methods to characterize uncertainties. Interval method applies for the situations where it is challenging to obtain the probability distribution of the imprecisely defined parameter, but its upper and lower bounds can be determined. In such case, the bounds of the outputs of the model can also be estimated accordingly. The implementations of interval method for uncertainty analysis can be found in literatures covering numerical modeling of various engineering problems (Muhanna and Mullen, 2001; Xu et al., 2006; Shary, 2014; Yang et al., 2015). However, as a drawback of this method, it is not possible to adequately reveal the nature of the output uncertainties by simply assigning one arithmetic interval (Kutscher and Schulze, 1993).

Fuzzy method deals with uncertainties due to the vagueness of definition, in particular for linguistic terms, rather than randomness. Based on fuzzy theory, statements of a modeling system regarding certain attributes can be described in terms of membership functions, which are continuous and normally fall in a range (0, 1) instead of being restricted to a discrete form 0 or 1.

Fuzzy method has been used independently, or hybrid with other types of uncertainty analysis methods in various fields of studies (Nie et al., 2007; Hanss and Turrin, 2010; Jing et al., 2013a; Jing et al., 2013b; Adhikari and Khodaparast, 2014).

Stochastic method is commonly applied in handling uncertainties that originated from the randomness of parametric values. Monte Carlo simulation is one of the most common stochastic methods involving random sampling with certain types of distributions, and it has been widely applied in environmental systems by propagating the parameter uncertainties and evaluating their impacts on the model output (Helton, 1993; Isukapalli et al., 1998; Maqsood, 2004; Li et al., 2014). Especially, Monte Carlo simulation is popular to address parametric uncertainties within subsurface flow and transport models. Some recent studies in this field are reviewed as follows.

Qin et al. (2008a) developed a factorial-design-based stochastic modeling system (FSMS) to systematically study the parametric uncertainties associated with hydrocarbon contaminant transportation in the aquifers. The FSMS was built by integrating a transport model, factorial analysis, and Monte Carlo simulations into a framework. However, the applicability of the FSMS was restricted by the limited data available for the generation of information regarding probability distribution functions (PDFs).

He et al. (2012) presented a global uncertainty and sensitivity analysis framework for modeling free product migration and recovery from petroleum contaminated aquifers by employing the Quasi-Monte Carlo (QMC) sampling method. The QMC method can generate a subsequence of random samples with low discrepancy, thus to avoid obtaining unevenly distributed parameters within the sampling intervals. It also has proven advantages in alleviation of computational effort through parameters screening by using global sensitivity analysis.

Pasetto et al. (2014) performed Monte Carlo simulations based on a reduced-order surrogate model for saturated groundwater flow under randomly distributed transmissivities. By comparing the number of iterations as well as the discrepancy between the sample distributions of hydraulic heads computed using the full and the reduced-order model, it was concluded that the reduced-order model was accurate and computational efficient for flow scenarios when small variance and/or a large correlation length of the log-transmissivity field was involved.

2.3.3 Calibration and verification

The traditional method of model calibration is essentially a trial and error process which uses iterations to adjust the relevant parameters until the simulated outputs are sufficiently close to the experimental data. This method is still popular and has been embedded in commercial modeling tools for automatic calibration (Solomatine et al., 1999; Sonnenborg et al., 2003; Mugunthan et al., 2005; Razavi and Tolson, 2012).

Exiting studies have focused on optimizing the mathematical algorithms to achieve a more efficient calibration process (Duan et al., 1992; Holland, 1992; Gupta et al., 1999; Zhao et al., 2013; Wu et al., 2014). Calibration methods have also been improved by applying parameter estimation, zonation, and global optimization within reasonable predefined intervals (Kitanidis and Vomvoris, 1983; Christensen and Cooley, 1999; Doherty, 2003; Moore and Doherty, 2006; Lovison et al., 2013; Kang, 2014; Plasencia et al., 2014; Yen et al., 2014; Zhang et al., 2015).

Despite that a good fit can be expected, it should not be ignored that some major limitations such as extensive computational requirements, low physical plausibility, and over-parameterization exist when traditional calibration methods are employed (Neuman, 1973; Daliakopoulos et al., 2005; Van Griensven et al., 2006; Whittaker et al., 2010; Okamoto and Akella, 2012)

Verification is an essential process of model development that quantifies the confidence and predictive accuracy of the built simulation models. The purpose of verification is to improve a model's credibility for practitioners (Carson, 2002; Thacker et al., 2004). Typically, observed data obtained from experiments are used to conduct verification processes by comparing to the simulated results of the numerical models, and the group of data applied for verification should be independent from the one used for calibration (Sargent, 2015). However, verification does not ensure the model meets a specified set of requirements as implemented in future predictions, thus precise reflections of real world processes are often not guaranteed (Macal, 2005).

2.3.4 Design of experimental aided parameterization

DOE is a well-known statistical methodology, which can unveil the interrelationships between parameters and the corresponding responses by conducting controlled experiments (Park, 2007). By using DOE, it is possible to simultaneously study several parameters and their interactions (Czitrom, 1999; Veličković et al., 2013; Sarikaya and Güllü, 2015). Factorial design and Response surface method (RSM) are two types of the most commonly used DOE models. Factorial design is adequate to generate the final response model if the model is linear. However, if the model is nonlinear, RSM is commonly applied to investigate the relationship between response and parameters. Optimization of the DOE model usually helps to find the maximum or minimum responses, which can also be reflected in the curvatures of the three-dimensional plots (Li et al., 2008; Khawas et al., 2011).

DOE was originally developed to guide the planning and setup for physical experiments, and it could considerably reduce the number of experiments required to identify the significance of parameters and their interactions (Kirk, 1982). Considering that the complexity and cost can increase dramatically with the growing number of input variables, numerical simulation tools

have been taking advantages of DOE method and extensively involved with proven effectiveness and computational efficiency in achieving the optimal responses. Some examples of recent studies are stated as follows.

Wu et al. (2012) used a DOE aided method to conduct sensitivity analysis and parameterization for a hydrological model SLURP and optimized the predicted regression equation, which has resulted in a greater goodness of fit value compared to the one achieved by the automatic calibration function within the model.

Zahraee et al. (2013) introduced DOE in modeling a real-world construction process to achieve optimal resource levels and maximize the process productivity.

In the study of Al-Shalabi et al. (2014), seven uncertain design parameters for a low salinity water injection process were screened by using DOE method, followed by the optimization of cumulative oil recovery using the RSM.

Though DOE aided methods have proven advantages in conducting parameterization for numerical models, it is not totally evident to accept the optimized responses as the final calibration results without considering the uncertainties associated with these parameters. However, this concern has not been addressed in the existing studies. Also, few studies have been reported regarding using DOE aided method in parameterizing subsurface models, in which uncertainties commonly exist and knowledge concerning complicated interactions between each parameter is far from adequate (Qin et al., 2008a). Especially for modeling BSEAR processes, no studies have integrated DOE aided parameterization methods with Monte Carlo simulations to investigate the influence from stochastic parameters, and calibrate the simulation model within reduced ranges.

2.4 Summary

In this chapter, both physical simulation and numerical simulation of subsurface contamination and remediation processes were reviewed. Previous attempts coupling both types of models were also reviewed. Emphasis has been put on remediation processes involving biosurfactnants. For physical simulation, it was found that most of the studies involved either lab-scale column experiments, which cannot demonstrate multi-dimensional and heterogeneous subsurface scenarios, or pilot-scale soil reactors, which require significant amount of biosurfactants and challenge the control of experimental conditions. As a trade-off option, ISFCs were occasionally deployed; however, biosurfactants were rarely introduced in the existing studies. For numerical simulation, among many available simulation packages, UTCHEM is the major type of simulator used in modeling BSEAR processes, however, its complicated parameters associated with biosurfactants are difficult to define, which correspondingly poses extensive data requirements and computational demand. Simpler numerical models such as BioF&T 3D require much fewer data and exhibit potential as surrogate model for UTCHEM in modeling BSEAR processes. Nevertheless, no studies have been reported regarding advancement of simpler numerical models in simulating complicated BSEAR processes with identification of biosurfactant related parameters. Also, ISFCs were rarely coupled with numerical simulations in modeling BSEAR processes.

Different parameterization methods for numerical models were also reviewed, including sensitivity analysis, uncertainty analysis, calibration and verification of numerical models. As a type of commonly used statistic tool, DOE models are able to identify significant parameters as well as their interactions, thus to aid parameterization of numerical models. Though demonstration of DOE aided parameterization method was found in hydrology models, its

application in parameterizing subsurface models were limited. Additionally, parametric uncertainties, which are critical in parameterizing subsurface modeling especially for BSEAR processes, have seldom been addressed and integrated with the DOE aided parameterization method in previous studies.

CHAPTER 3: AN INTEGRATED PHYSICAL AND NUMERICAL MODELING APPROACH

3.1 Background

Hydrocarbon leakage from global petroleum production and consumption activities has brought up increasing environmental concerns in soil and groundwater contaminations (Li et al., 2012; Hickenbottom et al., 2013). In order to achieve a better understanding of the fate of subsurface contaminants, physical models at different scales were widely employed. Efforts were also put into developing numerical models for simulating multidimensional, multicomponent and multiphase transportation of contaminants within porous media. Generally, physical models are built to provide numerical models with observed data for calibration and verification. Verified numerical models can then be implemented in predictions and further to support decision making on field-scale remediation practices (Demissie et al., 2009; McKnight et al., 2010; Ostermann and Seidel, 2015; Sargent, 2015).

According to the literature reviews, most of the existing studies were conducted based on lab-scale one-dimensional physical models such as column experiments, which restrain the reflection of heterogeneities scenarios in practices. By contrast, physical models involving pilot-scale soil reactor experiments or field-scale monitoring practices often require long durations and complex systems for data acquisitions, which lack flexibility and generality (Maqsood, 2004). As a tradeoff option, Song and Seagren (2008) proposed an ISFC system integrated with the commercial simulators RT3D and MODFLOW. It was able to interpret relatively large-scale physical, chemical, and biological processes, while keep the complexities of the modeling

system under controlled laboratory conditions. The ISFC system was then applied to study limiting factors for in situ bioremediation under different controlled scenarios (Johnson et al., 2013; Song et al., 2014).

Except for the studies mentioned above, however, previous attempts to integrate physical and numerical models at similar scales were limited. To enrich the existing studies, this chapter aims to couple flow cell experiments with a commercial multidimensional and multicomponent simulator named BioF&T 3D, and to establish an integrated physical and numerical modeling approach which is robust and generally applicable to different types of hydrocarbon contamination and remediation processes.

3.2 Physical Model

3.2.1 An intermediate scale flow cell system

In this study, the physical model was built based on a set of two pre-manufactured ISFCs, which were designed to collect aqueous samples and prescribe the simulation domain focused on the longitudinal and vertical directions. As shown in Figure 3.1, the flow cell was fabricated with transparent organic glass materials and was installed on an aluminum framed mobile base. Twenty sampling ports with five on each layer and 15 cm distance between the neighboring ones were equipped on the front panel of the flow cell. The dimension of the flow cell is 82.5 cm × 55 cm × 4 cm. Tap water is introduced from the top left corner where a water inlet port was installed, and the effluent can be discharged through the outlet port with a globe valve at the bottom right corner of the flow cell. Two vertical water retaining zones were created using screening meshes at both ends of the flow cell with three functions: 1) to guarantee the water seepage flow occurs simultaneously at the entire depth of the simulated aquifer; 2) to indicate the

water levels at both ends as hydraulic heads; 3) to enable the pumping out of the accumulated floating oil during the operation when necessary. Globe valves were installed on the bottom three layers for aqueous samples collections.

Prior to soil loading, water proof of the flow cell was carefully checked with water submerging all the four layers of the sampling ports for up to 24 hours. Purchased white play sand with the brand name SHAW® were screened with a 2 mm mesh size sieve. The measured porosity varied from 0.30 to 0.38, and the soil bulk density was determined as 1.643 g/cm^3. Particle size analysis was then conducted using the sieving method, and the size distribution results were given in Table 3.1. A homogenous sandy profile right below the first layer of sampling ports was then created after the soil loading. A variable speed peristaltic pump was employed to create a water flow at approximately 12 ml/min. In order to maintain the water levels at both end and achieve a steady boundary between unsaturated zone and saturated zone, sampling port #5, as illustrated in Figure 3.2, was left open and connected to the drainage. The water levels were measured at 35 cm and 30 cm when stabilized for upstream and downstream respectively. Clear diesel fuel was gradually injected into the flow cell units and BTEX were targeted compounds.

A Bacillus sp. Bacterial strain isolated from the Atlantic Ocean was selected to culture biosurfactant in the Northern Region Persistent Organic Pollution Control (NRPOP) Lab (Cai et al., 2014). The CMC of the crude biosurfactant solution was determined to be 0.01% and the detailed production processes were provided by Zhang (2015). The crude biosurfactant solution was introduced through a one-time injection into the left water retaining zone of the flow cell for BSEAR experiments.

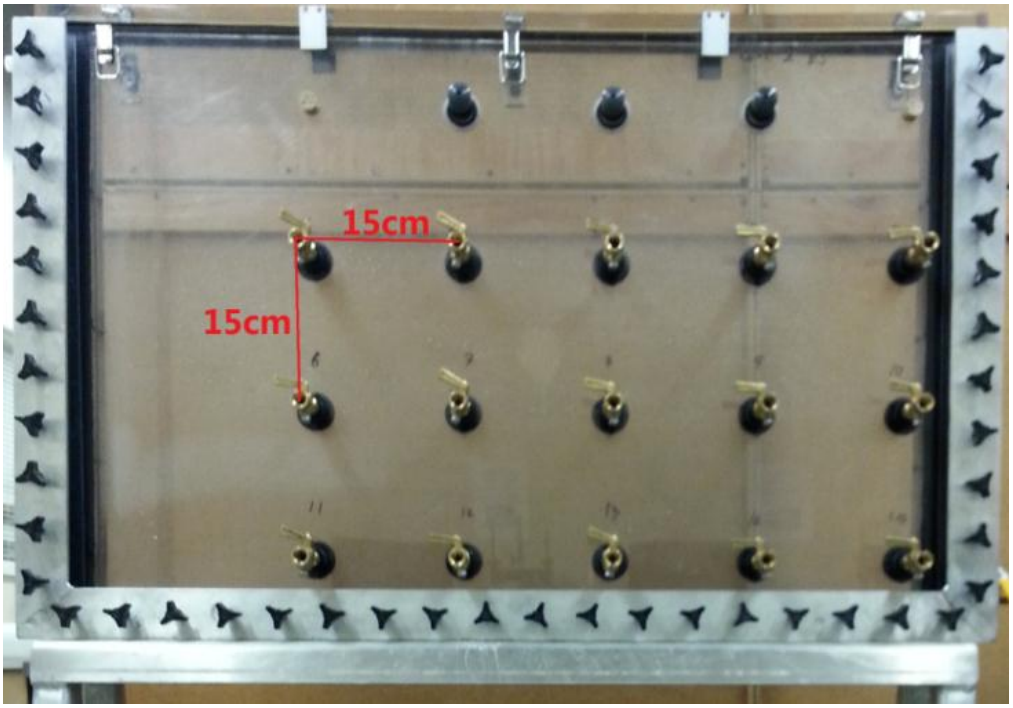

Figure 3.1 Outlook of the ISFC

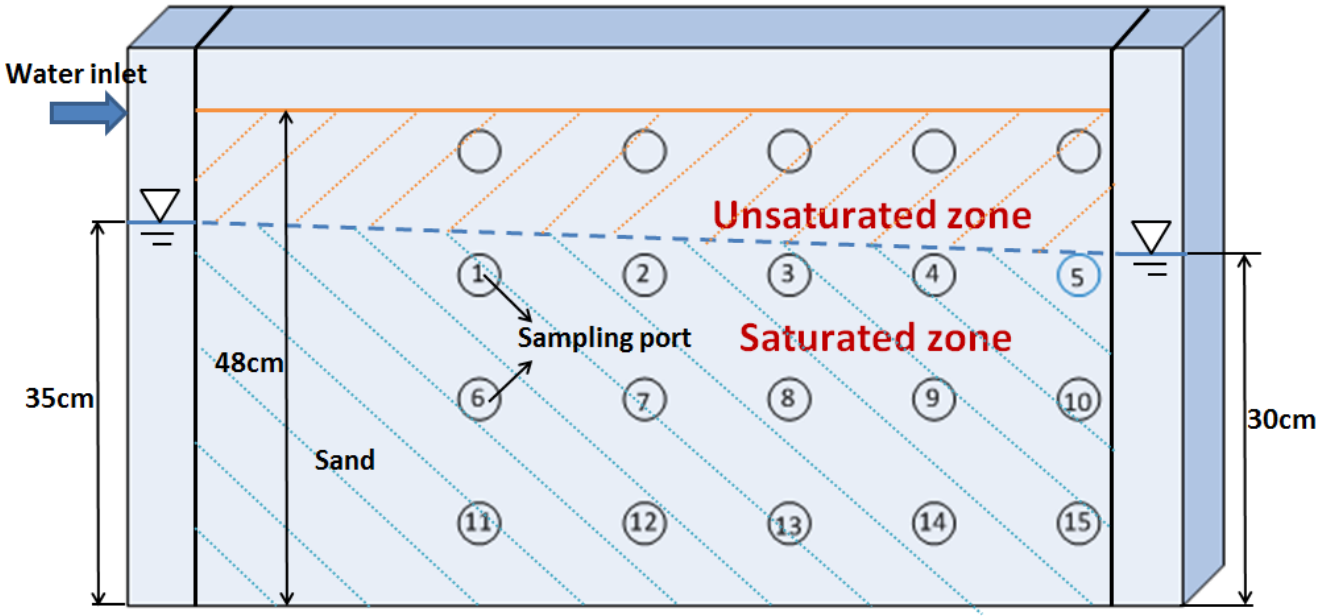

Figure 3.2 Sketch of the ISFC setup

Table 3.1 Soil particle size distribution

Particle	Diameter (mm)	Size Distribution (%)
Coarse Sand	0.5-2	4.6%
Medium Sand	0.25-0.5	36.4%
Fine Sand	0.125-0.25	47.1%
Very Fine Sand	0.0625-0.125	10.8%
Silt	<0.0625	1.1%

3.2.2 Experimental design and sample analysis

Aqueous samples were collected from specific sampling ports at a certain time interval, and immediately transferred into a 40 ml caped vial, which was fulfilled with distilled water to have the headspaces removed. Details of experimental design including sampling schedules were illustrated in Chapter 4 and Chapter 5. The samples were then processed and the concentrations of BTEX were analyzed using the Stratum PTC^{TM} in series with the Agilent 7890A Gas Chromatography (GC), which was equipped with the J&W 122-5532 30 m × 250 μm × 0.25 μm column and the Agilent 5975C Mass Spectrum (MS). Helium was used as the carrying gas for both PTC and GC-MS. The purge flow was set at 40 ml/min for 11 mins and desorb flow was set at 450 ml/min for 4 mins. The oven temperature for GC was programed and maintained at 40 °C for 14 mins during the analyzing schedules.

Calibration curves for BTEX were established using fluorobenzene as the internal standard. The linearity was good for the analyzing method with the coefficient higher than 0.999, and the detection limits for the analyzing method was determined as 3 ppb for benzene, toluene, and ethylbenzene, and as 5 ppb for xylene.

3.3 Numerical Simulator

3.3.1 Structure and Compositions

An existing three-dimensional aquifer simulator named BioF&T 3D was employed for numerical simulation in this study. The software was developed by Scientific Software Group to model subsurface flow and contaminants transportation in three dimensions using finite element method (Katyal, 1997a). It has been mainly applied in real world petroleum sites contamination

and natural attenuation practices, but its application in academic research were dated and not common due to the challenges in modifying and upgrading the code (Chen et al., 2002; Kumar, 2002; Mulligan and Yong, 2004).

The software package includes a mesh editor to define the simulation domain, a pre-processor for input parameters specification and boundary schedules configuration, and a post-processor for output presentation (Katyal, 1997b).

3.3.2 Governing equations

The general governing flow equations integrated in this model are expressed as

$$\frac{1}{x_i}\left[K_{ij}k_{rw}\left(\frac{\psi}{x_j}+u_j\right)\right]=\left(S_wS_s+\phi\frac{dS_w}{d\psi}\right)\frac{\psi}{t}-q_s \tag{3.1}$$

where K_{ij} is the saturated hydraulic conductivity tensor, k_{rw} is the relative permeability, ψ is the pressure head, x_i , x_j (i, j = 1, 2, 3) are the spatial coordinates, t is time, u_j is the unit vector pointing in the vertical direction upward, S_w is the water saturation, S_s is the specific storage, ϕ is porosity, and q_s is the source/sink volumetric rate per unit volume of the porous medium.

BioF&T 3D provides two constitutive models for selection with regard to connections between permeability, saturation and pressure. These are Van Genuchten constitutive model and linear constitutive mode. Van Genuchten model and parameters were used in building the numerical model in this study, presented as

$$\bar{S_w}=[1+(\alpha\psi)^n]^{-m} \tag{3.2}$$

$$k_{rw}=\bar{S_w}^{0.5}\left[1-(1-\bar{S_w})^{1/m}\right]^2 \tag{3.3}$$

Where $\bar{S_w}=\frac{S_w-S_m}{1-S_m}$ is the effective water saturation, S_m is the irreducible water saturation, α and n are porous medium parameters, and $\mathrm{m}=1-{}^{1}/_{n}$.

The initial conditions can be expressed as

$$\psi(x_i, 0) = \psi_0(x_i) \tag{3.4}$$

The first type of boundary condition prescribes the fixed pressure head ψ_p, which is expressed as

$$\psi(x_i, \mathrm{t}) = \psi_p \tag{3.5}$$

The second type of boundary condition prescribes the outward water flux$-q_n$, with the unit vector n_i normal to the boundary, expressed as

$$q_i n_i = -q_n \tag{3.6}$$

q_i is the Darcy velocity, defined as

$$q_i = -K_{ij} k_{rw} \left(\frac{\psi}{x_i} + u_j\right) \tag{3.7}$$

Point sources and sinks are assigned to specific node locations with a certain volumetric flow rate, while for spatially distributed sources or sinks, recharge/discharge areas are proportional to the number of representing nodes, with due weighting given to the associated transmissivity under heterogeneous conditions.

Five distinct regions are normally contained in a typical subsurface contaminants transport media, namely 1) voids with air, 2) mobile liquid phase, 3) immobile liquid phase, 4) a dynamic soil region, in contact with the mobile phase, 5) a stagnate soil region in which diffusion dominants mass transfer. In BioF&T 3D, subsurface contaminants transportation is governed by the general equation expressed as

$$\frac{C_{wm}}{t}(\theta_m + f\rho k_d) + \frac{C_{wim}}{t}[\theta_{im} + (1-f)\rho k_d]$$

$$= \frac{1}{x_i}\left(\theta_m D_{ij} \frac{C_{wm}}{x_j}\right) - \frac{1}{x_i}(q_i C_{wm}) - q_s(C_{ws} - C_{wm}) - \lambda_{wm} + H_w \tag{3.8}$$

Where θ_m and θ_{im} are the fraction of the soil filled with mobile and immobile water respectively, $\theta_{im} = 0$ when the porous media is not fractured, C_{wm} and C_{wim} are the concentration of species in the mobile and immobile water, q_i is the Darcy velocity, k_d is partitioning coefficient of species incorporating linear adsorption, f is the fraction of the sorption sites which is directly contacted with the mobile liquid, and equals to 1 for unfractured porous media, ρ is soil bulk density, q_s is the fluid injection/withdrawal volumetric flow rate per unit volume of the porous medium, C_{ws} is the concentration of species in the injected/withdrawn fluid, D_{ij} is the hydrodynamic dispersion tensor, λ_{wm} is decay loss from mobile liquid phase, and H_w is contaminant loading due to dissolution of NAPL from the source to the mobile phase, calculated by

$$H_w = H_{iw} + H_{gw} \tag{3.9}$$

where H_{iw} represents the proportion of loading caused by groundwater infiltration through the NAPL plume under equilibrium state, and H_{gw} is loaded by groundwater flowing under the NAPL plume.

For simulation within fractured media, the diffusive mass transfer between the mobile and immobile phases is expressed as

$$\frac{C_{wim}}{t}[\theta_{im} + (1-f)\rho k_d] = X\,(C_{wm} - C_{wim}) - \lambda_{wim} \tag{3.10}$$

where X is mass transfer coefficient, and λ_{wim} is decay loss from immobile liquid phase.

BioF&T 3D can estimate the decay losses from biodegradation and radioactive decay for up to five species, under aerobic and anaerobic conditions. For non-radioactive contaminants, the aerobic biodegradation rate can be estimated by either instantaneous reaction or Monod kinetics. When the concentration of species is much smaller than the half-maximum rate concentration, normally a first order decay approximation can be applied.

The initial and boundary conditions for transportation model are defined as

$$C_{wm}(x_i, 0) = C_{w0} \tag{3.11}$$

$$C_{wm}(x_i, t) = C_{wt} \tag{3.12}$$

$$\left(\theta_m D_{ij} \frac{C_{wm}}{x_j}\right) = q_{wD} \tag{3.13}$$

$$\left(\theta_m D_{ij} \frac{C_{wm}}{x_j}\right) - q_i \frac{C_{wm}}{x_i} = q_{wT} \tag{3.14}$$

where C_{w0} is the initial concentration of species at location x_i , equation (2) describes the first type of domain boundary where concentration is equal to C_{wt} , equation (3) and (4) are the second and third type of boundary conditions where dispersive flux $q_{wD}$and total solute mass fluxes q_{wT} are prescribed respectively.

3.3.3 Solution method

BioF&T 3D applies the Galerkin finite element method to approximate the governing equations in three dimensional spaces. With the introduction of initial and boundary conditions, the simulation domain is discretized into horizontal slices for individual sequential solutions to reduce the matrix size, and the Picard iterative approach is employed to generate the solutions among slices, such that the duration of large domain simulations can be considerably shortened (Katyal and Parker, 1992; Katyal, 1997a).

3.4 Summary

This chapter presented an integrated physical and numerical modeling approach for subsurface simulations. In this study, physical model mainly served to calibrate and parameterize the numerical models. The physical model was built based on ISFCs, which were equipped with multiple sampling ports on the X-Z plane for aqueous samples collections. Concentrations of the

targeted compounds within the aqueous samples can be analyzed to investigate the subsurface transportation and distribution of hydrocarbon contaminants. The numerical simulations were conducted using the three-dimensional multi-components and multi-stage subsurface flow and transportation simulator BioF&T 3D. The simulation domain and boundary conditions are well described based on the grids generated by the mesh editor, and the simulated concentrations from different ports and time stages are achieved based on the Galerkin finite element method, and further processed to be presented in the form of contours.

CHAPTER 4: A HYBRID STOCHASTIC-DESIGN OF EXPERIMENT AIDED PARAMETERIZATION METHOD

4.1 Background

Numerical models have been widely applied in simulating subsurface Non-aqueous phase liquid (NAPL) contamination processes. However, there is often a lack of fit existing due to the imprecisely defined parameter uncertainties. Therefore, it is essential to conduct uncertainty and sensitivity analysis for parameterization and calibration of the numerical model, such that discrepancies between simulated and observed data can be minimized.

Traditional parameterization and calibration methods are either not able to reveal the interactions between individual parameters, which might lead to the ignorance of the potentially significant variables (Saltelli, 1999; Montgomery, 2008; Peeters et al., 2014), or risky in over-parameterization and not economic in calculation requirements (Neuman, 1973; Daliakopoulos et al., 2005; Van Griensven et al., 2006; Whittaker et al., 2010; Okamoto and Akella, 2012).

To address this issue, this chapter aims to couple design of experiment (DOE) method with stochastic approaches to develop a new hybrid stochastic-design of experiment aided parameterization (HSDP) method.

4.2 Methodology

Based on the integrated physical and numerical modeling approach discussed in Chapter 3, the HSDP method was developed by integrating the DOE aided parameterization method with stochastic parameter values. Generally, the proposed HSDP method follows the sequence of:

1) Parameters ranking/screening by OFAT. It is conducted by adjusting one factor at a time within a certain range while keeping the others unchanged, thus to investigate if the numerical model is sensitive to the variation of individual parameters. In this way, the number of parameters involved in the DOE model can be reduced by excluding the insignificant parameters, which leads to fewer runs during parameterization;

2) DOE aided parameterization. Factorial design and RSM are two of the most widely applied DOE methodologies. Factorial design is satisfactory in dealing with linear problems, in which interacting effects between parameters are not significant without clear curvatures existing on the 3D response surface. However, factorial design is not adequate to generate nonlinear DOE models, in which parameter interactions cannot be neglected and the curvatures are significant. In this case, RSM should be applied to well fit the DOE models. The predicted regression equations from the DOE models are then optimized to achieve the optimal responses and parameter combinations. Considering that it is not possible to identify if interactions exist in parameters ranking/screening processes using OFAT, properly selecting DOE methods is not guaranteed. RSM can be directly applied providing that the number of included parameters is few. Another alternative is to first try factorial design, which serves to further screen parameters for RSM at a later stage if the curvature is significant;

3) Monte Carlo simulations. Monte Carlo simulation is one of the common approaches to deal with stochastic uncertainty problems. It is often realized by generating a large number of random data following a certain probability distribution as inputs of the models, and further to identify their impacts on the variations of the models' outputs. Traditional Monte Carlo simulation normally requires huge computational capacity; however, number of runs can be

significantly reduced by performing it within narrowed ranges based on the optimized parameters from the DOE aided parameterization processes.

The overall framework of applying the HSDP method is as illustrated by a flowchart in Figure 4.1.

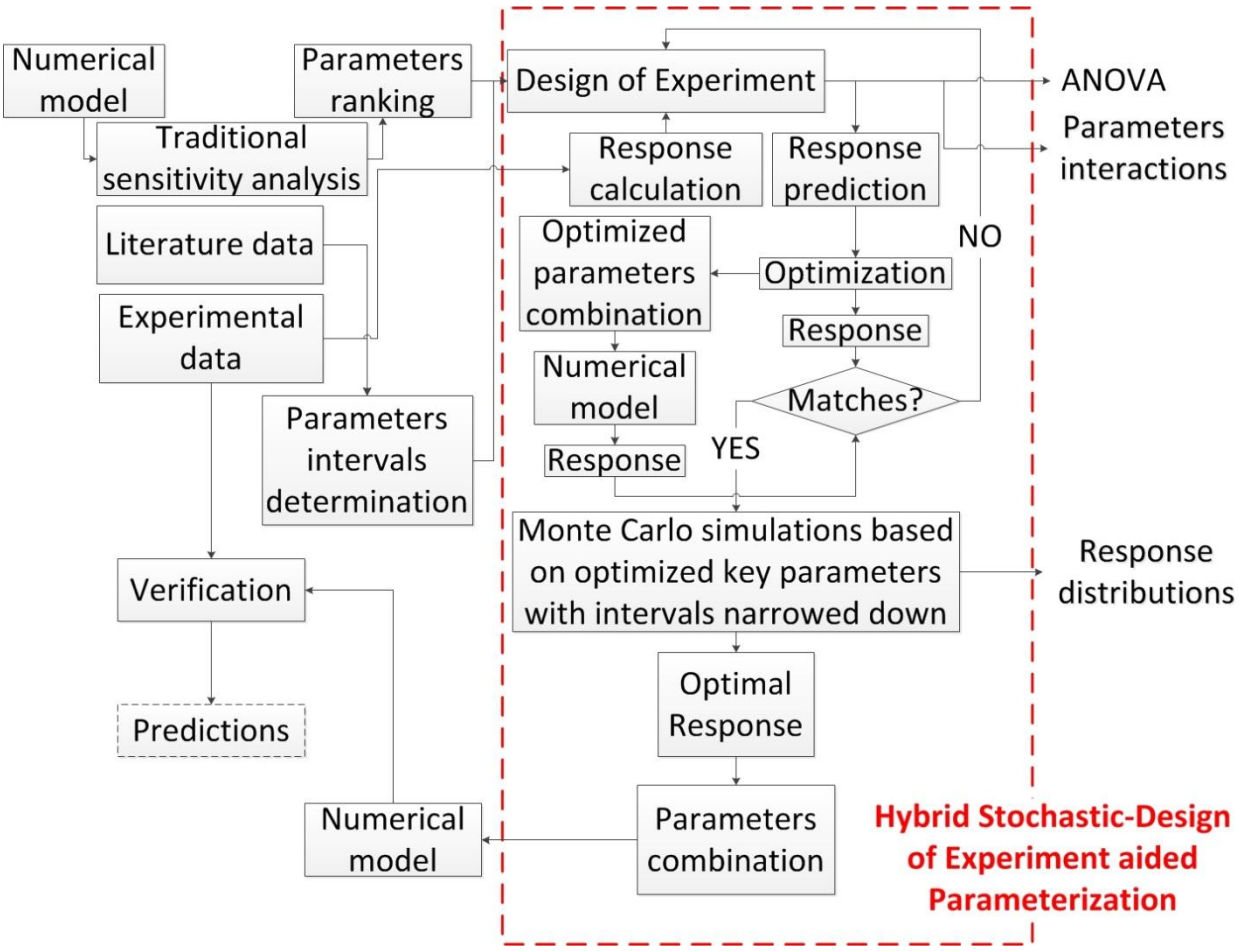

Figure 4.1 Framework of the proposed hybrid stochastic - DOE aided parameterization method

The detailed steps are summarized as follows:

Step 1: To build and preliminarily run the numerical model with all the input properties and boundary schedules specified. The input information regarding parameters and boundary schedules should be based on the suggested values from the instructions of the model.

Step 2: To conduct sensitivity analysis for the independent parameters, for example using OFAT, to screen the insensitive parameters and rank the remaining ones based on their relative significance.

Step 3: To determine the upper and lower bounds of the top ranked parameters in reasonable approaches, for example, from literatures and actual experimental measurements.

Step 4: To select and calculate the responses, which should be the common criteria that can represent the goodness of fit between experimental observations and numerical simulations.

Step 5: To analyze the relationships between responses and the corresponding parameter combinations using the DOE method. To collect the outputs such as Analysis of Variance (ANOVA), parameter interactions, and regression equations for predicted responses.

Step 6: To optimize the DOE predicted responses (to apply non-linear or linear optimization techniques depending on whether parameter interactions are significant or not) and record the optimal combination of parameters, which are then put back into the original numerical model to achieve actual responses.

Step 7: To compare the actual responses to the optimized responses from DOE predictions. To continue to step 8 if they are sufficiently close, otherwise, to update the DOE model by transformation or reselection of DOE method.

Step 8: To conduct Monte Carlo simulations and find the relationships between responses and key parameters within narrowed intervals centralized by the optimal parameters from step 6. Therefore, the number of runs does not have to be as much as traditional stochastic methods.

Step 9: To find the optimal response and the corresponding parameter combinations from step 8. Parameterization process ends hereby.

Step 10: To verify the numerical model for potential predictions.

In addition to the advantages of revealing parameter interactions, the proposed HSDP method can also reflect the effects from parameter uncertainties on the performance of numerical models. Moreover, different from conventional methods dealing with stochastic parameters, which rigidly apply Monte Carlo simulations at the beginning of the modeling, the HSDP method introduces stochastic parameters at a relatively later stage following the optimization of the DOE predicted responses. On the one hand, the reflections of effects of uncertain parameters would not be compromised by the significantly reduced number of runs, which corresponds to the considerable saving of computational requirements. On the other hand, by introducing iterations of screened significant parameters within narrowed intervals, an improvement of calibration results compared with simply using DOE aided parameterization method can be expected.

4.3 Case Study

4.3.1 Data acquisition

45ml diesel fuel was gradually injected to the same depth but 7.5 cm left to the sampling port #1 to simulate a NAPL leakage. Water flow was maintained at 12 ml/min. For the parameterization purpose, the first batch of aqueous samples was collected 48 hours after the

initial injection of diesel from ports #1, #2, #3, and #4 (ports indexes are as indicated in Figure 3.2). The second and third batches of aqueous samples were collected 24 hours and 72 hours afterwards from ports #1, #2, #3, #6, and #7. The observed data were given in Table 4.1.

For the numerical model, the simulation domain reflecting the boundary and setups of flow cell was established by Mesh Editor. Flow boundary conditions were defined by assigning water and diesel volumetric flow rates at specific nodes, while transport boundary conditions were set with BTEX relative abundances in the injected diesel were determined as 80 ppm, 680 ppm, 600 ppm, and 3100 ppm for benzene, toluene, ethyl benzene, and xylene, respectively. The total duration of simulation was set to 120 hours with 24 hours output intervals.

Table 4.1 Observed BTEX concentrations

	48hours				72hours					120hours				
	#1	#2	#3	#4	#1	#2	#3	#6	#7	#1	#2	#3	#6	#7
Benzene	58	40	29	17	38	38	29	9	9	26	23	24	8	9
Toluene	416	306	185	113	286	249	225	80	75	114	174	164	63	58
Ethyl benzene	363	250	136	47	208	195	188	58	45	132	128	135	65	63
Xylene	1697	1134	788	270	1076	981	820	168	166	603	583	689	294	319

Through traditional sensitivity analysis using OFAT, six parameters, namely porosity, first order decay coefficient, distribution coefficient, Henry's constant, as well as diffusion coefficient in water and in air, ranked top in significance as independent parameters and were represented by factors A to F, respectively. Meanwhile, lower and upper bounds of these parameters were reasonably determined based on measurements and/or literatures, as given in Table 4.2.

Table 4.2 Selected parameters for the DOE models

Parameters	Unit		Lower bound	Upper bound	References
A: porosity	-		0.30	0.38	Lab measurements
B: first order decay coefficient (DCAY)	/day	Benzene:	0	1.4E-3	(Borden et al., 1997; Suarez and Rifai, 1999; Newell et al., 2002; Agah et al., 2013)
		Toluene:	0	6.3E-3	
		Ethyl benzene:	0	5.8E-3	
		Xylene:	0	3.5E-3	
C: distribution coefficient (AKD)	-	Benzene:	2.06	2.16	(Chiou et al., 1982; Paschke and Popp, 1999; Nardi, 2003; Braeutigam et al., 2009; Eom, 2011)
		Toluene:	2.51	2.73	
		Ethyl benzene:	2.84	3.15	
		Xylene:	2.86	3.20	
D: Henry's constant (GAMA)	-	Benzene:	0.23	0.24	(Pankow et al., 1996; Miller and Stuart, 2000; Mozo et al., 2012)
		Toluene:	0.26	0.28	
		Ethyl benzene:	0.25	0.37	
		Xylene:	0.21	0.31	
E: diffusion coefficient in water (DIFW)	m^2/day	Benzene:	9.4E-5	12.6E-5	(Katyal, 1997b; Rowe et al., 2005; Lahoz-Martín et al., 2014)
		Toluene:	8.2E-5	10.5E-5	
		Ethyl benzene:	6.2E-5	9.8E-5	
		Xylene:	6.2E-5	8.3E-5	
F: diffusion coefficient in air (DIFA)	m^2/day	Benzene:	0.76	1.08	(Yaws, 1995; Katyal, 1997b; Rowe et al., 2005; De Biase et al., 2014)
		Toluene:	0.68	0.97	
		Ethyl benzene:	0.61	0.87	
		Xylene:	0.61	0.84	

The response for this design was Root Mean Square Deviation (RMSD), as given by equation (4-1). The coefficient of determination (R^2), which is a common statistical indicator to evaluate the goodness of fit for groundwater models, was also calculated during the parameterization processes, as given by equation (4-2).

$$\mathrm{RMSD} = \sqrt{\frac{\sum_{i=1}^{N}(y_i - \hat{y}_i)^2}{N}} \tag{4.1}$$

$$R^2 = 1 - \frac{\sum_{i=1}^{N}(y_i - \hat{y}_i)^2}{\sum_{i=1}^{N}(y_i - \bar{y})^2} \tag{4.2}$$

In which, y_i is observed data, $\hat{y}_i$ is simulated data, N is the number of groups of observed/simulated data, $\bar{y}$ is the mean value of the observed data. Ideally, a perfectly fit model would have RMSD=0 and $R^2 = 1$, though it is not likely in practice (Daliakopoulos et al., 2005; Sun et al., 2009).

4.3.2 Parameterization

23 groups of simulations were conducted by running BioF&T 3D with different combinations of parameters A to F. The sequence of simulations was randomly generated by using the minimum run resolution V factorial design with Design Expert 7.1®. The ANOVA results were summarized in Table 4.3. As shown in Figure 4.2, different parameters and their interactions stand out as significant factors for different contaminant species. Factor A soil porosity, factor C distribution coefficient (AKD), and factor D Henry's Constant (GAMA) were the most influential parameters for improving the goodness of fit for numerical simulations. It is also important to look at factor B first order decay coefficient (DCAY) for its interactions with other significant parameters. Factor E diffusion coefficient in water (DIFW) and factor F diffusion coefficient in air (DIFA) were proven to be insignificant. Positive or negative effects

from individual factors were clearly identified, and the interaction effects of two parameters were also presented as 3D surface graphs in Figures 4.3, 4.4, 4.5, 4.6, and 4.7. It also showed that the center point was not far from the DOE predicted surface, and minimum curvature was observed, which suggest the interaction effects were not predominant and the selected factorial design is acceptable in predicting the responses. These interactions between parameters cannot be identified by using OFAT. Also, minimum run resolution V factorial design uses less number of runs than full factorial design.

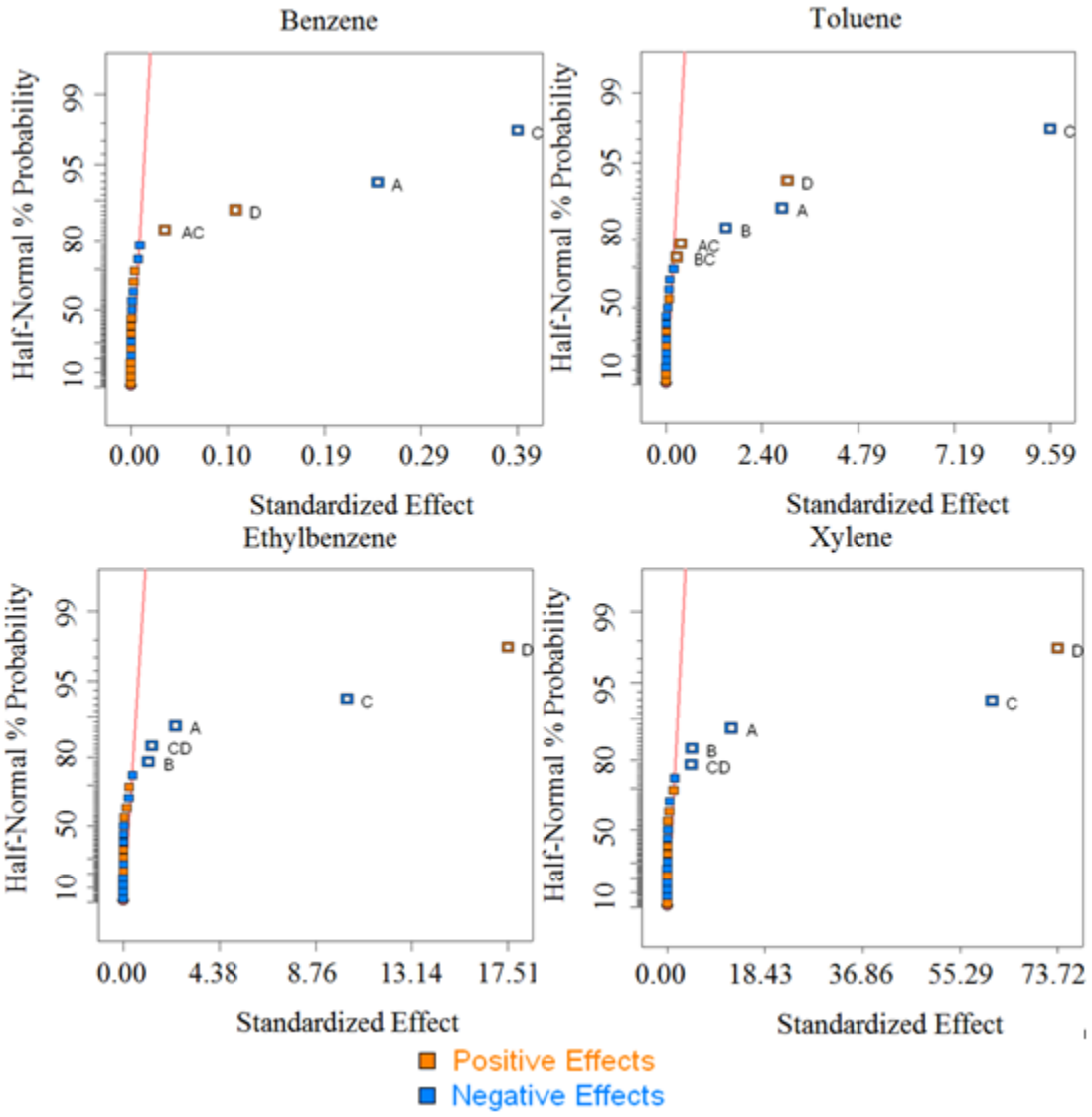

Figure 4.2 Half-normal probability plots

Table 4.3 ANOVA results of minimum run resolution V design

Source	Sum of squares (b/t/e/x)*	df (b/t/e/x)	Mean square (b/t/e/x)	F value (b/t/e/x)	p-value (Prob>F) (b/t/e/x)
Model	1.37/683.97	4/6/5/5	0.34/114	4003.81/3268.29	< 0.0001/ < 0.0001
	2504.12/56692.45		500.82/11338.49	2887.18/5770.61	< 0.0001/< 0.0001
A - Porosity	0.33/43.81	1/1/1/1	0.33/43.81	3816.75/1255.93	< 0.0001/< 0.0001
	29.5/774.25		29.5/774.25	170.14/394.05	< 0.0001/< 0.0001
B - DCAY	-/11.72	-/1/1/1	-/11.72	-/336.04	-/< 0.0001
	6.96/114.29		6.96/114.29	40.15/58.17	< 0.0001/< 0.0001
C - AKD	0.80/479.24	1/1/1/1	0.8/479.24	9385.06/13740.12	< 0.0001/< 0.0001
	543.02/19650.38		543.02/19650.33	3130.44/10000.85	< 0.0001/< 0.0001
D - GAMA	0.059/48.18	1/1/1/1	0.059/48.18	692.13/1381.23	< 0.0001/< 0.0001
	1602/28384.22		1602/28384.22	9235.31/14445.85	< 0.0001/< 0.0001
AC	0.006/0.71/-/-	1/1/-/-	0.006/0.71/-/-	72.37/20.33/-/-	< 0.0001/0.0004/-/-
BC	-/0.39/-/-	-/1/-/-	-/0.39/-/-	-/11.15/-/-	-/0.0045/-/-
CD	-/-/8.92/105.94	-/-/1/1	-/-/8.92/105.94	-/-/51.4/53.92	-/-/ < 0.0001/< 0.0001
Residual	0.001/0.52	17/15/16/16	0/0.035/0.17/1.96		
	2.78/31.44				
Cor Total	0.37/684.58	22/22/22/22			
	2508.53/56739.44				

*(b/t/e/x) denotes benzene, toluene, ethylbenzene, and xylene.

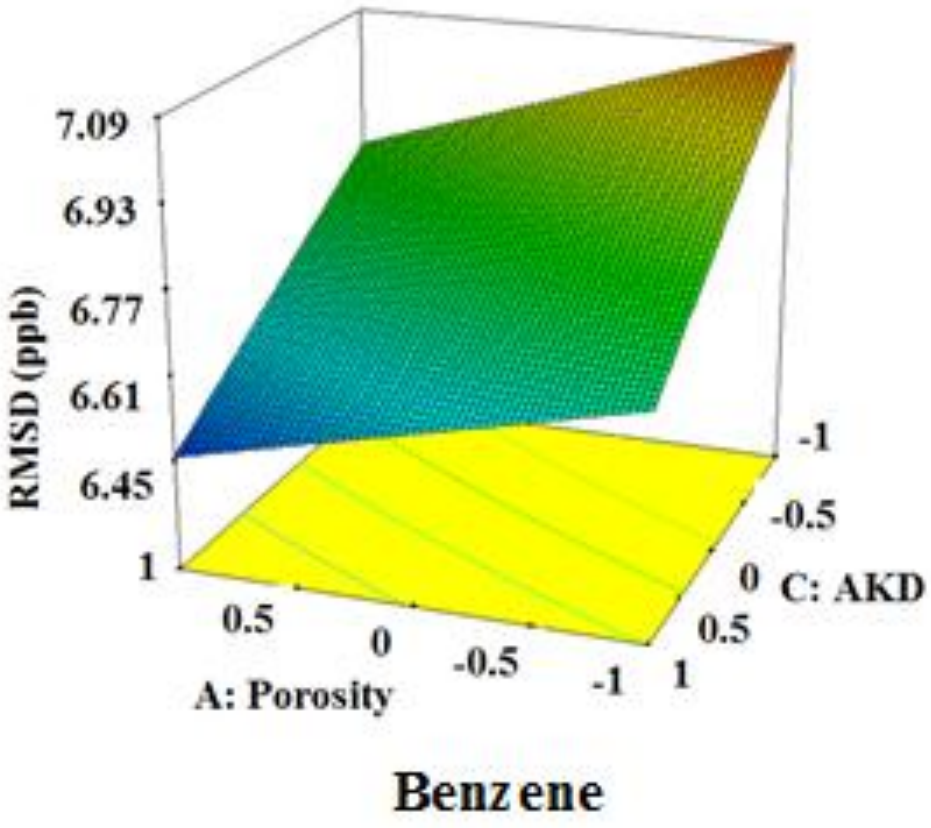

Figure 4.3 3D surface graph of factors A and C interactions for benzene

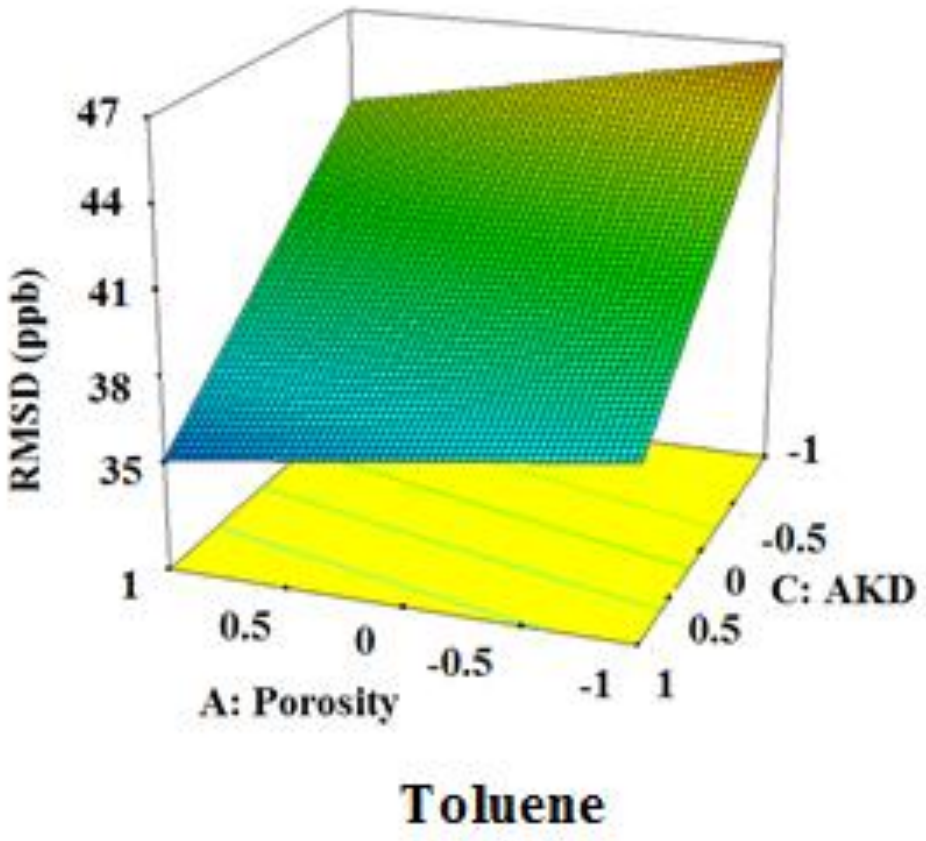

Figure 4.4 3D surface graph of factors A and C interactions for toluene

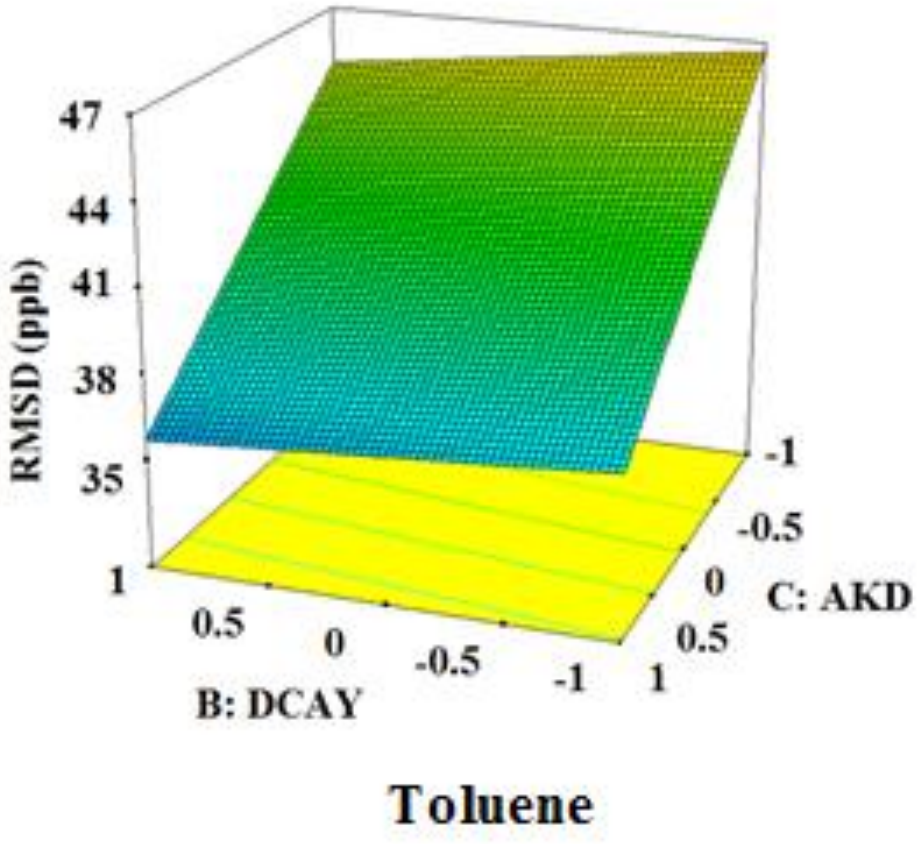

Figure 4.5 3D surface graph of factors B and C interactions for toluene

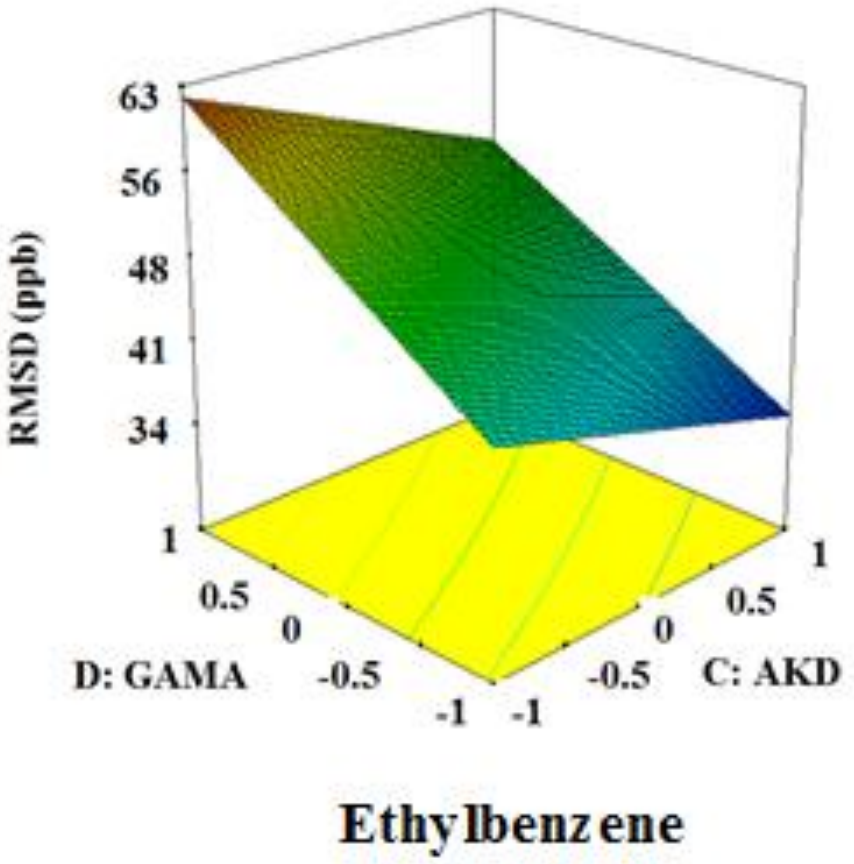

Figure 4.6 3D surface graph of factors C and D interactions for ethylbenzene

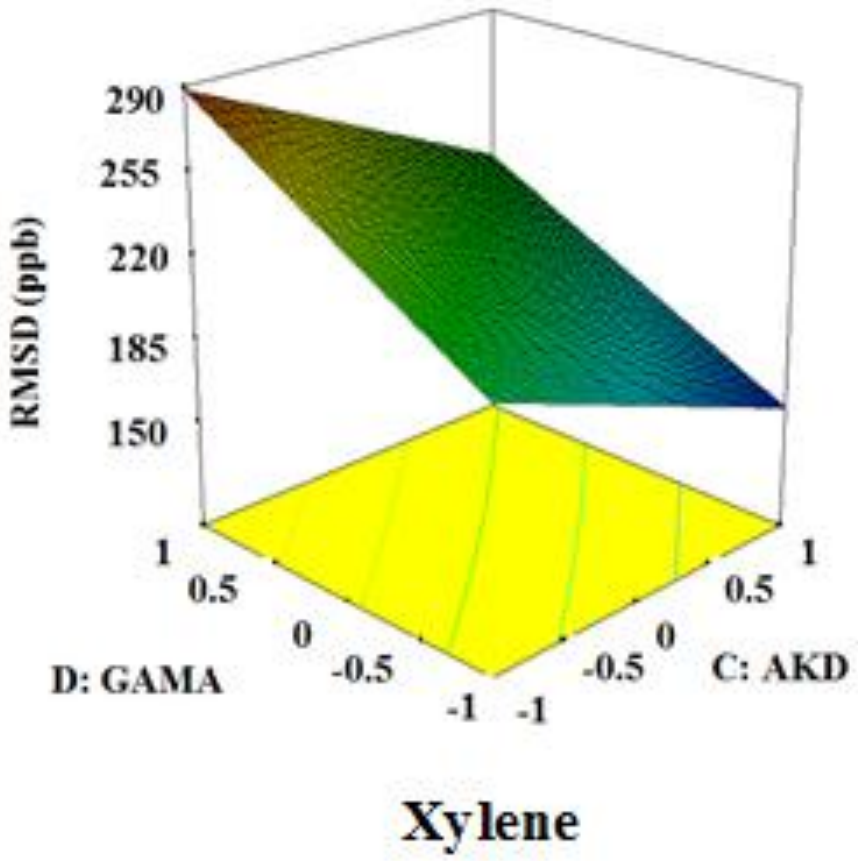

Figure 4.7 3D surface graph of factors C and D interactions for xylene

Based on the ANOVA results, factor E and F can be excluded due to the insignificances at their corresponding ranges. Meanwhile, the 3D surface graphs indicated that the combination of a lower Henry's constant, a higher porosity, and a higher distribution coefficient would be in favor of improving the performance of the model. The predicted regression equation for RMSD in terms of coded factors is given in equations (4.3), (4.4), (4.5), and (4.6) as follows:

$$\mathrm{RMSD_b} = 6.76 - 0.12\mathrm{A} - 0.19\mathrm{C} + 0.053\mathrm{D} + 0.017\mathrm{AC} \quad (4.3)$$

$$\mathrm{RMSD_t} = 41.04 - 1.45\mathrm{A} - 0.75\mathrm{B} - 4.72\mathrm{C} + 1.54\mathrm{D} + 0.19\mathrm{AC} + 0.14\mathrm{BC} \quad (4.4)$$

$$\mathrm{RMSD_e} = 47.74 - 1.19\mathrm{A} - 0.58\mathrm{B} - 5.02\mathrm{C} + 8.63\mathrm{D} - 0.66\mathrm{CD} \quad (4.5)$$

$$\mathrm{RMSD_x} = 219.86 - 6.09\mathrm{A} - 2.34\mathrm{B} - 30.22\mathrm{C} + 36.32\mathrm{D} - 2.28\mathrm{CD} \quad (4.6)$$

As objectives, the RMSD predictions are then minimized by using nonlinear optimization. An optimization software package Lingo®, was applied in this process. The optimized parameters were then fed back to the simulation models to achieve actual responses and R^2 value. The comparisons of predicted and actual responses after optimization were made and summarized in Table 4.4.

Table 4.4 Summary of predicted and actual responses after optimization of the DOE models

	Optimized parameters				Predicted	Actual	
	A: Porosity	B: DCAY (day-1)	C: AKD	D: GAMA	Response RMSD (ppb)	Response RMSD (ppb)	R^2
Benzene	0.38	1.4E-3	2.16	0.23	6.33	6.41	0.79
Toluene	0.38	6.3E-3	2.73	0.26	28.20	33.02	0.90
Ethylbenzene	0.38	5.8E-3	3.15	0.25	33.11	33.37	0.85
Xylene	0.38	3.5E-3	3.20	0.21	127.02	148.32	0.88

As can be noticed, the DOE predicted responses reasonably match the ones achieved by using the suggested sets of parameters in the simulation model. Nevertheless, it cannot be justified as the best calibration. Thus, further tests involving stochastics parameters were conducted for two purposes: firstly, to reflect the impact from uncertain parameters on response distributions; secondly, to minimize the ignorance of parameter combinations for better responses. Stochastic parameters are introduced into the targeted numerical models by Monte Carlo simulations. After the effective parameterization by DOE, the computational requirements can be dramatically reduced with fewer parameters and narrower ranges. It was found that factors A, B, C, and D were involved in the predicted regression equations, however, the coefficient of factor B was significantly lower relative to the other three factors, and its value was low. Hence, stochastic values were only introduced into factor A, C, and D in this study. Uniform distribution was applied to generate 60 groups of data for these three selected parameters. Their updated intervals were generated by centralizing the optimized parameters and expanding with ±20% of their initial intervals, which are still within reasonable ranges.

Sixty responses were generated and are shown in Figures 4.8, 4.9, and 4.10. These figures also represent the impacts from each individual parameter on the RMSD value for BTEX. It can be noticed that only parts of the results (AKD on benzene, toluene, and xylene, GAMA on ethylbenzene and xylene) reflected that the trends of responses distributions followed the sensitivity analysis on individual parameters. It was probably due to the limited number of runs within the narrowed intervals. On the other hand, it further manifested the efficiency of the proposed method in reducing computational requirements while dealing with uncertain parameters. Multiple points were found below the previously achieved RMSD values. Since the optimized parameters were all found at their upper or lower bound values, it is common to find

improved responses when half of the new intervals centered by these values were actually beyond the original boundaries. Only one combination of parameters within the initial intervals was found to be capable of generating a lower RMSD than the previously optimized one. That is for ethylbenzene, RMSD equals 29.57 ppb when porosity is 0.376, AKD is 3.145, and GAMA is 0.268. All the other improved responses had at least partially involved parameters exceeding the initial ranges, which indicated the high accuracy of the predictions from the selected DOE method. The final calibration results are summarized in Table 4.5, with the comparison of the results achieved without introducing stochastic parameters by Monte Carlo simulations.

Table 4.5 Summary of the final parameterization results without / with Monte Carlo simulations

	Selected parameters			Calibrated results	
	A: Porosity	C: AKD	D: GAMA	RMSD (ppb)	R^2
Benzene	0.38/0.394	2.16/2.179	0.23/0.230	6.41/6.33	0.79/0.80
Toluene	0.38/0.378	2.73/2.774	0.26/0.257	33.02/31.31	0.90/0.91
Ethylbenzene	0.38/0.376	3.15/3.145	0.25/0.268	33.37/29.57	0.85/0.89
Xylene	0.38/0.389	3.20/3.260	0.21/0.196	148.32/131.33	0.88/0.90

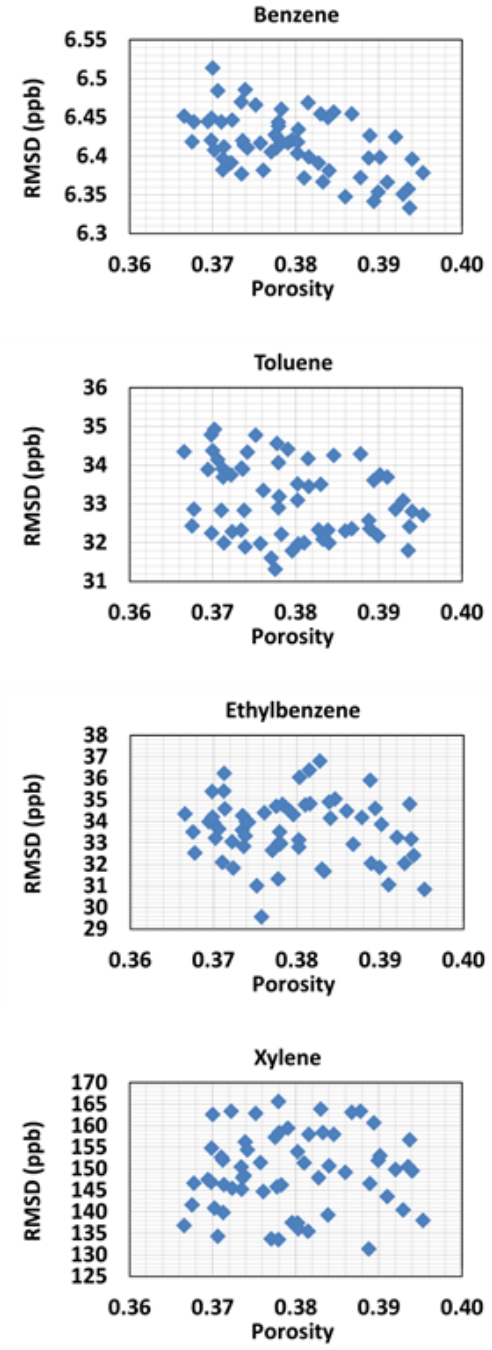

Figure 4.8 Effects of Porosity uncertainties on RMSD

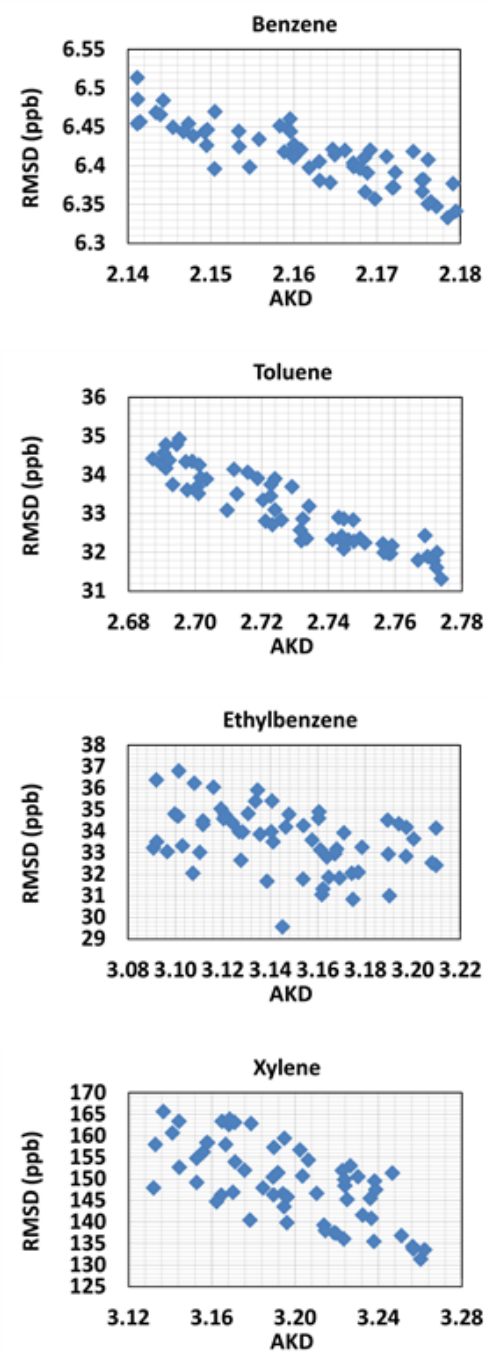

Figure 4.9 Effects of AKD uncertainties on RMSD

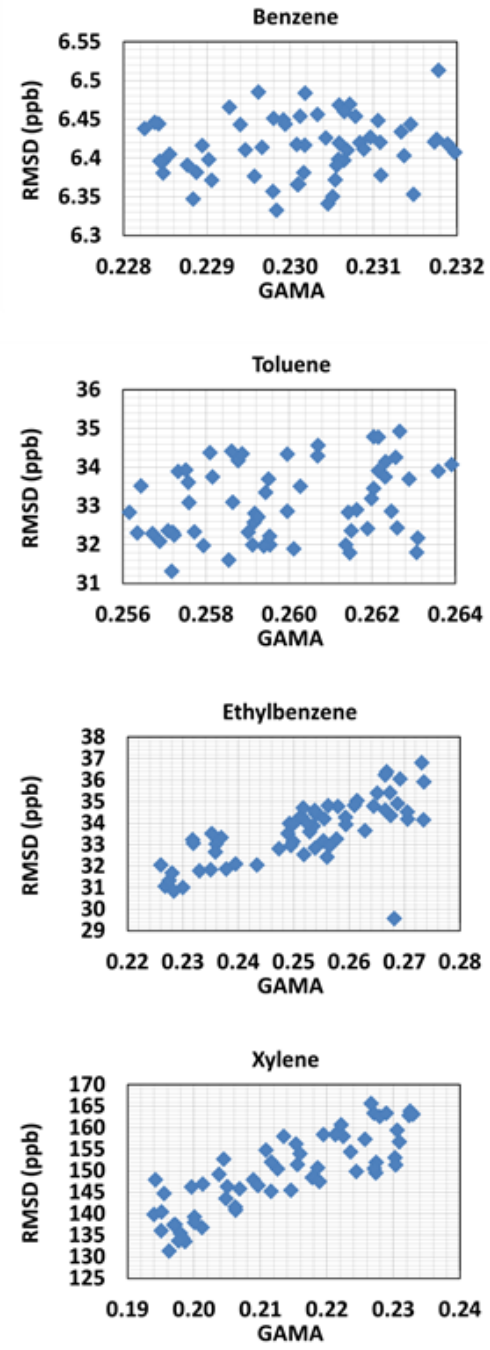

Figure 4.10 Effects of GAMA uncertainties on RMSD

4.3.3 Verification

For verification of the simulation model, another set of flow cell experiments were conducted. The diesel injection location was moved right into the sampling port #1, and the quantity of diesel was changed from 45 ml to 35 ml. Aqueous samples were collected from sampling ports #2, #3, #4, and #6 at five time stages (12 hours, 36 hours, 60 hours, 72 hours, and 84 hours after the initial diesel injection) and analyzed. The inputs for model verification are presented in Table 4.6. Simulation results at different time stages in the form of BTEX concentrations contours at the X-Z plane are shown in Figures 4.11, 4.12, 4.13, and 4.14. The migrations of contaminates over time were found reasonably close to practice. The comparisons of simulated and observed xylene concentrations from each sampling port were presented in Figures 4.15, 4.16, 4.17, and 4.18. The results demonstrated an overall satisfactory level of fit, with RMSD value at 5 ppb and R^2 value at 0.76 for benzene, RMSD value at 26 ppb and R^2 value at 0.87 for toluene, RMSD value at 31 ppb and R^2 value at 0.82 for ethylbenzene, and RMSD value at 126 ppb and R^2 value at 0.90 for xylene.

Some mismatches exist between the observed and simulated data at specific sampling ports and time stages. The spatial and temporal variations of goodness of fit in this study could be caused by the inexact retardation effects and the uncertainties from the applied soil materials, which were assumed homogenous but not possible for flow cell loading. Additionally, the flow rate of water could not be consistently maintained during the experiments without accurate controlling countermeasures, which led to the deviation from the defined boundary schedules in the simulations.

Table 4.6 BioF&T 3D model inputs for verification

Parameter	Value				Unit
Species properties	Benzene	Toluene	Ethyl benzene	Xylene	
Specific gravity of residual hydrocarbon	0.878	0.878	0.878	0.878	-
Water solubility	1780	515	152	152	g/m^3
Oil-water mass transfer coefficient	1.25	1.25	1.25	1.25	$/cm^3$
First order decay coefficient	0.0014	0.0063	0.0058	0.0035	/day
Distribution coefficient	2.179	2.774	3.145	3.260	-
Henry's constant	0.230	0.257	0.268	0.196	-
Diffusion coefficient in water	12.6E-5	10.5E-5	9.8E-5	8.3E-5	m^2/day
Diffusion coefficient in air	1.08	0.97	0.87	0.84	m^2/day
Concentration in NAPL	80	680	600	3100	ppm
General inputs					
NAPL spill amount		35			ml
Simulation period		96			hours
Hydraulic gradient		0.036			m/m
Saturated hydraulic conductivity		350			cm/day
Porosity		0.38			-
Residual water		0.1			-
Van Genuchten Paramater α		0.124			1/cm
Van Genuchten Paramater n		2.28			-
Longitudinal dispersivity for soil		8			cm
Transverse dispersivity for soil		0.8			cm
Soil bulk density		1.643			g/cm^3

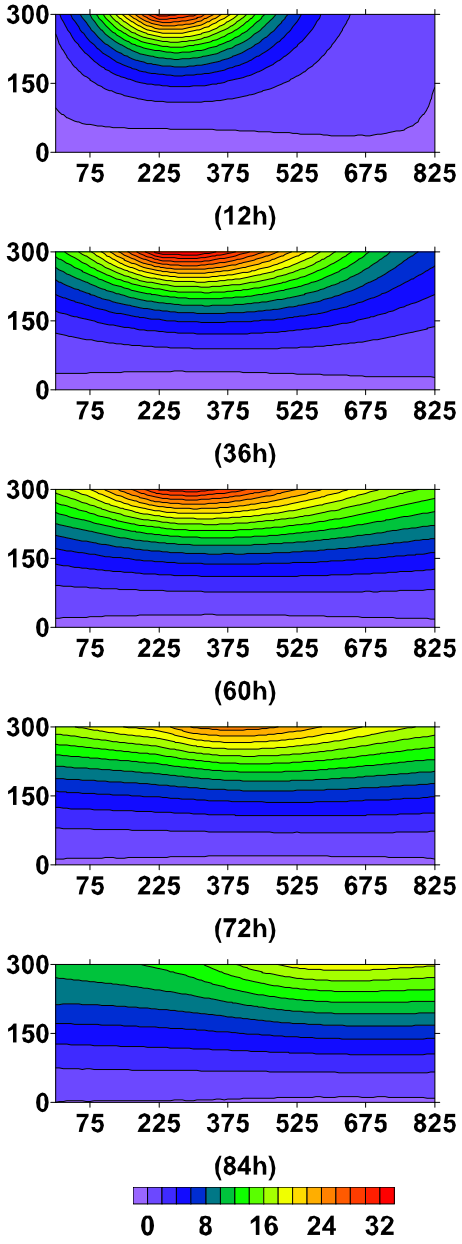

Figure 4.11 Simulated benzene concentration (in ppb) contours at the X-Z plane (in cm) at different time stages after initial diesel injection

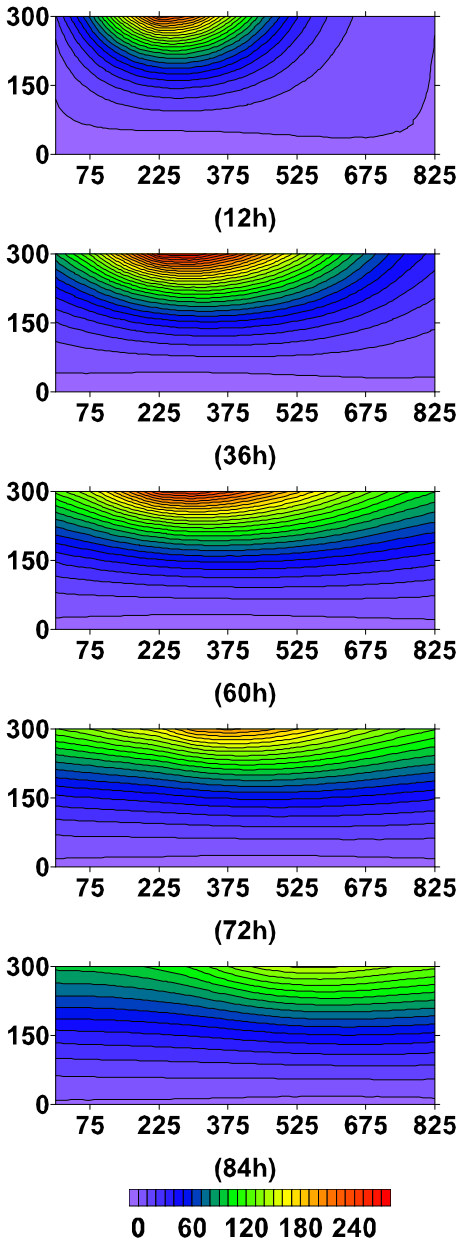

Figure 4.12 Simulated toluene concentration (in ppb) contours at the X-Z plane (in cm) at different time stages after initial diesel injection

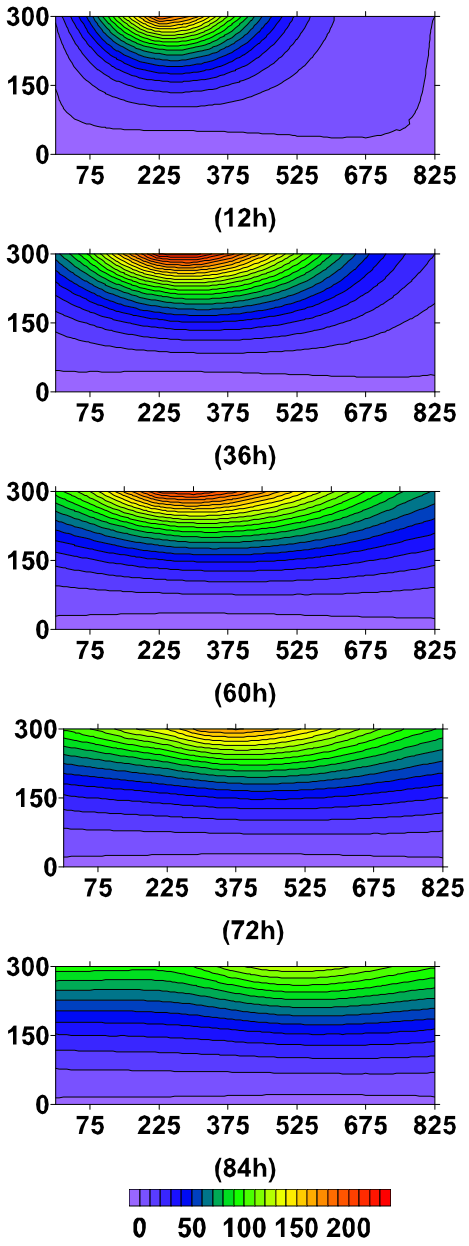

Figure 4.13 Simulated ethylbenzene concentration (in ppb) contours at the X-Z plane (in cm) at different time stages after initial diesel injection

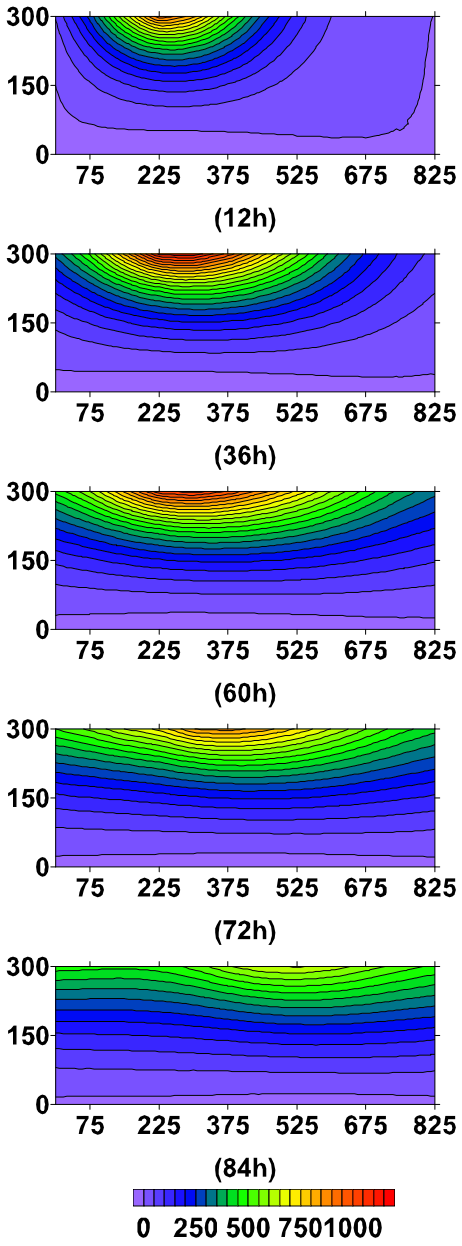

Figure 4.14 Simulated xylene concentration (in ppb) contours at the X-Z plane (in cm) at different time stages after initial diesel injection

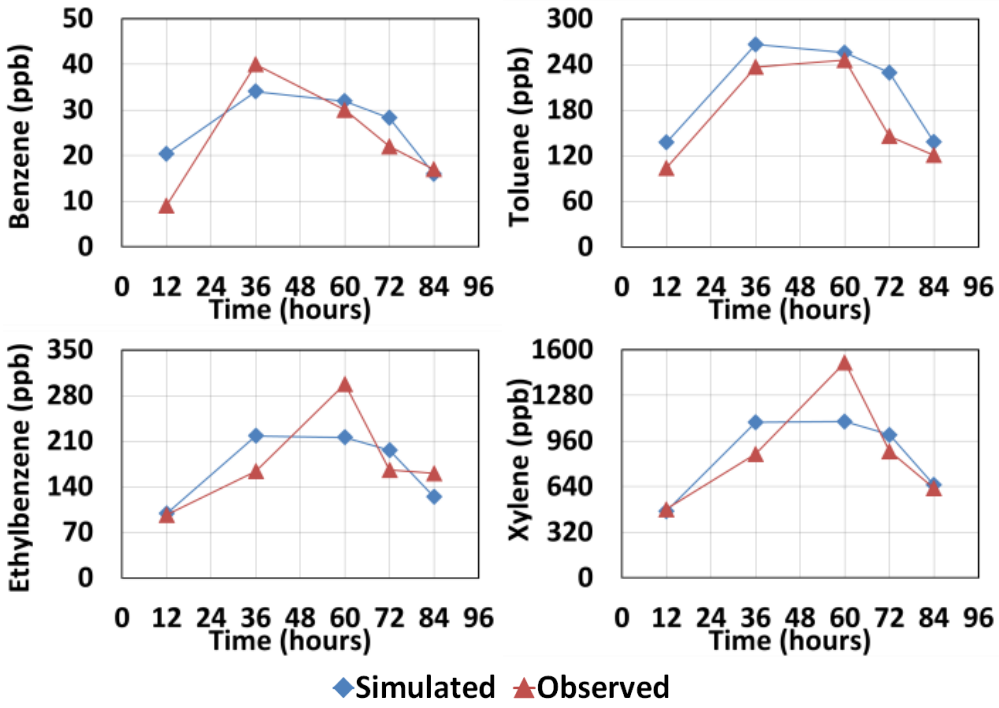

Figure 4.15 BTEX verification results for sampling port #2

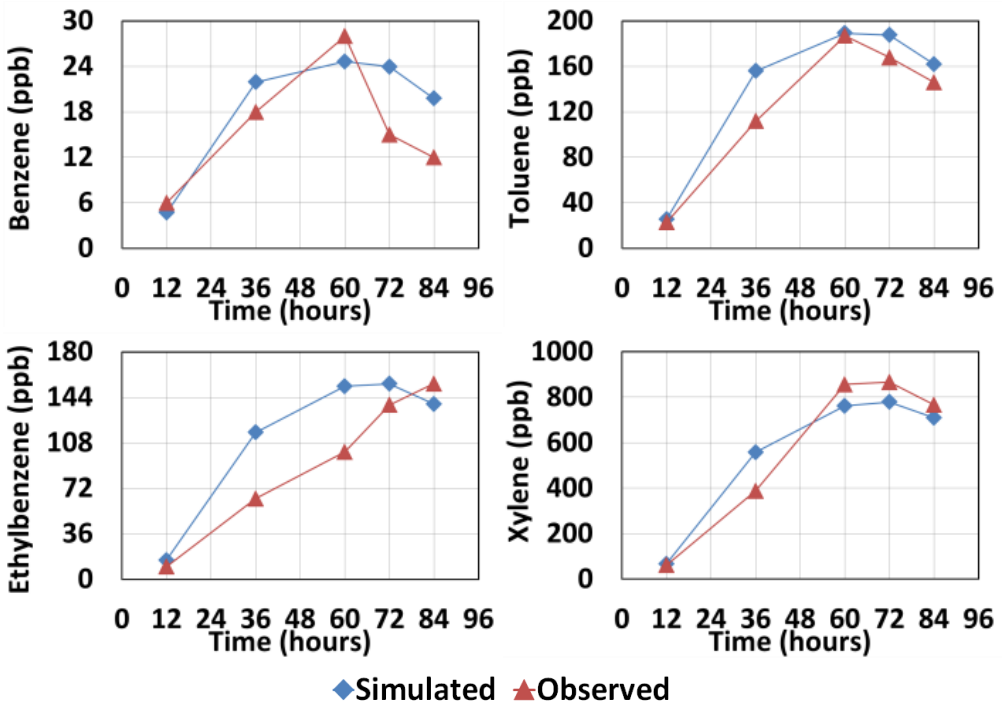

Figure 4.16 BTEX verification results for sampling port #3

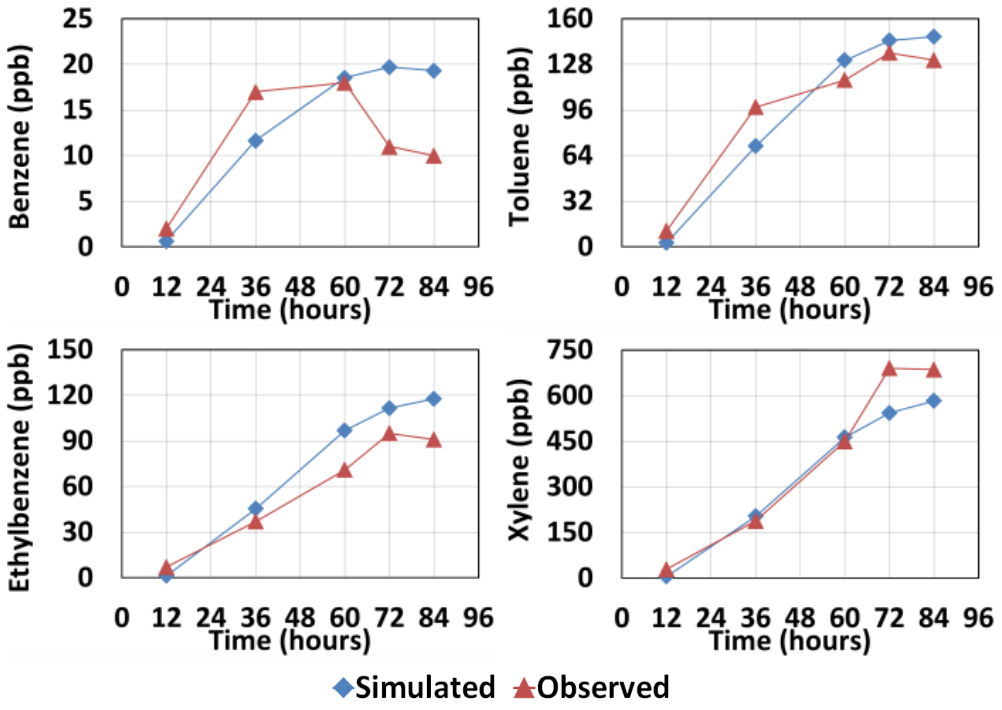

Figure 4.17 BTEX verification results for sampling port #4

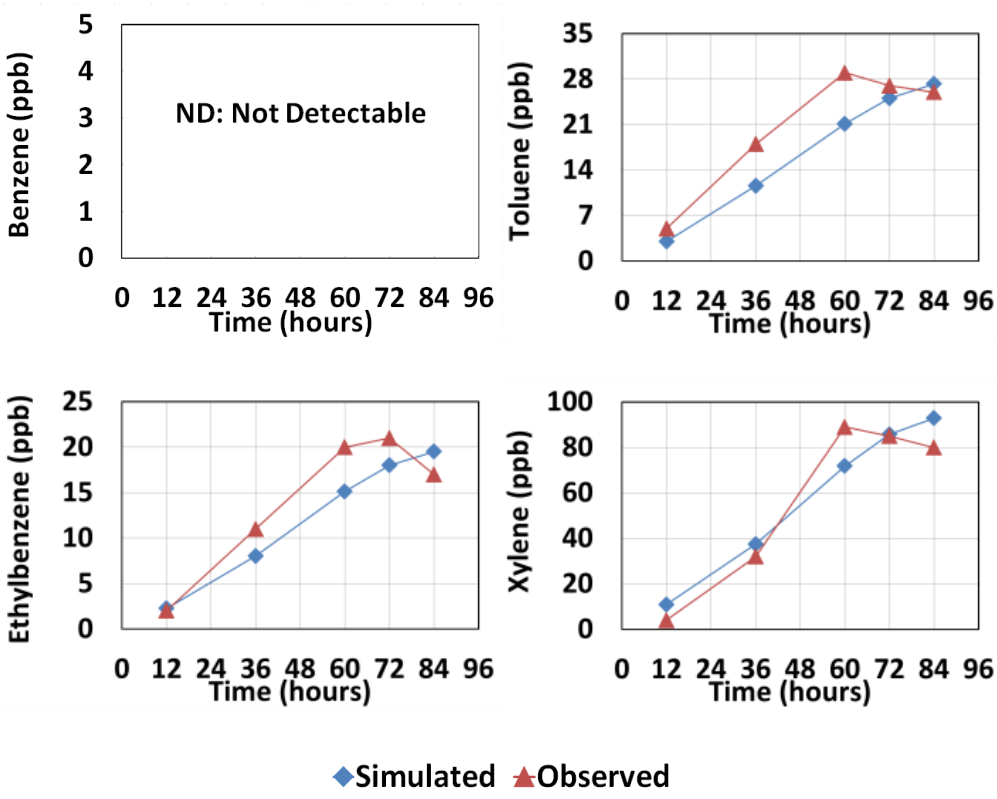

Figure 4.18 BTEX verification results for sampling port #6

4.4 Summary

In this research, flow cell experiments were conducted to physically simulate BTEX contamination and natural attenuation processes in the subsurface. A commercial groundwater modeling tool BioF&T 3D was applied to conduct numerical simulations. A new hybrid stochastic – DOE aided parameterization method was developed to improve the modeling performance and implemented in a case study.

It was found that the developed HSDP method can efficiently identify key parameters and their interactions for the simulation models. After optimizing the regression equations predicted by DOE, the obtained responses closely followed those achieved from simulations of the numerical models. The impacts of individual parameters on the model's overall goodness of fit were reflected by conducting Monte Carlo simulations within the narrowed intervals based on the DOE optimized parameters, and the combination of parameters was further updated as better responses were found. For verification, a good level of fit between the simulated and observed data from flow cell experiments was presented.

The application of the HSDP method can also be potentially extended to different subsurface models, in which parameter uncertainties and interactions need to be identified in a robust and efficient way. More complicated spatial and temporal simulation domains, such as variation of temperature, different recharging schedules, and heterogeneous soil profiles, can be involved to investigate the generality of the HSDP method in future studies.

CHAPTER 5: SIMULATION OF BIOSURFACTANT ENHANCED AQUIFER REMEDIATION PROCESSES

5.1 Background

Aquifer contamination from petroleum hydrocarbons spills has been causing widespread concerns. It often leads to severe and long-term impacts on the environment and threatens human health (Langwaldt and Puhakka, 2000; Wang et al., 2012; Pasha et al., 2014). In order to control the risk of subsurface hydrocarbon contamination and mitigate its negative consequences, it is crucial to develop and deploy effective in-situ remediation technologies.

Many countermeasures have been well studied and able to meet the remediation requirements under different circumstances, such as bioremediation, pump-and-treat, and soil flushing (Huang et al., 2006a; Atteia et al., 2013; Yadav et al., 2014). Especially during the recent decade, surfactant enhanced aquifer remediation (SEAR) as a promising approach has gained increasing attention (Childs et al., 2006; Paria, 2008; Zhao et al., 2014). By forming the oil-swollen micelles, surfactant enhances the mobility and solubility of hydrophobic non-aqueous phase liquid (NAPL), which can thus significantly promote the physical removal rate and accelerate the biodegradation of hydrocarbons (Qin et al., 2007; Peng et al., 2011; Zheng et al., 2012; Li et al., 2015b). Compared to chemical synthetized surfactants, biosurfactants produced by microorganisms are more favorably considered in environmental applications due to its biodegradability, low toxicity, and competitive effectiveness (Mulligan, 2005; Zhang et al., 2011; Liu et al., 2014).

Previous studies mainly involved lab scale column experiments to evaluate the performance of biosurfactant, whereas larger scale experiments based on multidimensional reactors were rarely conducted (Gudiña et al., 2012; Joshi and Desai, 2013; Bolobajev et al., 2015). Additionally, most of the researches of biosurfactant focused on rhamnolipid, which is a type of well-studied biosurfactant at the current stage. Studies for other types of biosurfactant such as surfactin, however, were limited.

On the other hand, for numerical simulation of SEAR processes, a simulator named UTCHEM has been the dominant option. Its complex kinetic equations describing non-equilibrium flow and mass transfer processes due to the presence of surfactant, however, make it a heavy computational burden to specifically identify all the surfactant properties or to introduce stochastic parameters for sensitivity/uncertainty analysis and model calibration (He et al., 2008; Luo and Lu, 2014). It is particularly true considering the types of biosurfactants and their application methods may vary from case to case, which can bring significant inconvenience to practical applications. Despite that existing simulators designated for BSEAR are rare; it is common to find substitutive models that are capable of simulating the fate of subsurface NAPL contaminants when surfactant is not presented. As an example, BioF&T 3D has been a mature simulator developed by Katyal (1997a) to solve multiphase and multicomponent biodegradation, flow, and transport in porous media. Its input parameters are much simplified compared to UTCHEM, and it has been widely used in multiple previous studies (Suk et al., 2000; Lee et al., 2001; Liu et al., 2004; Qin et al., 2008b; Kumar, 2012). Therefore, it is highly desired to study the possibility of developing a surrogate model for UTCHEM, so that the simulation of SEAR processes can be more efficiently, robustly, and flexibly conducted in practices.

To help fill the knowledge gap, this chapter focuses on advancing BioF&T 3D and enabling it to simulate BSAER processes. The objective is to be realized by conducting parallel flow cell experiments and employing the hybrid Stochastic – DOE aided parameterization (HSDP) method to provide a combination of calibrated parameters for BioF&T 3D. The method was demonstrated in Chapter 4 with proven efficiency and effectiveness in modeling a soil washing process without the addition of surfactant. A type of lab synthetized surfactin crude biosufactant solution is selected and deployed in soil flushing processes for its performance assessed.

5.2 Methodology

5.2.1 Materials and Experimental Setups

In order to provide experimental data for model parameterization, calibration and verification, the same integrated physical and numerical modeling approach as described in Chapter 3 was deployed in this study. The sketch of flow cell experiments involving biosurfactant was illustrated in Figure 5.1. Details of flow cell setups, soil loading processes, aqueous samples collecting as well as analyzing methods were also provided in Chapter 3.

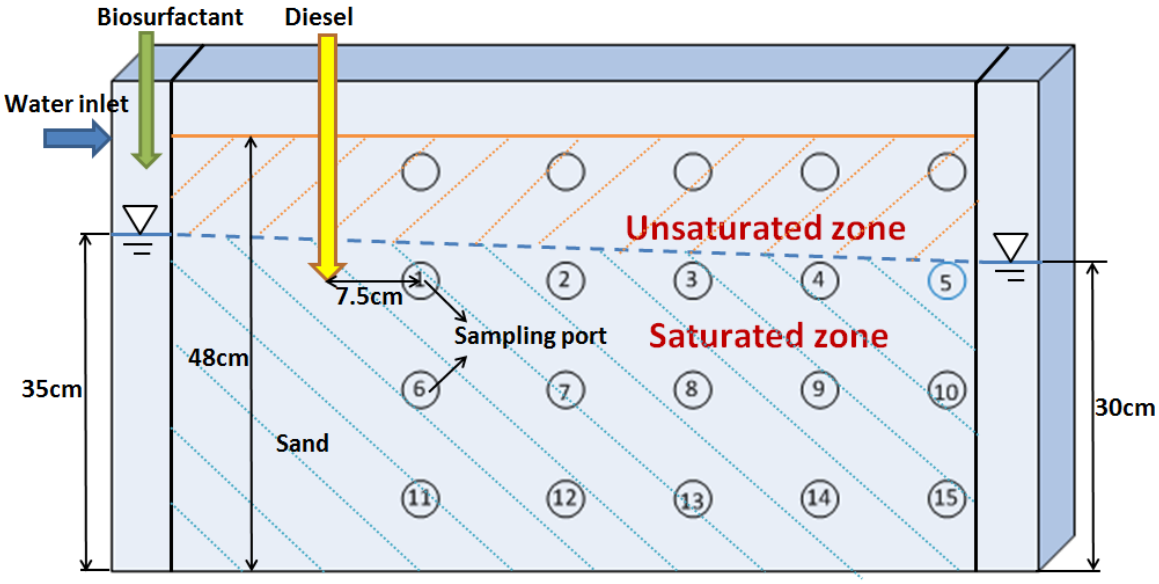

Figure 5.1 Flow cell experiments with biosurfactant injection

Two experiments were conducted in parallel using identical flow cells: unit 1 was for soil flushing without introducing biosurfactant (NOBS Scenario), whereas unit 2 was for biosurfactant enhanced soil flushing (BS Scenario). Clear diesel fuel was injected at one time to the same depth as but 7.5 cm left to the sampling port #1 to mimic a NAPL leakage in both of the flow cells, and BTEX within the aqueous phase was the compounds to be analyzed.

The introduced crude biosurfactant was surfactin generated by *Bacillus* subtilis and synthetized by the NRPOP Lab. According to the study of Zhang (2015), the CMC of the same type of surfactin was determined as 0.01% and the suggested concentration for PCB removal using soil washing was 0.5%. The amount of 45 ml water and surfactin at the inlet were injected in Unit 1 and 2, respectively. The water flow rate was kept at 12 ml/min for both flow cells, which could sustain a biosurfactant concentration level approximating to 0.5% during the first 12 hours after the diesel was injected. Aqueous samples were collected from the sampling ports #1, #2, #3, #5, and #6, and analyzed at a 12 hours interval during the first two days, after which 24 hours interval was applied until 120 hours after the initial diesel injection.

5.2.2 Parameterization

The HSDP method was modified and used in this study to advance BioF&T 3D in simulating biosurfactant enhanced soil flushing, and further to investigate the sensitivities and potential interactions between relevant parameters.

Generally, the HSDP method was performed by: 1) building the DOE models based on screened parameters and defined responses, which could reflect the goodness of fit between observed and simulated data; 2) identifying the significances and interactions of parameters; 3) optimizing the DOE predicted responses; 4) introducing stochastic data within reduced intervals

based on the optimized parameters; 5) running Monte Carlo simulation to find the optimal responses with the corresponding combinations of parameters.

Detailed steps of the HSDP method, as well as its demonstration in a case study based on the similar setups of flow cell experiments for the NOBS scenario, can be found in Chapter 4.

5.3 Result and Discussion

5.3.1 Flow cell experiment

Table 5.1 shows the concentration of BTEX monitored with both of the flow cell units from multiple sampling ports including the effluents during a 120-hour period. The BTEX concentration in effluents from both flow cell units was plotted in Figure 5.2. In this study, the abundance of BTEX in diesel was determined as 76 ppm, 768 ppm, 815 ppm, and 3380 ppm for benzene, toluene, ethylbenzene, and xylene, respectively.

Table 5.1 Monitored BTEX concentration from parallel flow cell experiments

	Sampling Ports	12hours		24hours		36hours		48hours		72hours		96hours		120hours	
		BS	NO BS	BS	NO BS	BS	NO BS	BS	NO BS	BS	NO BS	BS	NO BS	BS	NO BS
Benzene	#1	17	10	12	12	8	14	-	14	-	4	-	-	-	-
	#2	9	6	8	8	7	9	-	9	-	5	-	4	-	-
	#3	7	4	7	8	7	10	5	8	-	8	-	6	-	5
	#6	-	-	-	-	5	4	6	4	-	4	-	-	-	-
	Effluent #5	25	8	11	12	4	8	-	7	-	3	-	-	-	-
Toluene	#1	146	96	116	122	100	124	69	113	10	76	10	24	8	21
	#2	120	60	102	94	81	103	67	94	28	61	16	26	14	7
	#3	45	26	57	51	56	55	56	47	9	44	-	28	-	7
	#6	7	-	12	17	13	21	18	24	16	17	10	9	-	-
	Effluent #5	74	35	64	43	22	23	26	15	13	10	9	10	7	8
Ethyl	#1	151	104	128	115	64	129	46	112	15	22	-	13	-	10
benzene	#2	100	37	64	69	56	80	61	78	32	26	-	12	-	11
	#3	45	25	52	40	68	44	34	59	13	32	8	23	7	16
	#6	8	-	10	8	15	10	20	12	-	18	-	9	-	9
	Effluent #5	60	18	41	21	16	18	18	10	6	9	6	7	-	-
Xylene	#1	656	418	383	534	346	436	145	400	123	196	137	104	98	109
	#2	277	227	295	279	332	300	273	326	107	191	79	54	73	41
	#3	193	53	215	148	203	212	168	249	41	217	25	88	20	55
	#6	15	8	31	13	41	32	66	54	75	93	74	116	58	84
	Effluent #5	147	12	76	38	26	94	30	45	30	40	28	33	16	33

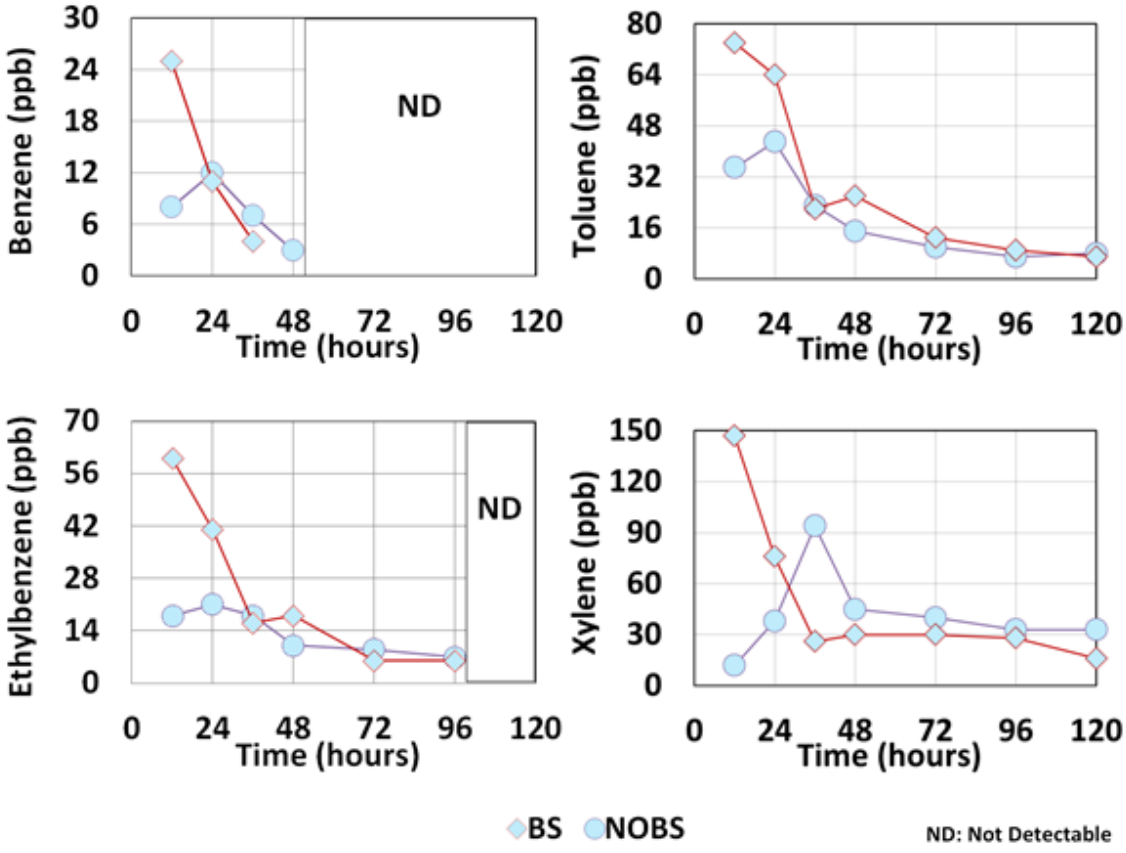

Figure 5.2 Analyzed BTEX concentrations in the effluents

As can be observed, the concentration of BTEX in the effluent peaked after 12 hours of diesel injection for the BS scenario, whereas the concentration peaks were retarded for the NOBS scenario. This phenomenon indicated that the targeted contaminants tend to migrate along with the water flow in a quicker manner after the introducing of the biosurfactant. It suggested that the biosurfactant could lead to the enhanced dissolution of BTEX and increased mobility of diesel. Additionally, it was also noticed that the distinctions between BS and NOBS scenarios regarding the BTEX concentration in the effluent were predominate during the first 12 hours after the diesel injection, which should be highlighted in the parameterization processes.

5.3.2 Parameterization

According to Chapter 4, in which HSDP method was applied and demonstrated in case study of parameterizing the NOBS scenario, porosity, distribution coefficient (AKD), and Henry's constant (GAMA) were identified as significant factors in the simulation model. Therefore, they were defined in this study as well. Additionally, it was also found that the ratio of targeted contaminants loaded into the subsurface system during the first 12 hours to the quantity loaded within the entire duration (120 hours) would affect the time when the concentration peak appears at each location in the simulation domain. This factor can be adjusted by modifying the number of simulation time steps set for each concentration output interval. Therefore, the first 12 hours loading ratio (12LR) was also included in parameterizing BioF&T 3D for modeling biosurfactant enhanced soil flushing processes, whereas it was kept constant as 0.35 for modeling the processes without the addition of biosurfactant.

The response selected for the DOE model was Root Mean Square Deviation (RMSD) with the coefficient of determination (R^2) also calculated during the whole parameterization process. Traditional sensitivity analysis method One-factor-at-a-time (OFAT) was applied to screen the

parameters and identify their corresponding ranges as inputs of the DOE model. The upper bounds and lower bounds of porosity, AKD, and GAMA were determined based on Chapter 4. The ranges of 12LR were upgraded by exceeding the original value of 0.35, given that a higher loading speed could normally be anticipated from the addition of biosurfactant. The lower bound and upper bound of each screened parameter were summarized in Table 5.2.

Table 5.2 Screened parameters and their ranges for the DOE models

Parameters	Unit		Lower bound	Upper bound
A: 12LR	-	BTEX	0.40	0.75
B: porosity	-	BTEX	0.30	0.38
C: distribution coefficient (AKD)	-	Benzene:	1.50	3.50
		Toluene:	2.00	3.20
		Ethyl benzene:	2.40	4.00
		Xylene:	2.40	4.00
D: Henry's constant (GAMA)	-	Benzene:	0.20	0.30
		Toluene:	0.20	0.40
		Ethyl benzene:	0.20	0.40
		Xylene:	0.15	0.33

For each compound of BTEX, 30 groups of simulations including six center points were conducted by running the simulation model with different combinations of parameters A to D. To model the possible curvatures generated by the selected parameters and response, the central composite design (CCD) with Design Expert 7.1® was applied. The Analysis of Variance (ANOVA) results is summarized in Table 5.3.

The results indicated that interactions of factors C (distribution coefficient) and D (Henry's constant), A^2 (quadratic term of the first 12 hours loading ratio), and C^2 (quadratic term of distribution coefficient) were significant model terms in general with the p-values much lower or close to 0.05. Also, the interaction of factors A and C was involved specifically in modeling ethylbenzene. Even though for different species, some of the p-values for the individual factors A, C, or D were much higher than 0.05, these factors were also included in predicting the responses for the DOE models. Factor B (porosity), however, was not considered as a significant factor and excluded by the CCD models in this case. The interactions of factors C and D for all the four species of BTEX, as well as interaction of factors A and C for ethylbenzene were plotted using CCD and illustrated in Figures 5.3, 5.4, 5.5, 5.6, and 5.7. Obvious curvatures were observed within all the 3D graphs, which suggested pronounced interacting effects between the involved factors. Taking the interaction of factors C and D as an example, a lower level of factor D would contribute to the decrease of the RMSD when factor C was at its lower level. However, decreasing the value of factor D when factor C was at its higher level would lead to the rising of the RMSD instead. These interaction effects also indicated that assuming distribution coefficient of BTEX increases, which was reasonable considering the enhanced dissolution effects from biosurfactant, the Volatile Organic Compounds (VOCs) tended to stay in the aqueous phase (as

reflected by the increasing of Henry's constant). The interaction of 12LR and distribution coefficient for ethylbenzene, however, was complicated as the response was not in a monotonic relationship with the parameters in their corresponding ranges. The 3D graphs also provided a general idea of where the optimal responses were located under different factor settings, which was identified by the lowest points on the plotted surfaces.

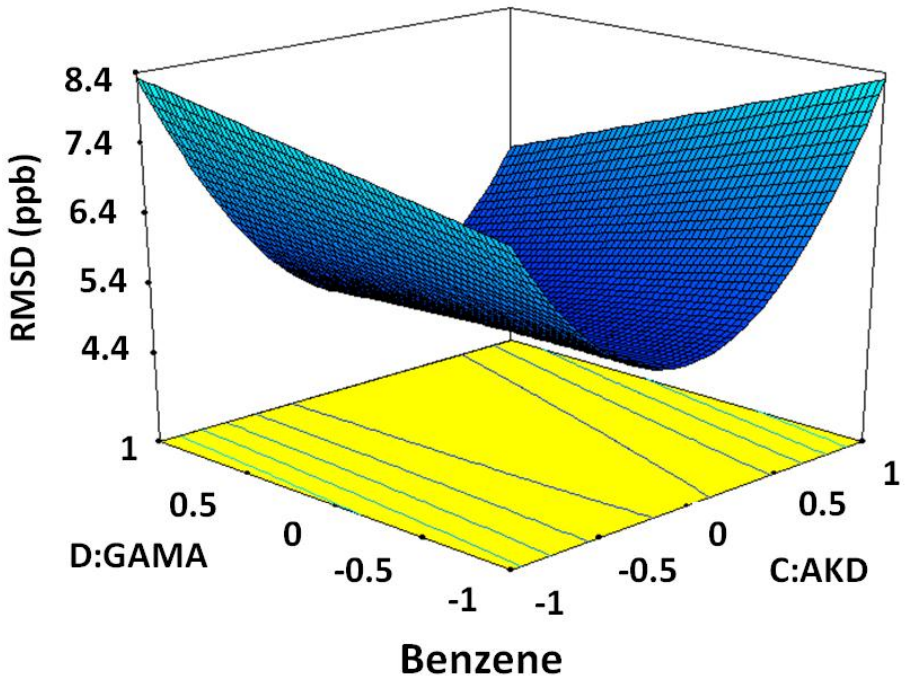

Figure 5.3 3D surface graph of factors C and D interactions for benzene

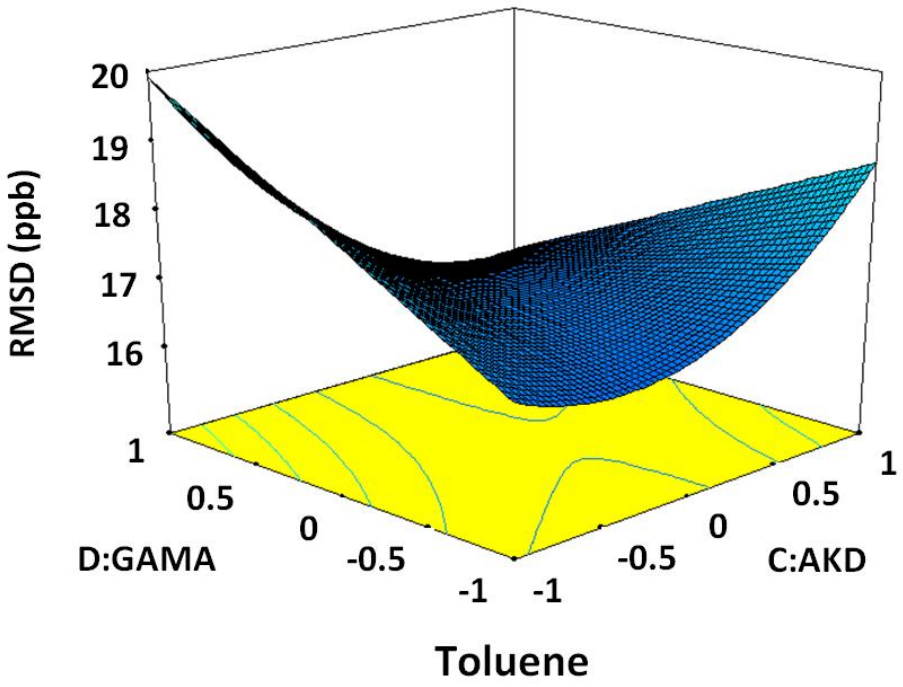

Figure 5.4 3D surface graph of factors C and D interactions for toluene

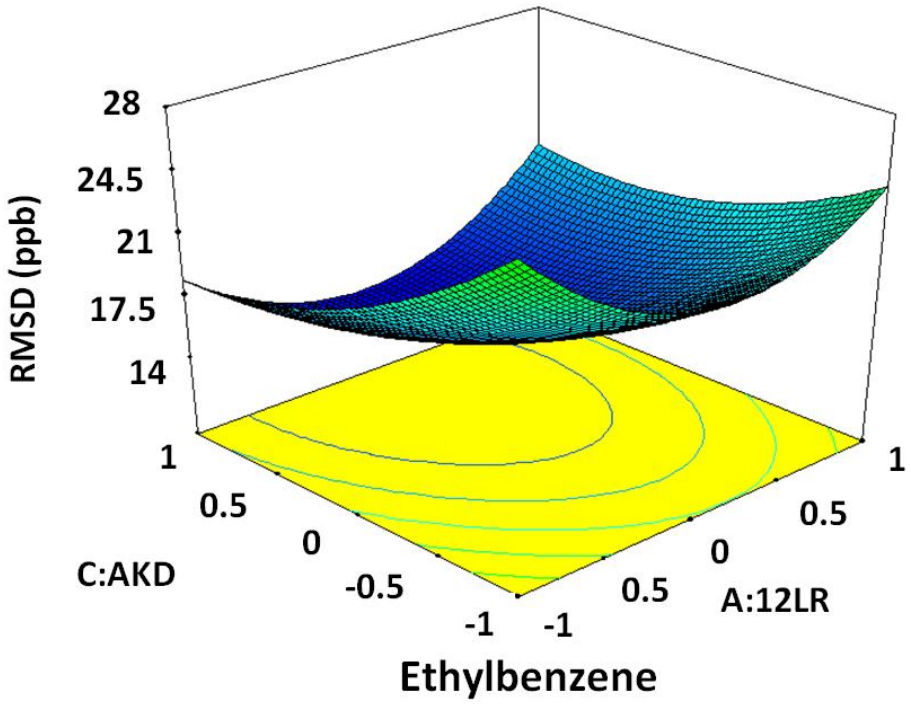

Figure 5.5 3D surface graph of factors A and C interactions for ethylbenzene

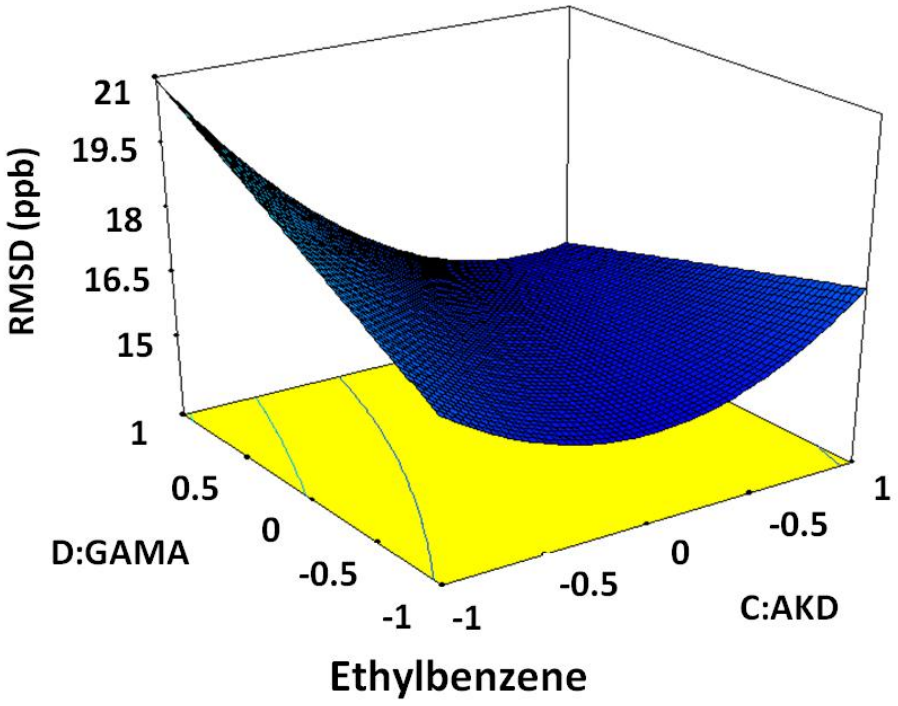

Figure 5.6 3D surface graph of factors C and D interactions for ethylbenzene

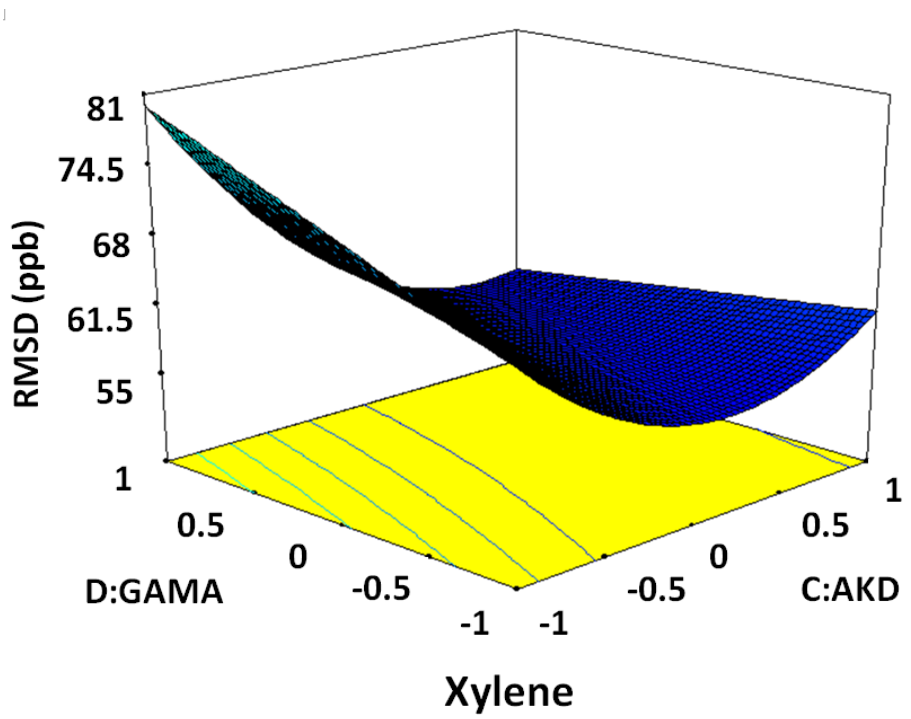

Figure 5.7 3D surface graph of factors C and D interactions for xylene

The predicted regression equation for RMSD in terms of coded factors was also given by CCD as follows:

$$RMSD_b = 30.60 - 59.85A - 9.92C + 33.45D - 15.47CD + 54.13A^2 + 2.70C^2 \quad (5.1)$$

$$RMSD_t = 54.68 - 137.57A - 10.33C + 68.06D - 25.64CD + 138.71A^2 + 3.30C^2 \quad (5.2)$$

$$RMSD_e = 98.57 - 204.16A - 20.75C + 75.25D + 7.99AC - 21.70CD + 153.10A^2 + 3.25C^2 \quad (5.3)$$

$$RMSD_x = 333.22 - 646.72A - 70.29C + 240.13D - 66.65CD + 578.83A^2 + 12.10C^2 \quad (5.4)$$

As objectives, the RMSD predictions were then minimized by using nonlinear optimization. An optimization software package Lingo®, was applied in this process. The optimized parameters were then put back to the simulation model to achieve actual responses and R^2 values. The comparisons of predicted and actual responses after optimization were summarized in Table 5.3, and acceptable matches between the CCD predicted responses and the actual ones achieved by taking the suggested sets of parameters in the simulation models.

Table 5.3 ANOVA results of central composite design

Source	Sum of squares (b/t/e/x)*	df (b/t/e/x)	Mean square (b/t/e/x)	F value (b/t/e/x)	p-value (Prob>F) (b/t/e/x)
Model	277.88/927.06 /830.56/11869.58	6/6/7/6	46.31/154.51 /118.65/1978.26	13.77/13.71 24.51/24.92	<0.0001/<0.0001 / <0.0001/<0.0001
A-12LR	4.21/354.26 /4.64/263.65	1/1/1/1	4.21/354.26 /4.64/263.65	1.25/31.44 0.96/3.32	0.2748/< 0.0001 /0.3381/0.0814
C-AKD	1.81/6.38 /54.32/1198.36	1/1/1/1	1.81/6.38 /54.32/1198.36	0.54/0.57 11.22/15.10	0.4704/0.4595 /0.0029/0.0007
D-GAMA	1.63/0.46 /8.13/140.14	1/1/1/1	1.63/0.46 /8.13/140.14	0.49/0.041 1.68/1.77	0.4931/0.8420 /0.2085/0.1970
CD	9.57/37.88 /48.20/368.45	1/1/1/1	9.57/37.88 /48.20/368.45	2.84/3.36/9.96/4.64	0.0052/0.0797 /0.0046/0.0419
AC	-/-/20.03/-	-/-/1/-	-/-/20.03/-	-/-/4.14/-	-/-/0.0542/-
A^2	78.16/513.32 /625.35/8938.32	1/1/1/1	78.16/513.32 /625.35/8938.32	23.24/45.56/129.17/112.60	<0.0001/<0.0001 /<0.0001/< 0.0001
C^2	207.59/40.16 /122.91/1706.30	1/1/1/1	207.59/40.16 /122.91/1706.30	61.73/3.56/25.39/21.50	<0.0001/0.0717 /<0.0001/0.0001
Residual	77.35/259.15 /106.51/1825.74	23/23/22/23	3.36/11.27 /4.84/79.38		
Cor Total	355.23/1186.21 /937.07/13695.32	29/29/29/29			

*(b/t/e/x) denotes benzene, toluene, ethylbenzene, and xylene.

Table 5.4 Summary of predicted and actual responses after optimization of the DOE models

	Optimized parameters			Predicted	Actual	
	A: 12LR	C: AKD	D: GAMA	Response RMSD (ppb)	Response RMSD (ppb)	R^2
Benzene	0.55	2.70	0.30	4.46	5.25	0.71
Toluene	0.50	2.34	0.20	16.08	12.31	0.91
Ethylbenzene	0.57	3.83	0.40	14.44	14.32	0.86
Xylene	0.56	4.00	0.40	54.43	53.56	0.86

Despite that the RMSD values obtained by DOE parameterization were reasonably low with well acceptable R^2 values; it was not sufficiently evident to assume these results as the best calibration sets for the simulation models given that only 30 groups of parameter combinations were examined by CCD. In order to further improve the parameterization results, stochastic values were introduced based on the reduced ranges of parameters optimized by CCD. Consequently, the impact from uncertain parameters on response distributions could be quantified, and the risk of ignoring parameter combinations for better responses could also be reduced.

Uniform distribution was applied to generate 60 groups of data for each of the three selected parameters, which were factors A, C, and D. Their updated intervals were generated by centralizing the optimized parameters and expanding with ±20% of their initial intervals. Monte Carlo simulations running the simulation models based on the 60 stochastic parameter combinations were conducted. The relationships between selected parameters and responses distributions were shown in Figures 5.8, 5.9, and 5.10.

It was noticed that only parts of the results (12LR on toluene, ethylbenzene, and xylene, AKD on benzene) showed clear trends of responses distributions due to the changes of individual parameters, whereas the others were randomly scattered. This phenomenon further manifested that interaction effects between parameters could hardly be revealed by simply using the traditional uncertainty and sensitivity analysis methods based on iterations. At the same time, multiple points were found lower than the previously RMSD values obtained by the DOE aided parameterization processes, leading to the improved calibration results. The final calibration

results were summarized in Table 5.5, including the comparison of the results achieved without introducing stochastic parameters by Monte Carlo simulations.

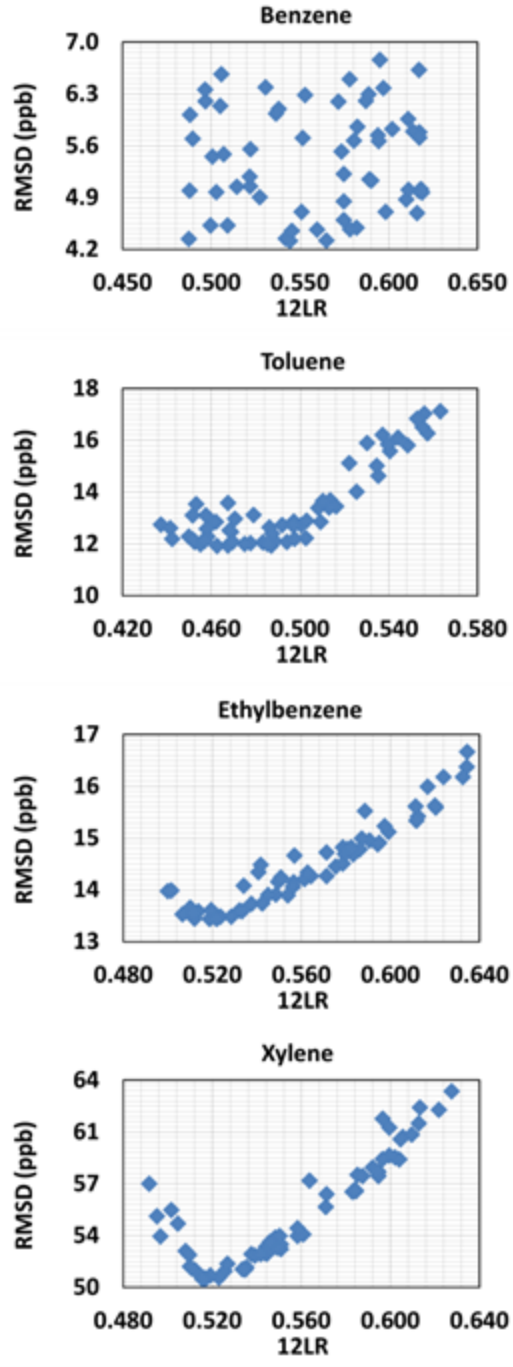

Figure 5.8 Effects of 12LR uncertainties on RMSD

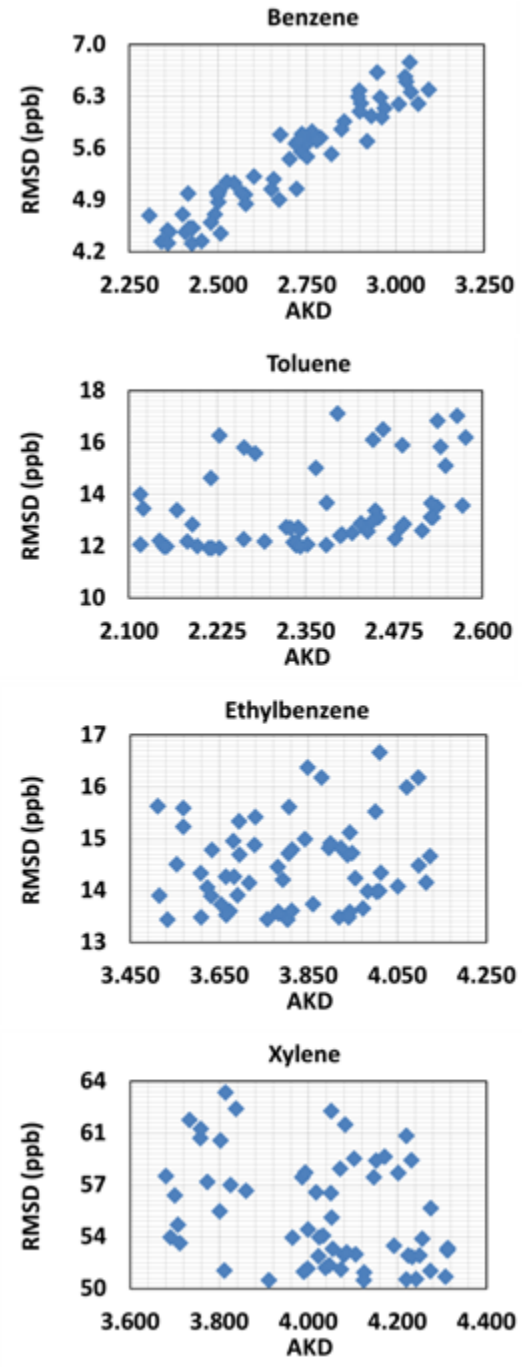

Figure 5.9 Effects of AKD uncertainties on RMSD

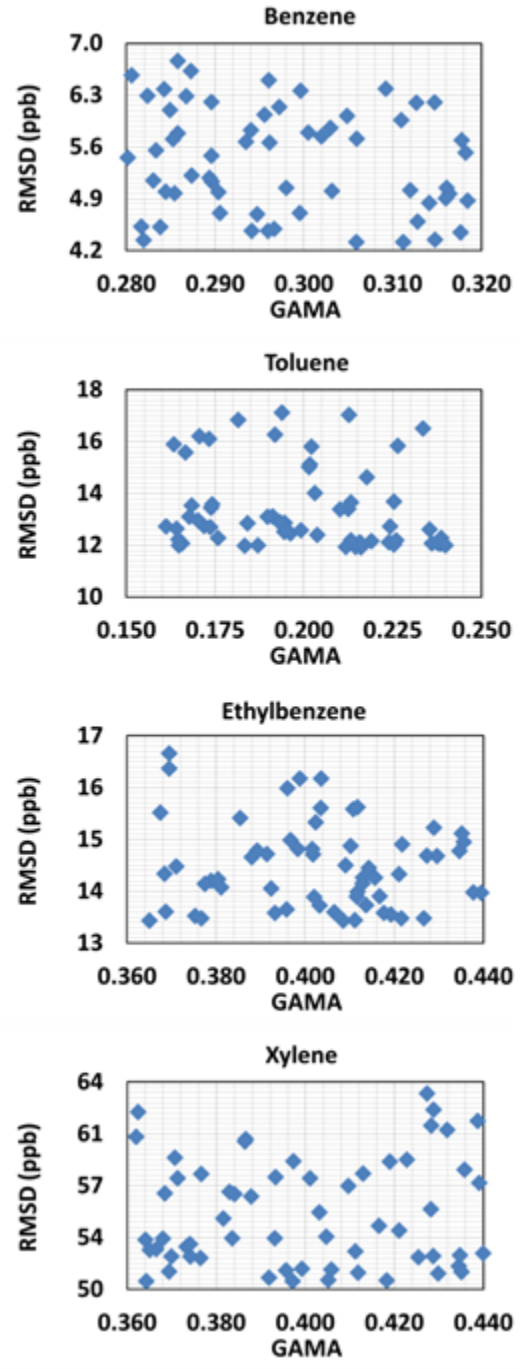

Figure 5.10 Effects of GAMA uncertainties on RMSD

Table 5.5 Summary of the final parameterization results without / with Monte Carlo simulations

	Selected parameters			Calibrated results	
	A: 12LR	C: AKD	D: GAMA	RMSD (ppb)	R^2
Benzene	0.55/0.544	2.70/2.426	0.30/0.311	5.25/4.31	0.71/0.80
Toluene	0.50/0.463	2.34/2.217	0.20/0.216	12.31/11.92	0.91/0.92
Ethylbenzene	0.57/0.522	3.83/3.534	0.40/0.365	14.32/13.43	0.86/0.88
Xylene	0.56/0.517	4.00/3.912	0.40/0.364	53.56/50.57	0.86/0.87

Table 5.6 and Table 5.7 summarized the goodness of fit between simulated data and observed ones in both temporal and spatial scales. It was found that the concentrations of BTEX were more accurately modeled at earlier time stages and at sampling ports which were closer to the diesel spilling location, especially for the first time stage (e.g. 0.94 for Ethylbenzene) and sampling port #1 (e.g. 0.98 for Toluene). However, the goodness of fit was not satisfactory for later time stages and sampling ports remoter from the spilling location. One explanation could be that simulation was conducted under the assumption of homogenous soil profile, which was not possible to be realized during the loading of sand in this flow cell experiment. Especially in the vertical directions, stratifications were observed. On the other hand, the lack-of-fit effects for the relatively lower concentrations from later sampling stages and distant sampling ports were more dominant than higher concentration levels, and slight deviations might lead to the decreasing R^2 value. However, the overall R^2 values were to a large extent controlled by higher concentration levels, which makes the calculations of goodness of fit from latter sampling stages and remoter sampling ports less significant.

Table 5.6 R^2 values of all the sampling ports at different time stages

	12h	24h	36h	48h
Benzene	0.84	0.59	0.30	-
Toluene	0.91	0.89	0.83	0.85
Ethylbenzene	0.94	0.76	0.73	0.33
Xylene	0.92	0.93	0.85	0.62

Table 5.7 R^2 values during the entire sampling period from different sampling ports

	#1	#2	#3
Benzene	0.68	0.65	0.57
Toluene	0.98	0.88	0.33
Ethylbenzene	0.88	0.57	0.70
Xylene	0.84	0.87	0.69

5.3.3 Comparison of BS and NOBS processes

The comparisons of BS and NOBS were conducted mainly from two aspects. Firstly, the values of parameters from both scenarios were compared after the parameterizations as summarized in Table 5.8. For the BS scenario, factors A, C, and D were optimized while factor B was kept constant as deterministic parameter according to the ANOVA results from CCD. For the NOBS scenario, factor A was kept constant whereas the other three factors were optimized based on factorial design.

Secondly, taking each individual parameter into consideration, a higher factor A (12 LR) suggested that compared to the NOBS scenario, a larger proportion of NAPL contaminants were loaded into the simulation system during the first 12 hours for the BS scenario. This variation of parameter also indicated an enhancement of dissolution effects of the NAPL contaminants from the addition of biosurfactant. For B (porosity), C (distribution coefficient), as well as D (Henry's constant), the regularity of variation was not found.

After parameterization, simulated and observed BTEX concentrations for BS and NOBS scenarios from each sampling port were presented in Figures 5.11, 5.12, 5.13, and 5.14. For the BS scenario, earlier concentration peaks were observed from sampling ports #1 and #2 compared to the NOBS scenario, which further confirmed the enhanced dissolution effects from the applied crude biosurfactant even though at a low concentration. However, the trends were not obvious for sampling ports #3 and #6. Not many observed data were available for benzene due to its relatively low abundance in diesel, which led to the challenges for analyzing low concentration samples below the detection limits of the applied analyzing methods.

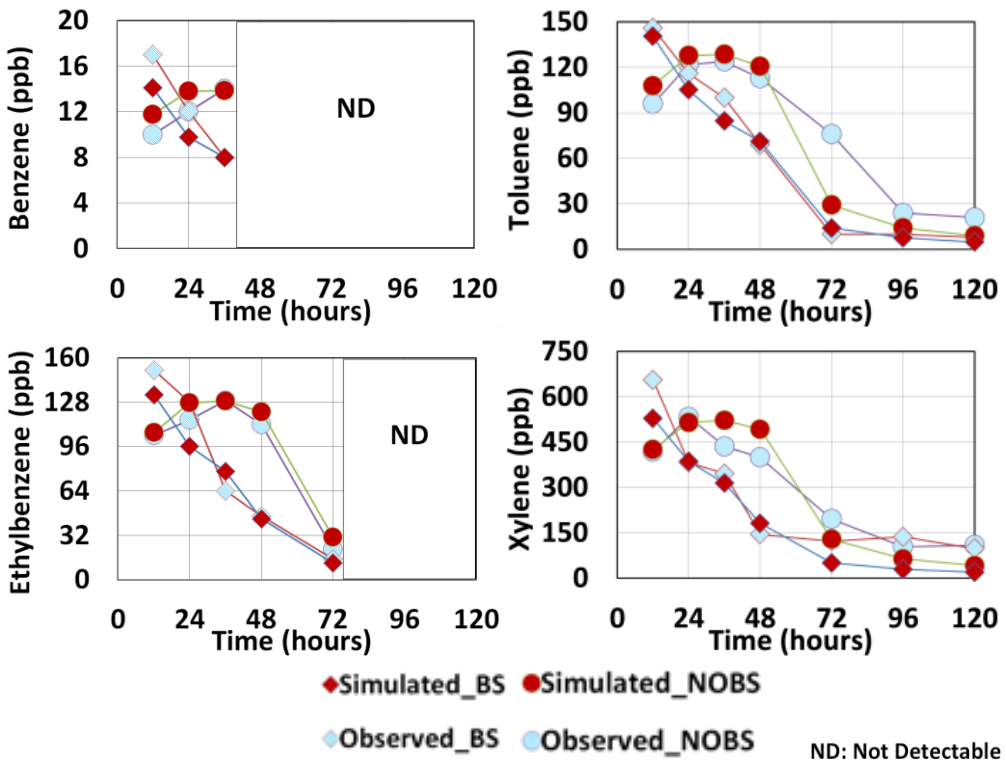

Figure 5.11 Effects comparison of BS and NOBS after the parameterization at sampling port #1

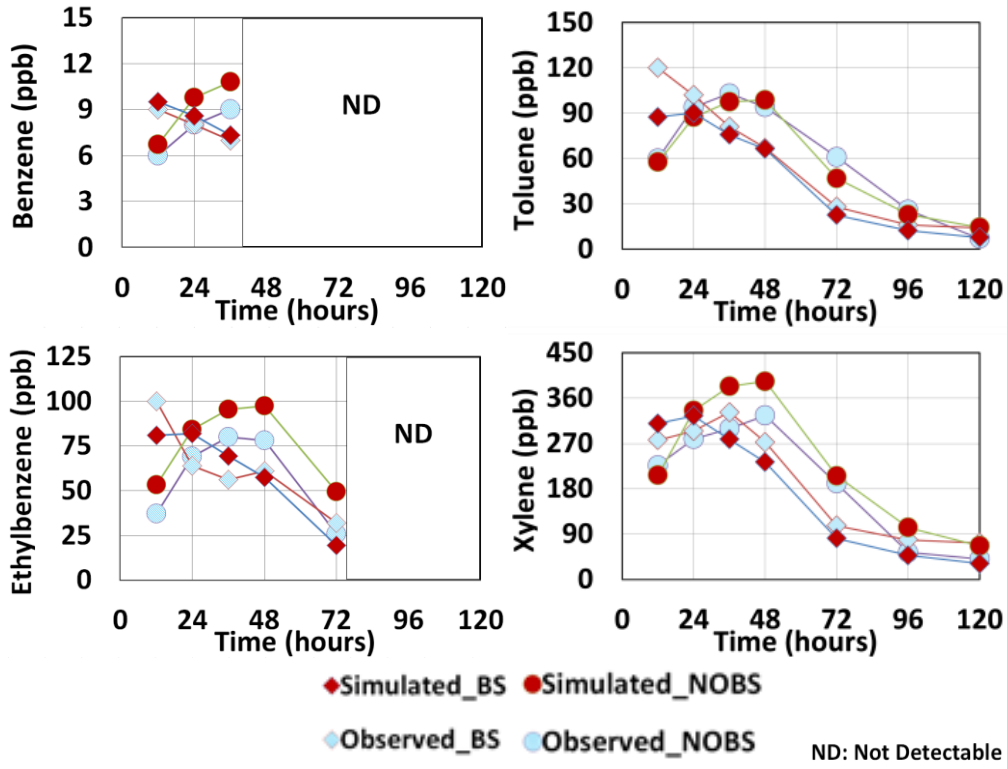

Figure 5.12 Effects comparison of BS and NOBS after the parameterization at sampling port #2

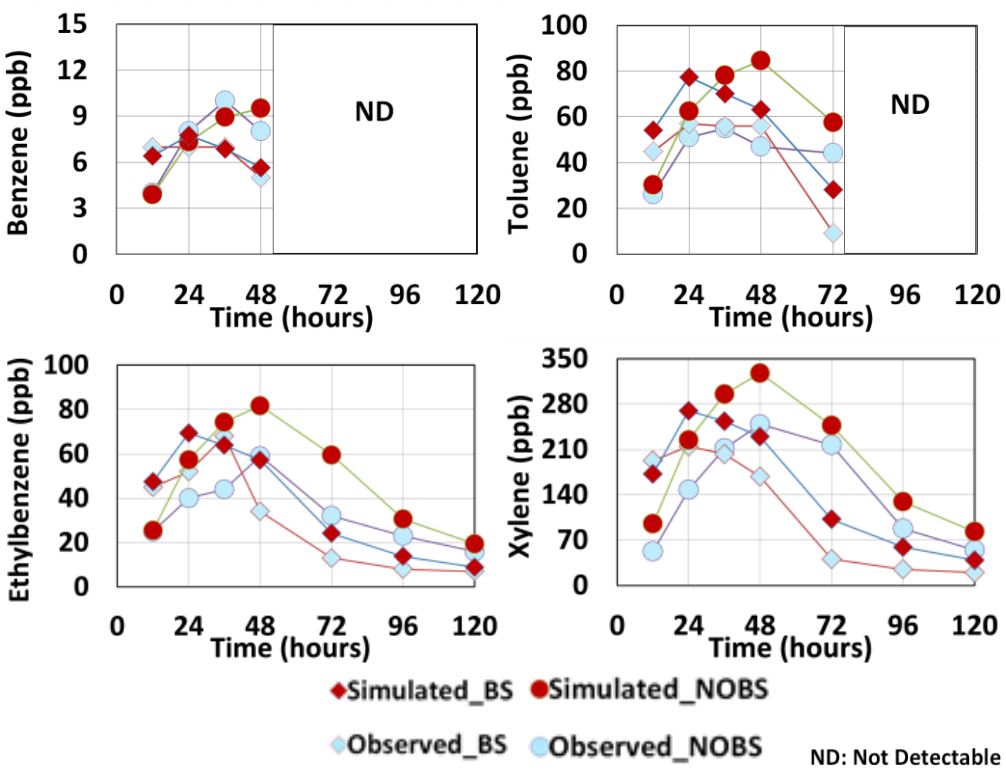

Figure 5.13 Effects comparison of BS and NOBS after the parameterization at sampling port #3

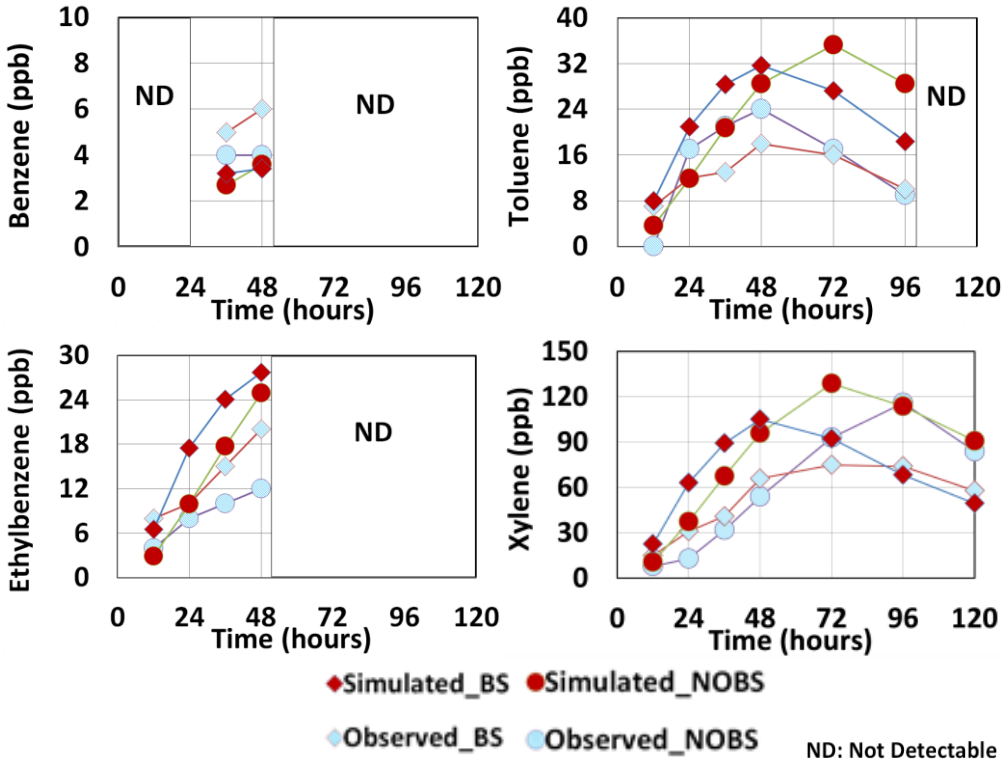

Figure 5.14 Effects comparison of BS and NOBS after the parameterization at sampling port #6

Table 5.8 Comparisons of parameters values for BS / NOBS processes after the final parameterization

	A: 12LR	B: Porosity	C: AKD	D: GAMA
Benzene	0.544/0.350	0.380/0.394	2.426/2.179	0.311/0.230
Toluene	0.463/0.350	0.380/0.378	2.217/2.774	0.216/0.257
Ethylbenzene	0.522/0.350	0.380/0.376	3.534/3.145	0.365/0.268
Xylene	0.517/0.350	0.380/0.389	3.912/3.260	0.364/0.196

5.3.4 Verification

The verification of the simulation model was undertaken by changing the volume of the diesel introduced into the system from 15 ml to 20 ml, while keeping the same quantity of crude biosurfactant injection as 45 ml. The water flow rate was maintained 12 ml/min. Hence, it was assumed the equivalent biosurfactant concentration is identical to the one used for parameterization processes. The comparisons of simulated and observed BTEX concentrations from each sampling port were presented in Figures 5.15, 5.16, 5.17, and 5.18. The results demonstrated an overall satisfactory level of fit, with the overall R^2 value reaches 0.76, 0.81, 0.83, and 0.81 for benzene, toluene, ethylbenzene, and xylene, respectively.

Simulation results at different time stages in the form of BTEX concentrations contours at the X-Z plane are shown in Figures 5.19, 5.20, 5.21, and 5.22. The migrations of contaminates over time were found reasonably close to practice during the first 36 hours after the diesel injection. As appeared in the concentration contours for the following periods, the majority of remaining BTEX was observed migrate to the downstream. The boundary effects might be the cause of higher concentrations accumulated at the downstream boundaries of the simulation domain. Also, the concentration levels adjacent to the source of spill after 36 hours might not be reflect the practical situation. It was due to the limited number of BioF&T 3D transport schedules, which were mostly taken to describe the earlier time stages with higher concentration levels. However, the behaviors of contaminants transportation were not sufficiently revealed after the first 36 hours, which could lead to the deficits of concentration at the source of spill.

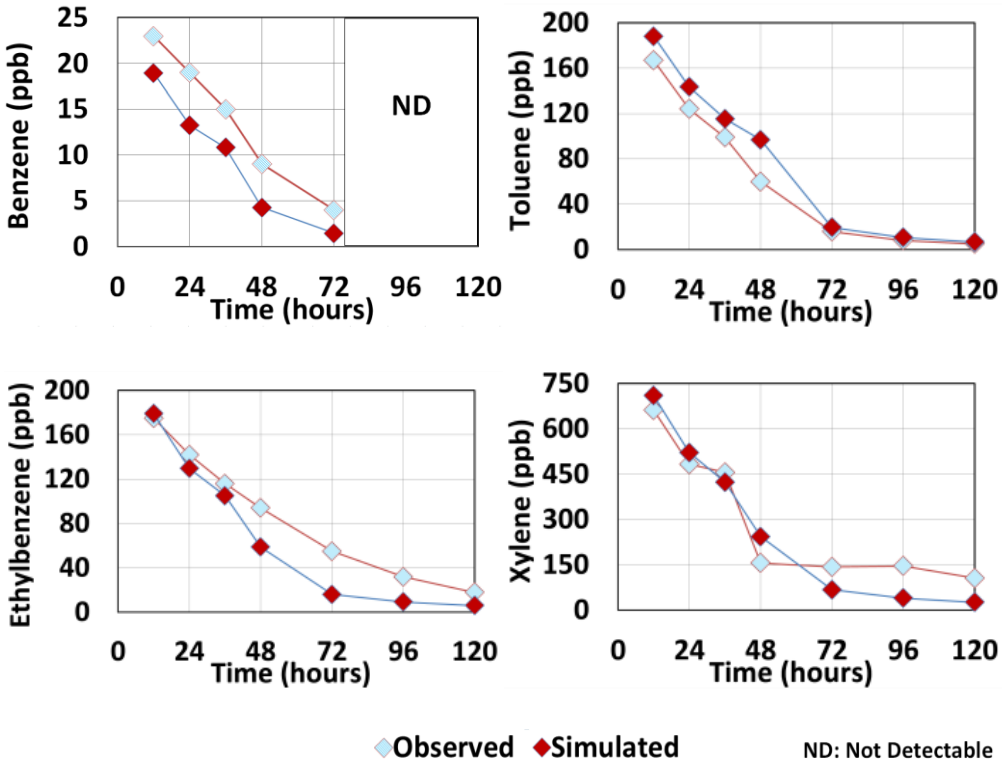

Figure 5.15 BTEX verification results for sampling port #1

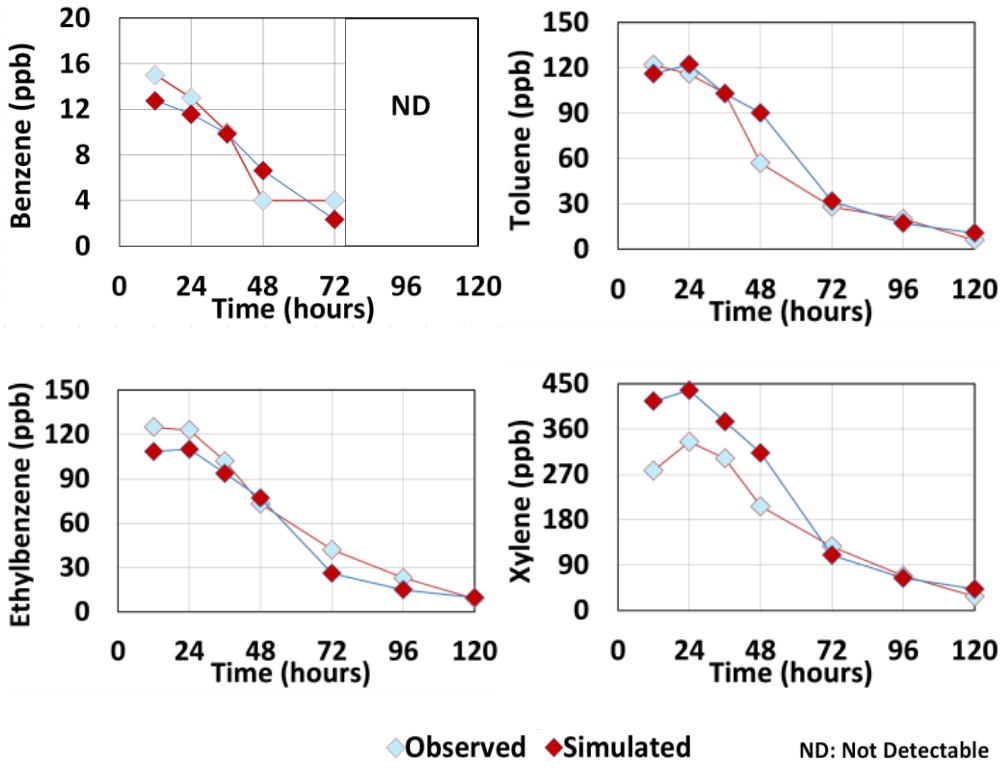

Figure 5.16 BTEX verification results for sampling port #2

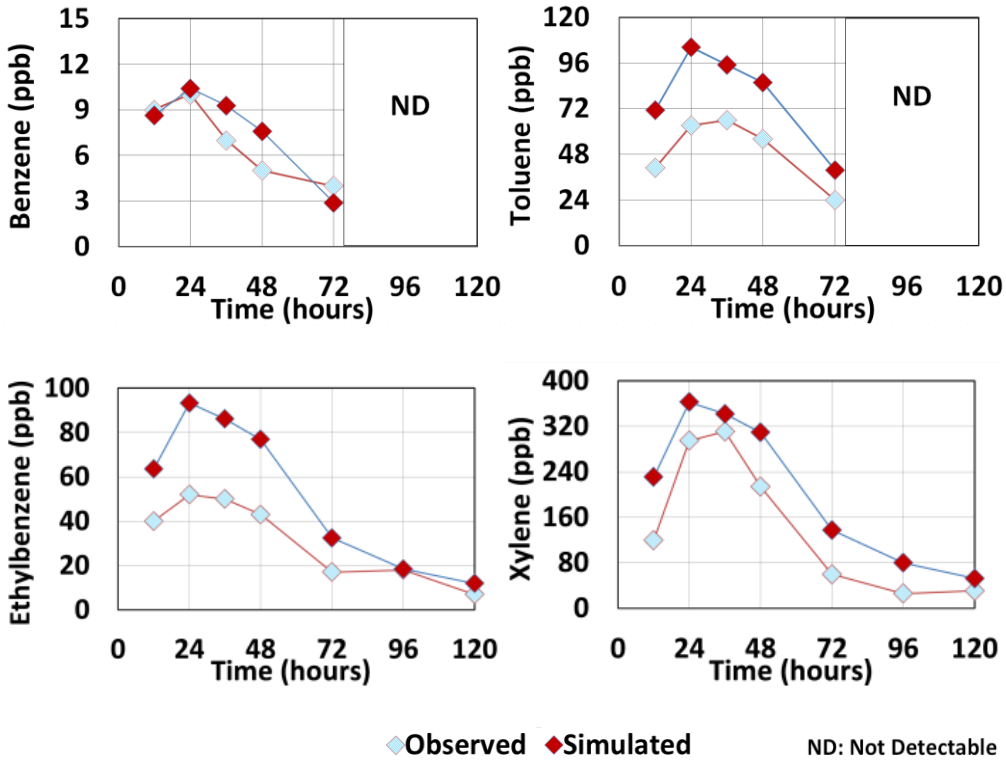

Figure 5.17 BTEX verification results for sampling port #3

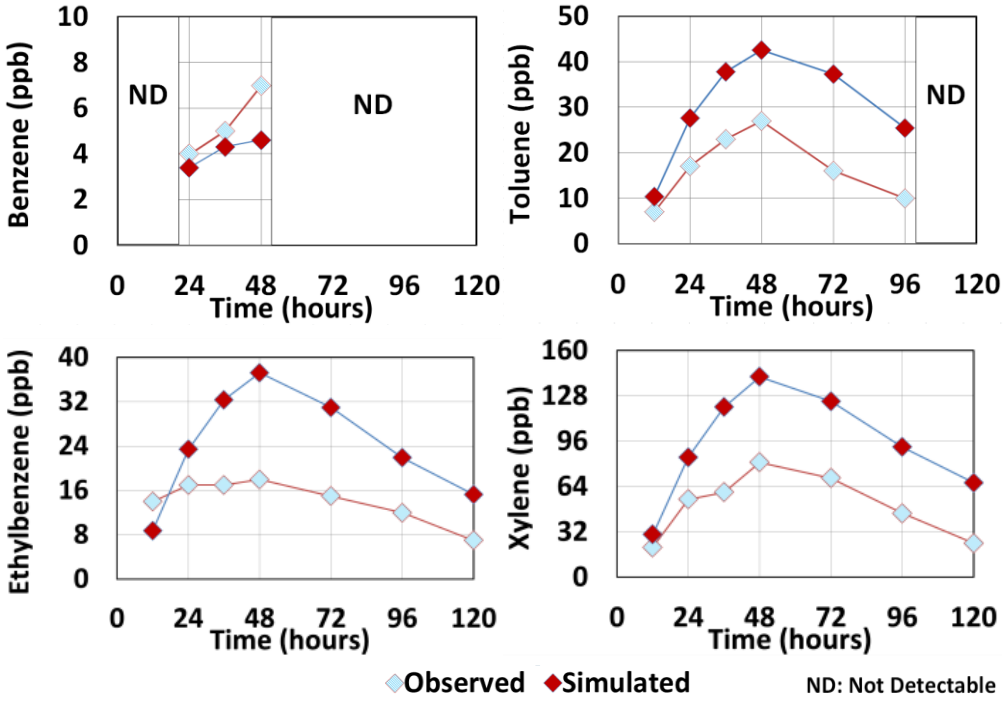

Figure 5.18 BTEX verification results for sampling port #6

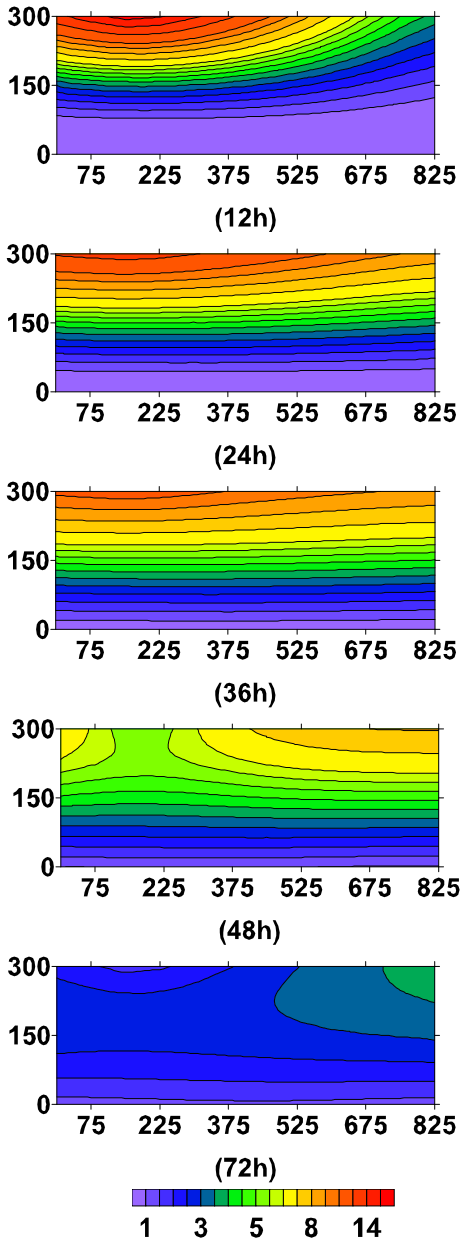

Figure 5.19 Simulated benzene concentration (in ppb) contours at the X-Z plane (in cm) at different time stages after initial diesel injection

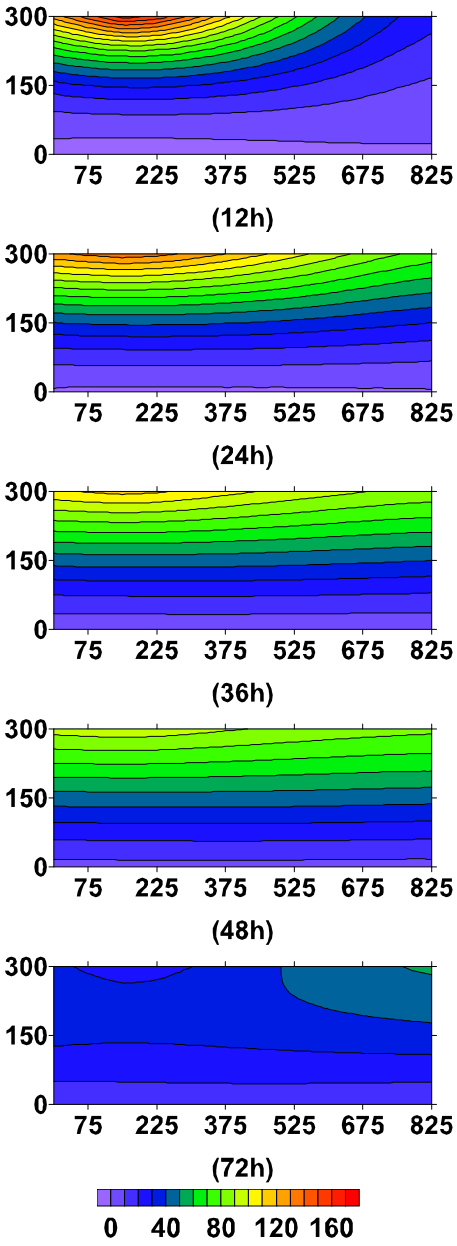

Figure 5.20 Simulated toluene concentration (in ppb) contours at the X-Z plane (in cm) at different time stages after initial diesel injection

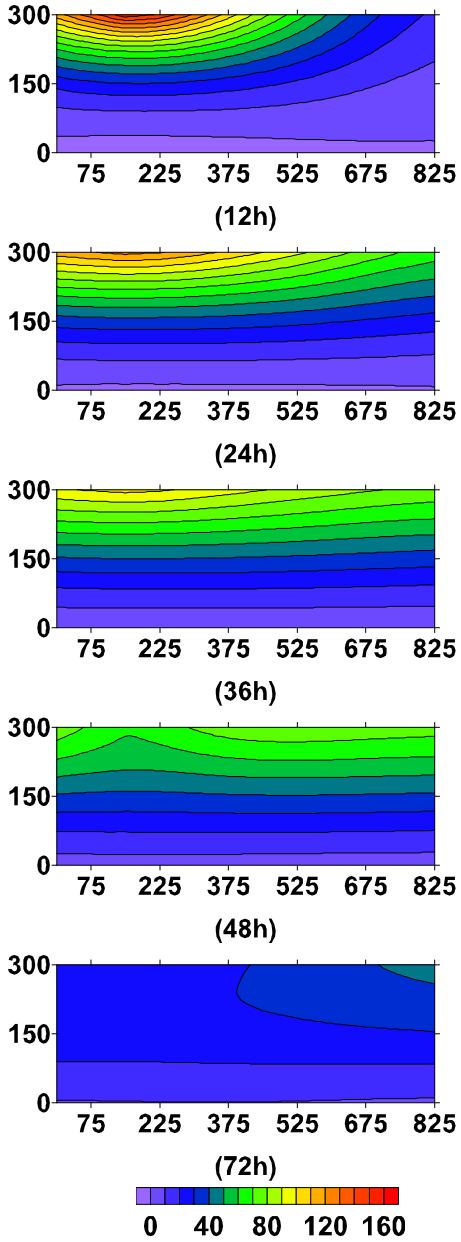

Figure 5.21 Simulated ethylbenzene concentration (in ppb) contours at the X-Z plane (in cm) at different time stages after initial diesel injection

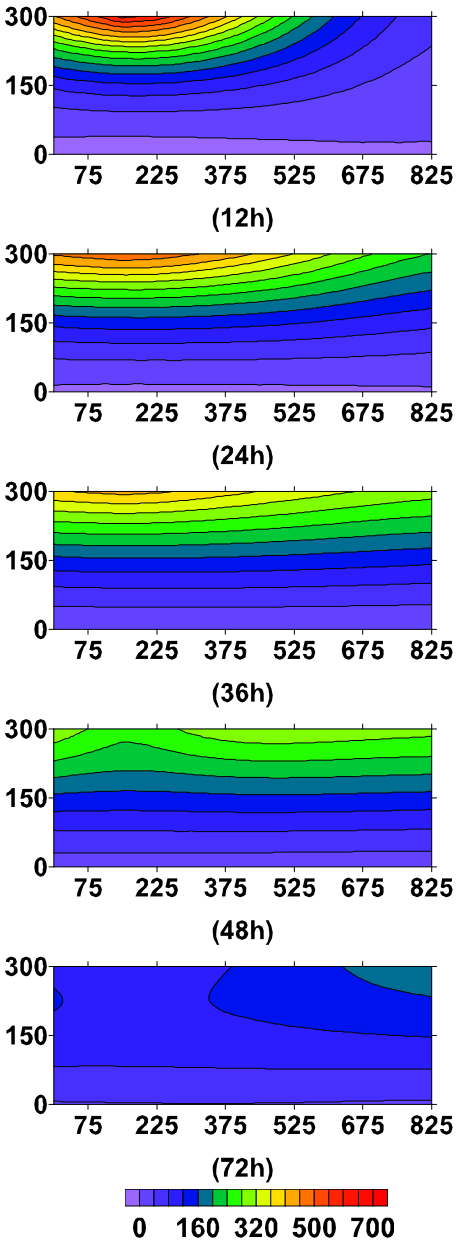

Figure 5.22 Simulated xylene concentration (in ppb) contours at the X-Z plane (in cm) at different time stages after initial diesel injection

5.4 Summary

In this study, parallel flow cell experiments were conducted to investigate the performance of lab synthetized surfactin solution in enhancing aquifer remediation processes. BioF&T 3D was advanced to simulate BSEAR processes based on data collection from flow cell experiments using the HSDP method.

Based on the parameterization results, three parameters namely the first 12 hours loading ratio, distribution coefficient, and Henry's constant were examined by the DOE model with their interactions revealed. The overall goodness-of-fit represented as R^2 values for both calibration and verification were satisfactory after the parameterization. In the meantime, through the comparisons between BS and NOBS processes, it can also be concluded that mobility and solubility of contaminants were enhanced by introducing the studied surfactin biosurfactant. These effects could also be reflected in the modification of parameters, especially for the increase of 12LR.

This study initiated the attempts to advance simpler surrogate simulators such as BioF&T 3D in modeling BSEAR processes. Compared to UTCHEM, which is predominately used to simulate SEAR processes, the solution proposed in this study exhibits the advantages of simplicity and robustness. Especially for applications in practices, explicitly defining specific surfactant related parameters, which might vary from case to case, is a critical challenge. As a consequence of this study, the computational demand can be considerably lowered for sensitivity and uncertainty analysis of the corresponding parameters, thus to more efficiently facilitate practical operations.

In future studies, continuously injection of biosurfcant solution with constant concentration is recommended, providing that the quantity requirements of biosurfactant can be satisfied.

CHAPTER 6: CONCLUSIONS AND RECOMMENDATIONS

6.1 Summary

Targeting subsurface hydrocarbon contamination and biosurfactant enhanced aquifer remediation (BSEAR) processes, this dissertation research has focused on developing a new parameterization method, and applying it to examine modeling uncertainties and improve simulation performances. A brief summary of this research is as follows:

1) An integrated physical and numerical modeling approach for subsurface simulations has been established by coupling flow cell experiments with a commercial multidimensional and multicomponent simulator BioF&T 3D.

2) Based on the proposed modeling approach, a new hybrid stochastic-design of experiment aided parametrization (HSDP) method has been developed. The HSDP method is able to quantify the significance of modeling parameters and reveal their interactions, as well as to assess the influence from parameter uncertainties. Also, the application of the HSDP method has been demonstrated through a case study, which involves the simulation of soil flushing processes. After parameterization, the influences from parameter uncertainties on the overall goodness of fit have been efficiently evaluated based on the optimized parameters from the design of experiment (DOE) models. It has also led to a satisfactory overall goodness of fit between simulated and observed concentrations of contaminants species according to the verification results (R^2 = 0.76, 0.87, 0.82, and 0.90 for benzene, toluene, ethylbenzene, and xylene, respectively).

3) The HSDP method has been further used to advance BioF&T 3D in simulating BSEAR processes. Parallel flow cell experiments have been conducted to investigate the performance of

a type of lab synthetized surfactin in enhancing aquifer remediation processes. Based on the parameterization results, three parameters namely the first 12 hours loading ratio (12LR), distribution coefficient, and Henry's constant were examined by the DOE model with their interactions revealed. The overall goodness of fit for verification was satisfactory after the parameterization (R^2 = 0.76, 0.81, 0.83, and 0.81 for benzene, toluene, ethylbenzene, and xylene, respectively). In the meantime, through the comparisons between biosurfactant enhanced soil flushing (BS) and soil flushing without introducing biosurfactant (NOBS) scenarios, it can also be concluded that mobility and solubility of contaminants were enhanced by introducing the surfactin solution. These effects could also be reflected in the adjustments of parameters, especially for the increase of 12LR (from 0.350 to 0.544, 0.462, 0.522, and 0.517 for benzene, toluene, ethylbenzene, and xylene, respectively).

6.2 Research Achievements

A new HSDP method has been developed and demonstrated within an integrated physical and numerical modeling approach. The HSDP method is capable of not only identifying the significance of individual parameters, but also revealing their interactions. Meanwhile, the influence from stochastic parameters were reflected and further contributed to an improved calibration results for the numerical model. The efficiency and effectiveness in achieving high goodness of fit between simulated and experimental observed data have also been proven. In addition to subsurface simulations, the application of the HSDP method can also be potentially extended to different types of numerical models, such as hydrology models, hydrodynamic models, and water quality models, to identify parameter uncertainties and interactions in a robust and efficient way.

This research has also initiated the attempts to advance simpler numerical models in modeling complicated BSEAR processes. By employing the HSDP method, physical meanings of the adjustments of parameters were well explained and were in accord with the observed data from the flow cell experiments. Compared to UTCHEM, which has predominately been used in existing studies, the solution proposed in this study exhibited the advantages of simplicity and robustness. Especially for applications in practices, explicitly defining specific surfactant related parameters, which might vary from case to case, can be a critical challenge. As a consequence of this study, the computational demand can be considerably lowered for sensitivity and uncertainty analysis of the corresponding parameters, thus to more efficiently facilitate practical operations.

Based on this dissertation research, two journal papers have been generated:

1. **Li, Z.,** Chen, B., Wu, H., and Ye, X. (2016). A hybrid stochastic - design of experiment aided parameterization method for modeling aquifer NAPL contaminations.
2. **Li, Z.,** Chen, B., Wu, H., Zhang, H., Ye, X., and Zhang, K. (2016). A parameterization study for modeling biosurfactant enhanced aquifer remediation processes based on flow cell experiments.

6.3 Recommendations for Future Research

Further studies of the BSEAR processes and applications of the HSDP method involving pilot-scale or field-scale simulations are recommended to be conducted. An existing pilot-scale soil reactor is ready to use in the Northern Region Persistent Organic Pollution Control (NRPOP) Lab. Based on this soil reactor, research plans have already been made targeting a real

contaminated site in Labrador, Canada. Soil loading is ongoing at the current stage. Different types of biosurfactants are also planned to be applied in the future studies.

Further effort can also be put on integrating numerical simulations of different aquifer remediation processes with optimizations to support decision makings in practice, particularly under more complicated spatial and temporal conditions such as the variation of temperature, different recharging schedules, and heterogeneous soil profiles.

Furthermore, the generalization of the HSDP method for parameterizing numerical models in different fields can also be conducted in future studies.

REFERENCES

Abriola, L. M., Dekker, T. J., and Pennell, K. D. (1993). Surfactant-enhanced solubilization of residual dodecane in soil columns. 2. Mathematical modeling. *Environmental Science & Technology, 27*(12), 2341-2351.

Abriola, L. M., Drummond, C. D., Hahn, E. J., Hayes, K. F., Kibbey, T. C., Lemke, L. D., . . . Rathfelder, K. M. (2005). Pilot-scale demonstration of surfactant-enhanced PCE solubilization at the Bachman road site. 1. Site characterization and test design. *Environmental Science & Technology, 39*(6), 1778-1790.

Adhikari, S. and Khodaparast, H. H. (2014). A spectral approach for fuzzy uncertainty propagation in finite element analysis. *Fuzzy Sets and Systems, 243*, 1-24.

Agah, A., Ardejani, F. D., and Ghoreishi, H. (2013). Two-dimensional numerical finite volume modeling of processes controlling distribution and natural attenuation of BTX in the saturated zone of a simulated semi-confined aquifer. *Arabian Journal of Geosciences, 6*(6), 1933-1944.

Akbari, A. and Ghoshal, S. (2014). Pilot-scale bioremediation of a petroleum hydrocarbon-contaminated clayey soil from a sub-Arctic site. *Journal of Hazardous Materials, 280*, 595-602.

Al-Mahallawi, K., Mania, J., Hani, A., and Shahrour, I. (2012). Using of neural networks for the prediction of nitrate groundwater contamination in rural and agricultural areas. *Environmental Earth Sciences, 65*(3), 917-928.

Al-Shalabi, E. W., Sepehrnoori, K., and Delshad, M. (2014). *Optimization of the Low Salinity Water Injection Process in Carbonate Reservoirs.* Paper presented at the International Petroleum Technology Conference.

Almasri, M. N. and Kaluarachchi, J. J. (2005). Modular neural networks to predict the nitrate distribution in ground water using the on-ground nitrogen loading and recharge data. *Environmental Modelling & Software, 20*(7), 851-871.

Alvarez, P. J. and Illman, W. A. (2005). *Bioremediation and natural attenuation: process fundamentals and mathematical models* (Vol. 27): John Wiley & Sons.

Ashraf, M. A., Sarfraz, M., Naureen, R., and Gharibreza, M. (2015). Remediation Approaches *Environmental Impacts of Metallic Elements* (pp. 315-358): Springer.

Atteia, O., Estrada, E. D. C., and Bertin, H. (2013). Soil flushing: a review of the origin of efficiency variability. *Reviews in Environmental Science and Bio/Technology, 12*(4), 379-389.

Bachmat, Y. and Bear, J. (1964). The general equations of hydrodynamic dispersion in homogeneous, isotropie, porous mediums. *Journal of Geophysical Research, 69*(12), 2561-2567.

Bai, G., Brusseau, M. L., and Miller, R. M. (1997). Biosurfactant-enhanced removal of residual hydrocarbon from soil. *Journal of Contaminant Hydrology, 25*(1), 157-170.

Banat, I., Thavasi, R., and Jayalakshmi, S. (2011). Biosurfactants from marine bacterial isolates.

Banat, I. M., Franzetti, A., Gandolfi, I., Bestetti, G., Martinotti, M. G., Fracchia, L., . . . Marchant, R. (2010). Microbial biosurfactants production, applications and future potential. *Applied Microbiology and Biotechnology, 87*(2), 427-444.

Bayer, D. M., Chagas-Spinelli, A. C., Gavazza, S., Florencio, L., and Kato, M. T. (2013). Natural Attenuation and Biosurfactant-Stimulated Bioremediation of Estuarine Sediments Contaminated with Diesel Oil. *Applied Biochemistry and Biotechnology, 171*(1), 173-188.

Bear, J. (1972). Dynamics of fluids in porous media. *Eisevier, New York, 764p*.

Bear, J. and Cheng, A.-D. (2010). *Modeling groundwater flow and contaminant transport* (Vol. 23): Springer Science & Business Media.

Bennett, N. D., Croke, B. F., Guariso, G., Guillaume, J. H., Hamilton, S. H., Jakeman, A. J., . . . Perrin, C. (2013). Characterising performance of environmental models. *Environmental Modelling & Software, 40*, 1-20.

Bezza, F. A. and Nkhalambayausi-Chirwa, E. M. (2015). Desorption kinetics of polycyclic aromatic hydrocarbons (PAHs) from contaminated soil and the effect of biosurfactant supplementation on the rapidly desorbing fractions. *Biotechnology & Biotechnological Equipment*(ahead-of-print), 1-9.

Bhandari, A., Surampalli, R. Y., Champagne, P., Ong, S. K., Tyagi, R., and Lo, I. M. (2007). Remediation Technologies for Soils and Groundwater Task Committee of the Environmental Council Environmental and Water Resources Institute (EWRI) of the American Society of Civil Engineers.

Bolobajev, J., Öncü, N. B., Viisimaa, M., Trapido, M., Balcıoğlu, I., and Goi, A. (2015). Column experiment on activation aids and biosurfactant application to the persulphate treatment of chlorophene-contaminated soil. *Environmental Technology, 36*(3), 348-357.

Borden, R. C., Daniel, R. A., LeBrun, L. E., and Davis, C. W. (1997). Intrinsic biodegradation of MTBE and BTEX in a gasoline-contaminated aquifer. *Water Resources Research, 33*(5), 1105-1115.

Borgonovo, E. and Plischke, E. (2015). Sensitivity analysis: a review of recent advances. *European Journal of Operational Research*.

Borsi, I. and Fasano, A. (2009). A general model for bioremediation processes of contaminated soils. *International Journal of Advances in Engineering Sciences and Applied Mathematics, 1*(1), 33-42.

Bouchard, D., Höhener, P., and Hunkeler, D. (2008). Carbon isotope fractionation during volatilization of petroleum hydrocarbons and diffusion across a porous medium: a column experiment. *Environmental science & technology, 42*(21), 7801-7806.

Braddock, J. F. and McCarthy, K. A. (1996). Hydrologic and microbiological factors affecting persistence and migration of petroleum hydrocarbons spilled in a continuous-permafrost region. *Environmental Science & Technology, 30*(8), 2626-2633.

Braeutigam, P., Wu, Z., Stark, A., and Ondruschka, B. (2009). Degradation of BTEX in aqueous solution by hydrodynamic cavitation. *Chemical Engineering & Technology, 32*(5), 745-753.

Bredehoeft, J. D. and Pinder, G. F. (1973). Mass transport in flowing groundwater. *Water Resources Research, 9*(1), 194-210.

Brown, C. L., Pope, G. A., Abriola, L. M., and Sepehrnoori, K. (1994). Simulation of surfactant-enhanced aquifer remediation. *Water Resources Research, 30*(11), 2959-2977.

Bu, P. X., AlSofi, A. M., Liu, J., Benedek, L., and Han, M. (2014). Simulation of single well tracer tests for surfactant–polymer flooding. *Journal of Petroleum Exploration and Production Technology*, 1-13.

Cai, Q., Zhang, B., Chen, B., Zhu, Z., Lin, W., and Cao, T. (2014). Screening of biosurfactant producers from petroleum hydrocarbon contaminated sources in cold marine environments. *Marine Pollution Bulletin, 86*(1), 402-410.

Camenzuli, D., Freidman, B. L., Statham, T. M., Mumford, K. A., and Gore, D. B. (2013). On-site and in situ remediation technologies applicable to metal-contaminated sites in Antarctica and the Arctic: a review. *Polar Research, 32*.

Campolongo, F. and Saltelli, A. (1997). Sensitivity analysis of an environmental model: an application of different analysis methods. *Reliability Engineering & System Safety, 57*(1), 49-69.

Cápiro, N. L., Da Silva, M. L., Stafford, B. P., Rixey, W. G., and Alvarez, P. J. (2008). Microbial community response to a release of neat ethanol onto residual hydrocarbons in a pilot-scale aquifer tank. *Environmental Microbiology, 10*(9), 2236-2244.

Carson, J. S. (2002). *Model verification and validation.* Paper presented at the Simulation Conference, 2002. Proceedings of the Winter.

Chang, J. S., Cha, D. K., Radosevich, M., and Jin, Y. (2015). Effects of biosurfactant-producing bacteria on biodegradation and transport of phenanthrene in subsurface soil. *Journal of Environmental Science and Health, Part A, 50*(6), 611-616.

Chatterjee, S. and Hadi, A. S. (2009). *Sensitivity analysis in linear regression* (Vol. 327): John Wiley & Sons.

Chen, Z., Huang, G., Chakma, A., and Li, J. (2002). Application of a GIS-based modeling system for effective management of petroleum-contaminated sites. *Environmental Engineering Science, 19*(5), 291-303.

Childs, J., Acosta, E., Annable, M. D., Brooks, M. C., Enfield, C. G., Harwell, J. H., . . . Sabatini, D. A. (2006). Field demonstration of surfactant-enhanced solubilization of DNAPL at Dover Air Force Base, Delaware. *Journal of Contaminant Hydrology, 82*(1), 1-22.

Chiou, C. T., Schmedding, D. W., and Manes, M. (1982). Partitioning of organic compounds in octanol-water systems. *Environmental Science & Technology*, *16*(1), 4-10.

Chokejaroenrat, C., Kananizadeh, N., Sakulthaew, C., Comfort, S., and Li, Y. (2013). Improving the sweeping efficiency of permanganate into low permeable zones to treat TCE: experimental results and model development. *Environmental Science & Technology, 47*(22), 13031-13038.

Christensen, S. and Cooley, R. L. (1999). Evaluation of prediction intervals for expressing uncertainties in groundwater flow model predictions. *Water Resources Research, 35*(9), 2627-2639.

Christofi, N. and Ivshina, I. (2002). Microbial surfactants and their use in field studies of soil remediation. *Journal of Applied Microbiology, 93*(6), 915-929.

Clement, T., Sun, Y., Hooker, B., and Petersen, J. (1998). Modeling multispecies reactive transport in ground water. *Groundwater Monitoring & Remediation, 18*(2), 79-92.

Clement, T. P., Johnson, C. D., Sun, Y., Klecka, G. M., and Bartlett, C. (2000). Natural attenuation of chlorinated ethene compounds: model development and field-scale application at the Dover site. *Journal of Contaminant Hydrology, 42*(2), 113-140.

Cooper, H. H. (1966). The equation of groundwater flow in fixed and deforming coordinates. *Journal of Geophysical Research, 71*(20), 4785-4790.

MDH Engineered Solutions Corporation (2005). Evaluation of Computer Models for Predicting The Fate and Transport of Hydrocarbons in Soil and Groundwater. Edmonton, Alberta.

Crawford, J. (1999). Geochemical Modelling–A Review of Current Capabilities and Future Directions.

Czitrom, V. (1999). One-factor-at-a-time versus designed experiments. *The American Statistician, 53*(2), 126-131.

da Rosa, C. F., Freire, D. M., and Ferraz, H. C. (2015). Biosurfactant microfoam: Application in the removal of pollutants from soil. *Journal of Environmental Chemical Engineering, 3*(1), 89-94.

Dagan, G. (1979). The generalization of Darcy's law for nonuniform flows. *Water Resources Research, 15*(1), 1-7.

Daliakopoulos, I. N., Coulibaly, P., and Tsanis, I. K. (2005). Groundwater level forecasting using artificial neural networks. *Journal of Hydrology, 309*(1), 229-240.

Damasceno, F., Freire, D., and Cammarota, M. (2014). Assessing a mixture of biosurfactant and enzyme pools in the anaerobic biological treatment of wastewater with a high-fat content. *Environmental Technology, 35*(16), 2035-2045.

De Biase, C., Loechel, S., Putzmann, T., Bittens, M., Weiss, H., and Daus, B. (2014). Volatile organic compounds effective diffusion coefficients and fluxes estimation through two types of construction material. *Indoor Air, 24*(3), 272-282.

Delshad, M., Pope, G., and Sepehrnoori, K. (1996). A compositional simulator for modeling surfactant enhanced aquifer remediation, 1 formulation. *Journal of Contaminant Hydrology, 23*(4), 303-327.

Demissie, Y. K., Valocchi, A. J., Minsker, B. S., and Bailey, B. A. (2009). Integrating a calibrated groundwater flow model with error-correcting data-driven models to improve predictions. *Journal of Hydrology, 364*(3), 257-271.

Dhail, S. and Jasuja, N. D. (2012). Isolation of biosurfactant-producing marine bacteria. *African Journal of Environmental Science and Technology, 6*(6), 263-266.

Di Julio, S. and Shallenberger, W. (2002). Bioslurping- horizontal radial flow- theory and experimental validation. *Journal of Hazardous Substance Research, 3*(6), 6_1.

Doherty, J. (2003). Ground water model calibration using pilot points and regularization. *Groundwater, 41*(2), 170-177.

Duan, Q., Sorooshian, S., and Gupta, V. (1992). Effective and efficient global optimization for conceptual rainfall-runoff models. *Water Resources Research, 28*(4), 1015-1031.

Eom, I. (2011). Estimation of Partition Coefficients of Benzene, Toluene, Ethylbenzene, and p-Xylene by Consecutive Extraction with Solid Phase Microextraction. *Bulletin of the Korean Chemical Society, 32*(5), 1463-1464.

Estrada, E. D. C., Bertin, H., and Atteia, O. (2015). Experimental Study of Foam Flow in Sand Columns: Surfactant Choice and Resistance Factor Measurement. *Transport in Porous Media, 108*(2), 335-354.

Falciglia, P. and Vagliasindi, F. (2015). Remediation of hydrocarbon polluted soils using 2.45 GHz frequency-heating: Influence of operating power and soil texture on soil temperature profiles and contaminant removal kinetics. *Journal of Geochemical Exploration, 151*, 66-73.

Farajzadeh, R., Matsuura, T., van Batenburg, D., and Dijk, H. (2012). Detailed modeling of the alkali/surfactant/polymer (ASP) process by coupling a multipurpose reservoir simulator to the chemistry package PHREEQC. *SPE Reservoir Evaluation & Engineering, 15*(04), 423-435.

Franzetti, A., Di Gennaro, P., Bevilacqua, A., Papacchini, M., and Bestetti, G. (2006). Environmental features of two commercial surfactants widely used in soil remediation. *Chemosphere, 62*(9), 1474-1480.

Gan, Y., Duan, Q., Gong, W., Tong, C., Sun, Y., Chu, W., . . . Di, Z. (2014). A comprehensive evaluation of various sensitivity analysis methods: A case study with a hydrological model. *Environmental Modelling & Software, 51*, 269-285.

Garson, D. G. (1991). Interpreting neural network connection weights.

Gerhard, J. I., Kueper, B. H., and Sleep, B. E. (2014). Modeling Source Zone Remediation *Chlorinated Solvent Source Zone Remediation* (pp. 113-144): Springer.

Gillespie, I. M. and Philp, J. C. (2013). Bioremediation, an environmental remediation technology for the bioeconomy. *Trends in Biotechnology, 31*(6), 329-332.

Gomes, H. I., Dias-Ferreira, C., and Ribeiro, A. B. (2013). Overview of in situ and ex situ remediation technologies for PCB-contaminated soils and sediments and obstacles for full-scale application. *Science of The Total Environment, 445*, 237-260.

Gomez, D. E., de Blanc, P. C., Rixey, W. G., Bedient, P. B., and Alvarez, P. J. (2008). Modeling benzene plume elongation mechanisms exerted by ethanol using RT3D with a general substrate interaction module. *Water Resources Research, 44*(5).

Gorelick, S. M. (1990). Large scale nonlinear deterministic and stochastic optimization: Formulations involving simulation of subsurface contamination. *Mathematical Programming, 48*(1-3), 19-39.

Gu, Y., Fu, R., Li, H., and An, H. (2015). A new two-dimensional experimental apparatus for electrochemical remediation processes. *Chinese Journal of Chemical Engineering*.

Gudiña, E. J., Pereira, J., Rodrigues, L., Coutinho, J., Teixeira, J., and Soares, L. P. (2012). *Biosurfactant producing microorganisms and its application to enhanced oil recovery at lab scale*. Paper presented at the SPE EOR Conference at Oil and Gas West Asia, Muscat, Oman.

Guo, P., Chen, W., Li, Y., Chen, T., Li, L., and Wang, G. (2014). Selection of surfactant in remediation of DDT-contaminated soil by comparison of surfactant effectiveness. *Environmental Science and Pollution Research, 21*(2), 1370-1379.

Gupta, H. V., Sorooshian, S., and Yapo, P. O. (1999). Status of automatic calibration for hydrologic models: Comparison with multilevel expert calibration. *Journal of Hydrologic Engineering, 4*(2), 135-143.

Hamby, D. (1994). A review of techniques for parameter sensitivity analysis of environmental models. *Environmental Monitoring and Assessment, 32*(2), 135-154.

Hanss, M. and Turrin, S. (2010). A fuzzy-based approach to comprehensive modeling and analysis of systems with epistemic uncertainties. *Structural Safety, 32*(6), 433-441.

Harbaugh, A. W. (2005). *MODFLOW-2005, the US Geological Survey modular ground-water model: The ground-water flow process*: US Department of the Interior, US Geological Survey Reston, VA, USA.

Harendra, S. and Vipulanandan, C. (2012). Determination of Sodium Dodecyl Sulfate (SDS) and Biosurfactants Sorption and Transport Parameters in Clayey Soil. *Journal of Surfactants and Detergents, 15*(6), 805-813.

Harvell, J. R. (2012). *Solubilization of multi-component immiscible liquids in homogeneous systems: A comparison of different flushing agents using a 2-D flow cell.* The University of Alabama Tuscaloosa.

Haryanto, B. and Chang, C.-H. (2014). Foam-enhanced removal of adsorbed metal ions from packed sands with biosurfactant solution flushing. *Journal of the Taiwan Institute of Chemical Engineers, 45*(5), 2170-2175.

He, L., Huang, G., Lu, H., Wang, S., and Xu, Y. (2012). Quasi-Monte Carlo based global uncertainty and sensitivity analysis in modeling free product migration and recovery from petroleum-contaminated aquifers. *Journal of Hazardous Materials, 219*, 133-140.

He, L., Huang, G., Lu, H., and Zeng, G. (2008). Optimization of surfactant-enhanced aquifer remediation for a laboratory BTEX system under parameter uncertainty. *Environmental Science & Technology, 42*(6), 2009-2014.

Helton, J. C. (1993). Uncertainty and sensitivity analysis techniques for use in performance assessment for radioactive waste disposal. *Reliability Engineering & System Safety, 42*(2), 327-367.

Hickenbottom, K. L., Hancock, N. T., Hutchings, N. R., Appleton, E. W., Beaudry, E. G., Xu, P., and Cath, T. Y. (2013). Forward osmosis treatment of drilling mud and fracturing wastewater from oil and gas operations. *Desalination, 312*, 60-66.

Higgins, M. R. and Olson, T. M. (2009). Life-cycle case study comparison of permeable reactive barrier versus pump-and-treat remediation. *Environmental Science & Technology, 43*(24), 9432-9438.

Holland, J. H. (1992). Adaptation in natural and artificial systems: an introductory analysis with applications to biology, control, and artific.

Holvoet, K., van Griensven, A., Seuntjens, P., and Vanrolleghem, P. (2005). Sensitivity analysis for hydrology and pesticide supply towards the river in SWAT. *Physics and Chemistry of the Earth, Parts A/B/C, 30*(8), 518-526.

Houska, T., Multsch, S., Kraft, P., Frede, H.-G., and Breuer, L. (2014). Monte Carlo-based calibration and uncertainty analysis of a coupled plant growth and hydrological model. *Biogeosciences, 11*(7), 2069-2082.

Hu, L., Wu, X., Liu, Y., Meegoda, J. N., and Gao, S. (2010). Physical modeling of air flow during air sparging remediation. *Environmental Science & Technology, 44*(10), 3883-3888.

Huang, G., Huang, Y., Wang, G., and Xiao, H. (2006a). Development of a forecasting system for supporting remediation design and process control based on NAPL-biodegradation simulation and stepwise-cluster analysis. *Water Resources Research, 42*(6).

Huang, G. and Loucks, D. (2000). An inexact two-stage stochastic programming model for water resources management under uncertainty. *Civil Engineering Systems, 17*(2), 95-118.

Huang, Y. (2004). *Development of environmental modeling methodologies for supporting system simulation, optimization and process control in petroleum waste management.* University of Regina.

Huang, Y., Huang, G., Wang, G., Lin, Q., and Chakma, A. (2006b). An integrated numerical and physical modeling system for an enhanced in situ bioremediation process. *Environmental Pollution, 144*(3), 872-885.

Huang, Y., Li, J., Huang, G., Chakma, A., and Qin, X. (2003). Integrated simulation-optimization approach for real-time dynamic modeling and process control of surfactant-enhanced remediation at petroleum-contaminated sites. *Practice Periodical of Hazardous, Toxic, and Radioactive Waste Management, 7*(2), 95-105.

Isukapalli, S., Roy, A., and Georgopoulos, P. (1998). Stochastic response surface methods (SRSMs) for uncertainty propagation: application to environmental and biological systems. *Risk Analysis, 18*(3), 351-363.

Isukapalli, S. S. (1999). *Uncertainty analysis of transport-transformation models.* Citeseer.

Jácome, L. A. P. and Van Geel, P. J. (2013). An initial study on soil wettability effects during entrapped LNAPL removal by surfactant flooding in coarse-grained sand media. *Journal of Soils and Sediments, 13*(6), 1001-1011.

Jácome, L. A. P. and Van Geel, P. J. (2015). Comparative study of the impacts of soil wettability during entrapped LNAPL removal by surfactant flooding in two different sand media. *Journal of Soils and Sediments, 15*(1), 24-31.

Jacques, J., Lavergne, C., and Devictor, N. (2006). Sensitivity analysis in presence of model uncertainty and correlated inputs. *Reliability Engineering & System Safety, 91*(10), 1126-1134.

Jean, J., Tsai, C., Ju, S., Tsao, C., and Wang, S. (2002). Biodegradation and transport of benzene, toluene, and xylenes in a simulated aquifer: comparison of modelled and experimental results. *Hydrological Processes, 16*(16), 3151-3168.

Jin, B., Jiang, H., Zhang, X., Wang, J., Yang, J., and Zheng, W. (2014). Numerical Simulation of Surfactant-Polymer Flooding. *Chemistry and Technology of Fuels and Oils, 50*(1), 55-70.

Jing, L. and Chen, B. (2011). Field investigation and hydrological modelling of a subarctic wetland-the Deer River watershed. *Journal of Environmental Informatics, 17*(1), 36-45.

Jing, L., Chen, B., and Zhang, B. (2014). Modeling of UV-Induced Photodegradation of Naphthalene in Marine Oily Wastewater by Artificial Neural Networks. *Water, Air, & Soil Pollution, 225*(4), 1-14.

Jing, L., Chen, B., Zhang, B., and Li, P. (2013a). A Hybrid Stochastic-Interval Analytic Hierarchy Process Approach for Prioritizing the Strategies of Reusing Treated Wastewater. *Mathematical Problems in Engineering, 2013*.

Jing, L., Chen, B., Zhang, B., and Peng, H. (2013b). A hybrid fuzzy stochastic analytical hierarchy process (FSAHP) approach for evaluating ballast water treatment technologies. *Environmental Systems Research, 2*(1), 1-10.

Johnson, M. A., Song, X., and Seagren, E. A. (2013). A quantitative framework for understanding complex interactions between competing interfacial processes and in situ biodegradation. *Journal of Contaminant Hydrology, 146*, 16-36.

Joshi, S. J. and Desai, A. J. (2013). Bench-scale production of biosurfactants and their potential in ex-situ MEOR application. *Soil and Sediment Contamination: An International Journal, 22*(6), 701-715.

Kaluarachchi, J. and Parker, J. (1989). An efficient finite element method for modeling multiphase flow. *Water Resources Research, 25*(1), 43-54.

Kaluarachchi, J. and Parker, J. (1990). Modeling multicomponent organic chemical transport in three-fluid-phase porous media. *Journal of Contaminant Hydrology, 5*(4), 349-374.

Kananizadeh, N., Chokejaroenrat, C., Li, Y., and Comfort, S. (2015). Modeling improved ISCO treatment of low permeable zones via viscosity modification: Assessment of system variables. *Journal of Contaminant Hydrology, 173*, 25-37.

Kang, S. (2014). *A Model Segmentation from Spectral Clustering: New Zonation algorithm and Application to Reservoir History Matching.* Paper presented at the SPE Annual Technical Conference and Exhibition.

Katyal, A. (1997a). BIOF&T flow and transport in the saturated and unsaturated zones in 2-or 3-dimensions: technical document & user guide. *Draper Aden Environmental Modelling, Inc., Blacksburg, VA.*

Katyal, A. (1997b). Bioslurp technical documentation & user guide: 4.Bioslurp input parameters.

Katyal, A. and Parker, J. (1992). An adaptive solution domain algorithm for solving multiphase flow equations. *Computers & Geosciences, 18*(1), 1-9.

Kermani, M. and Ebadi, T. (2012). The effect of oil contamination on the geotechnical properties of fine-grained soils. *Soil and Sediment Contamination: An International Journal, 21*(5), 655-671.

Khawas, A., Banerjee, A., and Mukhopadhyay, S. (2011). *A response surface method for design space exploration and optimization of analog circuits.* Paper presented at the VLSI (ISVLSI), 2011 IEEE Computer Society Annual Symposium on.

Khodadadi, A., Ganjidoust, H., and Razavi, S. S. (2012). Treatment of crude-oil contaminated soil using biosurfactants. *Journal of Petroleum and Gas Engineering Vol, 3*(6), 92-98.

Kim, J. and Corapcioglu, M. Y. (2003). Modeling dissolution and volatilization of LNAPL sources migrating on the groundwater table. *Journal of Contaminant Hydrology, 65*(1), 137-158.

Kirk, R. E. (1982). *Experimental design*: Wiley Online Library.

Kitanidis, P. K. and Vomvoris, E. G. (1983). A geostatistical approach to the inverse problem in groundwater modeling (steady state) and one-dimensional simulations. *Water Resources Research, 19*(3), 677-690.

Kobus, H., Barczewski, B., and Koschitzky, H.-P. (2012). *Groundwater and subsurface remediation: research strategies for in-situ technologies*: Springer Science & Business Media.

Konikow, L. F. (2011). The Secret to Successful Solute-Transport Modeling. *Groundwater*, *49*(2), 144-159.

Konikow, L. F. and Grove, D. B. (1977). Derivation of equations describing solute transport in ground water: US Geological Survey, Water Resources Division.

Kueper, B. H., Abbott, W., and Farquhar, G. (1989). Experimental observations of multiphase flow in heterogeneous porous media. *Journal of Contaminant Hydrology, 5*(1), 83-95.

Kumar, C. (2002). Groundwater flow models. *Scientist 'E1'National Institute of Hydrology Roorkee–247667 (Uttaranchal) publication*.

Kumar, C. (2012). Groundwater Modelling Software–Capabilities and Limitations. *J Environ Sci Toxicol Food Technol, 1*(2), 46-57.

Kutscher, S. and Schulze, J. (1993). Some Aspects of Uncertain Modelling Experiences in Applying Interval Mathematics to Practical Problems. *Mathematical Research, 68*, 62-62.

Kuyukina, M. S., Ivshina, I. B., Makarov, S. O., Litvinenko, L. V., Cunningham, C. J., and Philp, J. C. (2005). Effect of biosurfactants on crude oil desorption and mobilization in a soil system. *Environment International, 31*(2), 155-161.

Lahoz-Mart ń, F. D., Mart ń-Calvo, A., and Calero, S. (2014). Selective Separation of BTEX Mixtures Using Metal–Organic Frameworks. *The Journal of Physical Chemistry C, 118*(24), 13126-13136.

Langevin, C. D., Shoemaker, W. B., and Guo, W. (2003). MODFLOW-2000, the US Geological Survey Modular Ground-Water Model--Documentation of the SEAWAT-2000 Version

with the Variable-Density Flow Process (VDF) and the Integrated MT3DMS Transport Process (IMT).

Langwaldt, J. and Puhakka, J. (2000). On-site biological remediation of contaminated groundwater: a review. *Environmental Pollution, 107*(2), 187-197.

Lee, K., Suk, H., Choi, S., Lee, C., and Chung, S. (2001). Numerical evaluation of landfill stabilization by leachate circulation. *Journal of Environmental Engineering, 127*(6), 555-563.

Lee, M., Kim, J., and Kim, I. (2011). In-situ biosurfactant flushing, coupled with a highly pressurized air injection, to remediate the bunker oil contaminated site. *Geosciences Journal, 15*(3), 313-321.

Lenhart, T., Eckhardt, K., Fohrer, N., and Frede, H.-G. (2002). Comparison of two different approaches of sensitivity analysis. *Physics and Chemistry of the Earth, Parts A/B/C, 27*(9), 645-654.

Li, D., Sun, L., and Lian, M. (2015a). Application of Surfactants in Soil Remediation. *Journal of Chemical & Pharmaceutical Research, 7*(3).

Li, F., Zhu, L., Wang, L., and Zhan, Y. (2015b). Gene Expression of an Arthrobacter in Surfactant-Enhanced Biodegradation of a Hydrophobic Organic Compound. *Environmental Science & Technology, 49*(6), 3698-3704.

Li, J., Chakma, A., Zeng, G., and Liu, L. (2003). Integrated fuzzy-stochastic modeling of petroleum contamination in subsurface. *Energy Sources, 25*(6), 547-563.

Li, J., Zhang, J., Lu, Y., Chen, Y., Dong, S., and Shim, H. (2012). Determination of total petroleum hydrocarbons (TPH) in agricultural soils near a petrochemical complex in Guangzhou, China. *Environmental Monitoring and Assessment, 184*(1), 281-287.

Li, P., Chen, B., Zhang, B., Jing, L., and Zheng, J. (2014). Monte Carlo simulation-based dynamic mixed integer nonlinear programming for supporting oil recovery and devices allocation during offshore oil spill responses. *Ocean & Coastal Management, 89*, 58-70.

Li, Y., Li, Y., and Yu, S. (2008). Design optimization of a current mirror amplifier integrated circuit using a computational statistics technique. *Mathematics and Computers in Simulation, 79*(4), 1165-1177.

Liang, K. Y. and Zeger, S. L. (1993). Regression analysis for correlated data. *Annual Review of Public Health, 14*(1), 43-68.

Liu, H., Wang, H., Chen, X., Liu, N., and Bao, S. (2014). Biosurfactant-producing strains in enhancing solubilization and biodegradation of petroleum hydrocarbons in groundwater. *Environmental Monitoring and Assessment, 186*(7), 4581-4589.

Liu, L. (2005). Modeling for surfactant-enhanced groundwater remediation processes at DNAPLs-contaminated sites. *Journal of Environmental Informatics, 5*(2), 42-52.

Liu, L., Huang, G., Hao, R., and Cheng, S. (2004). An integrated subsurface modeling and risk assessment approach for managing the petroleum-contaminated sites. *Journal of Environmental Science and Health, Part A, 39*(11-12), 3083-3113.

Liu, Y., Ma, M., Shi, Z., Deng, Y., Zeng, X., and Hong, Y. (2012). A Study on Remediation of PCBs-Contaminated Soil by a Combination of Biosurfactant Washing, UV-Irradiation and Biodegradation. *Advanced Science Letters, 10*(1), 344-348.

Lotfabad, T. B., Ebadipour, N., and RoostaAzad, R. (2015). Evaluation of a recycling bioreactor for biosurfactant production by Pseudomonas aeruginosa MR01 using soybean oil waste. *Journal of Chemical Technology and Biotechnology*.

Lovison, A., Comola, F., Teatini, P., Janna, C., Ferronato, M., Putti, M., and Gambolati, G. (2013). *Model calibration of a geomechanical problem with efficient global optimization.* Paper presented at the Proceedings of DWCAA12.

Luo, J. and Lu, W. (2014). Sobol′ sensitivity analysis of NAPL-contaminated aquifer remediation process based on multiple surrogates. *Computers & Geosciences, 67*, 110-116.

Luo, J., Lu, W., Xin, X., and Chu, H. (2013). Surrogate model application to the identification of an optimal surfactant-enhanced aquifer remediation strategy for DNAPL-contaminated sites. *Journal of Earth Science, 24*, 1023-1032.

Macal, C. M. (2005). *Model verification and validation.* Paper presented at the Workshop on" Threat Anticipation: Social Science Methods and Models.

Mao, X., Jiang, R., Xiao, W., and Yu, J. (2014). Use of Surfactants for the Remediation of Contaminated soils: A Review. *Journal of Hazardous Materials*.

Maqsood, I. (2004). *Development of simulation-and optimization-based decision support methodologies for environmental systems management.* University of Regina.

Marchant, R. and Banat, I. M. (2012). Microbial biosurfactants: challenges and opportunities for future exploitation. *Trends in Biotechnology, 30*(11), 558-565.

Maszkowska, J., Kołodziejska, M., Białk-Bielińska, A., Mrozik, W., Kumirska, J., Stepnowski, P., . . . Kalbe, U. (2013). Column and batch tests of sulfonamide leaching from different types of soil. *Journal of Hazardous Materials, 260*, 468-474.

McKnight, U. S., Funder, S. G., Rasmussen, J. J., Finkel, M., Binning, P. J., and Bjerg, P. L. (2010). An integrated model for assessing the risk of TCE groundwater contamination to

human receptors and surface water ecosystems. *Ecological Engineering, 36*(9), 1126-1137.

Mesania, F. A. and Jennings, A. A. (2000). Modeling soil pile bioremediation. *Environmental Modelling & Software, 15*(4), 411-424.

Miller, C. T., Christakos, G., Imhoff, P. T., McBride, J. F., Pedit, J. A., and Trangenstein, J. A. (1998). Multiphase flow and transport modeling in heterogeneous porous media: challenges and approaches. *Advances in Water Resources, 21*(2), 77-120.

Miller, M. E. and Stuart, J. D. (2000). Measurement of aqueous Henry's law constants for oxygenates and aromatics found in gasolines by the static headspace method. *Analytical Chemistry, 72*(3), 622-625.

Mohammadi, H., Delshad, M., and Pope, G. A. (2009). Mechanistic modeling of alkaline/surfactant/polymer floods. *SPE Reservoir Evaluation & Engineering, 12*(04), 518-527.

Montgomery, D. C. (2008). *Design and analysis of experiments*: John Wiley & Sons.

Moore, C. and Doherty, J. (2006). The cost of uniqueness in groundwater model calibration. *Advances in Water Resources, 29*(4), 605-623.

Mozo, I., Lesage, G., Yin, J., Bessiere, Y., Barna, L., and Sperandio, M. (2012). Dynamic modeling of biodegradation and volatilization of hazardous aromatic substances in aerobic bioreactor. *Water Research, 46*(16), 5327-5342.

Mugunthan, P., Shoemaker, C. A., and Regis, R. G. (2005). Comparison of function approximation, heuristic, and derivative-based methods for automatic calibration of computationally expensive groundwater bioremediation models. *Water Resources Research, 41*(11).

Muhanna, R. L. and Mullen, R. L. (2001). Uncertainty in mechanics problems-interval-based approach. *Journal of Engineering Mechanics, 127*(6), 557-566.

Mulligan, C. N. (2005). Environmental applications for biosurfactants. *Environmental Pollution, 133*(2), 183-198.

Mulligan, C. N. and Wang, S. (2006). Remediation of a heavy metal-contaminated soil by a rhamnolipid foam. *Engineering Geology, 85*(1), 75-81.

Mulligan, C. N. and Yong, R. N. (2004). Natural attenuation of contaminated soils. *Environment International, 30*(4), 587-601.

Nardi, L. (2003). Determination of siloxane–water partition coefficients by capillary extraction–high-resolution gas chromatography: Study of aromatic solvents. *Journal of Chromatography A, 985*(1), 39-45.

Neuman, S. P. (1973). Calibration of distributed parameter groundwater flow models viewed as a multiple-objective decision process under uncertainty. *Water Resources Research, 9*(4), 1006-1021.

Newell, C. J., Rifai, H. S., Wilson, J. T., Connor, J. A., Aziz, J. A., and Suarez, M. P. (2002). *Calculation and use of first-order rate constants for monitored natural attenuation studies*: United States Environmental Protection Agency, National Risk Management Research Laboratory.

Nie, X., Huang, G., Li, Y., and Liu, L. (2007). IFRP: A hybrid interval-parameter fuzzy robust programming approach for waste management planning under uncertainty. *Journal of Environmental Management, 84*(1), 1-11.

Nilsson, B., Tzovolou, D., Jeczalik, M., Kasela, T., Slack, W., Klint, K. E., . . . Tsakiroglou, C. D. (2011). Combining steam injection with hydraulic fracturing for the in situ remediation of

the unsaturated zone of a fractured soil polluted by jet fuel. *Journal of Environmental Management, 92*(3), 695-707.

Nossent, J., Elsen, P., and Bauwens, W. (2011). Sobol'sensitivity analysis of a complex environmental model. *Environmental Modelling & Software, 26*(12), 1515-1525.

Nourani, V. and Fard, M. S. (2012). Sensitivity analysis of the artificial neural network outputs in simulation of the evaporation process at different climatologic regimes. *Advances in Engineering Software, 47*(1), 127-146.

Okamoto, M. and Akella, M. R. (2012). Adaptive control schemes specially designed for systems with unknown orthogonal matrix parameters. *Aerospace Science and Technology, 18*(1), 63-68.

Olden, J. D. and Jackson, D. A. (2002). Illuminating the "black box": a randomization approach for understanding variable contributions in artificial neural networks. *Ecological Modelling, 154*(1), 135-150.

Olden, J. D., Joy, M. K., and Death, R. G. (2004). An accurate comparison of methods for quantifying variable importance in artificial neural networks using simulated data. *Ecological Modelling, 178*(3), 389-397.

Ostermann, L. and Seidel, C. (2015). *The shallow water equations as a hybrid flow model for the numerical and experimental analysis of hydro power stations.* Paper presented at the Proceedings of The International Conference on Numerical Analysis and Applied Mathematics 2014

Pacwa-Płociniczak, M., Płaza, G. A., Piotrowska-Seget, Z., and Cameotra, S. S. (2011). Environmental applications of biosurfactants: recent advances. *International Journal of Molecular Sciences, 12*(1), 633-654.

Pankow, J. F., Rathbun, R. E., and Zogorski, J. S. (1996). Calculated volatilization rates of fuel oxygenate compounds and other gasoline-related compounds from rivers and streams. *Chemosphere, 33*(5), 921-937.

Paria, S. (2008). Surfactant-enhanced remediation of organic contaminated soil and water. *Advances in Colloid and Interface Science, 138*(1), 24-58.

Park, G. J. (2007). Design of experiments. *Analytic Methods for Design Practice,* 309-391.

Paschke, A. and Popp, P. (1999). Estimation of hydrophobicity of organic compounds. *Applications of Solid-Phase Microextraction*.

Pasetto, D., Guadagnini, A., and Putti, M. (2014). A reduced-order model for Monte Carlo simulations of stochastic groundwater flow. *Computational Geosciences, 18*(2), 157-169.

Pasha, A. Y., Hu, L., and Meegoda, J. N. (2014). Numerical simulations of a light nonaqueous phase liquid (LNAPL) movement in variably saturated soils with capillary hysteresis. *Canadian Geotechnical Journal, 51*(9), 1046-1062.

Peeters, L., Podger, G., Smith, T., Pickett, T., Bark, R., and Cuddy, S. (2014). Robust global sensitivity analysis of a river management model to assess nonlinear and interaction effects. *Hydrology and Earth System Sciences, 18*(9), 3777-3785.

Peng, S., Wu, W., and Chen, J. (2011). Removal of PAHs with surfactant-enhanced soil washing: influencing factors and removal effectiveness. *Chemosphere, 82*(8), 1173-1177.

Pereira, J. F., Gudiña, E. J., Costa, R., Vitorino, R., Teixeira, J. A., Coutinho, J. A., and Rodrigues, L. R. (2013). Optimization and characterization of biosurfactant production by Bacillus subtilis isolates towards microbial enhanced oil recovery applications. *Fuel, 111*, 259-268.

Peurrung, L. M., Fort, J. A., and Rector, D. R. (2013). *The Continued Need for Modeling and Scaled Testing to Advance the Hanford Tank Waste Mission*: Pacific Northwest National Laboratory.

Pfletschinger, H., Engelhardt, I., Piepenbrink, M., Königer, F., Schuhmann, R., Kallioras, A., and Schüth, C. (2012). Soil column experiments to quantify vadose zone water fluxes in arid settings. *Environmental Earth Sciences, 65*(5), 1523-1533.

Pinder, G. F. and Bredehoeft, J. (1968). Application of the digital computer for aquifer evaluation. *Water Resources Research, 4*(5), 1069-1093.

Plasencia, M., Pedersen, A., Arnaldsson, A., Berthet, J.-C., and Jónsson, H. (2014). Geothermal model calibration using a global minimization algorithm based on finding saddle points and minima of the objective function. *Computers & Geosciences, 65*, 110-117.

Treasury Board of Canada Secretariat (2015). Federal Contaminated Sites Inventory. Retrieved 2015.11.1, from http://www.tbs-sct.gc.ca/fcsi-rscf/classification-eng.aspx

Prasanphanich, J., Kalaei, M. H., Delshad, M., and Sepehrnoori, K. (2012). Chemical flooding optimisation using the experimental design approach and response surface methodology. *International Journal of Oil, Gas and Coal Technology, 5*(4), 368-384.

Qin, X., Huang, G., and Chakma, A. (2008a). Modeling groundwater contamination under uncertainty: a factorial-design-based stochastic approach. *Journal of Environmental Informatics, 11*(1), 11-20.

Qin, X., Huang, G., Chakma, A., Chen, B., and Zeng, G. (2007). Simulation-based process optimization for surfactant-enhanced aquifer remediation at heterogeneous DNAPL-contaminated sites. *Science of The Total Environment, 381*(1), 17-37.

Qin, X., Huang, G., Sun, W., and Chakma, A. (2008b). Optimization of remediation operations at petroleum-contaminated sites through a simulation-based stochastic-MCDA approach. *Energy Sources, Part A, 30*(14-15), 1300-1326.

Rahman, P. K. and Gakpe, E. (2008). Production, characterisation and applications of biosurfactants-Review. *Biotechnology, 7*(2), 360-370.

Ramsburg, C. A., Pennell, K. D., Abriola, L. M., Daniels, G., Drummond, C. D., Gamache, M., . . . Ryder, J. L. (2005). Pilot-scale demonstration of surfactant-enhanced PCE solubilization at the Bachman Road site. 2. System operation and evaluation. *Environmental Science & Technology, 39*(6), 1791-1801.

Rautela, R. and Cameotra, S. S. (2014). Role of Biopolymers in Industries: Their Prospective Future Applications *Environment and Sustainable Development* (pp. 133-142): Springer.

Razavi, S. and Tolson, B. (2012). *Efficient Auto-Calibration of Computationally Intensive Hydrologic Models by Running the Model on Short Data Periods.* Paper presented at the EGU General Assembly Conference Abstracts.

Rebello, S., Asok, A. K., Mundayoor, S., and Jisha, M. (2014). Surfactants: toxicity, remediation and green surfactants. *Environmental Chemistry Letters, 12*(2), 275-287.

Reddell, D. L. and Sunada, D. K. (1970). *Numerical simulation of dispersion in groundwater aquifers*: Colorado State University Fort Collins, Colorado.

Renard, P. and Allard, D. (2013). Connectivity metrics for subsurface flow and transport. *Advances in Water Resources, 51*, 168-196.

Rezanezhad, F., Couture, R.-M., Kovac, R., O'Connell, D., and Van Cappellen, P. (2014). Water table fluctuations and soil biogeochemistry: An experimental approach using an automated soil column system. *Journal of Hydrology, 509*, 245-256.

Rowe, R. K., Mukunoki, T., and Sangam, H. P. (2005). Benzene, Toluene, Ethylbenzene, m & p-Xylene, o-Xylene Diffusion and Sorption for a Geosynthetic Clay Liner at Two Temperatures. *Journal of Geotechnical and Geoenvironmental Engineering, 131*(10), 1211-1221.

Russo, A., Johnson, G., Schnaar, G., and Brusseau, M. (2010). Nonideal transport of contaminants in heterogeneous porous media: 8. Characterizing and modeling asymptotic contaminant-elution tailing for several soils and aquifer sediments. *Chemosphere, 81*(3), 366-371.

Saltelli, A. (1999). Sensitivity analysis: Could better methods be used? *Journal of Geophysical Research: Atmospheres (1984–2012), 104*(D3), 3789-3793.

Saltelli, A., Ratto, M., Tarantola, S., Campolongo, F., and Commission, E. (2006). Sensitivity analysis practices: Strategies for model-based inference. *Reliability Engineering & System Safety, 91*(10), 1109-1125.

Saltelli, A., Tarantola, S., Campolongo, F., and Ratto, M. (2004). *Sensitivity analysis in practice: a guide to assessing scientific models*: John Wiley & Sons.

Santa Anna, L. M., Soriano, A. U., Gomes, A. C., Menezes, E. P., Gutarra, M. L., Freire, D. M., and Pereira, N. (2007). Use of biosurfactant in the removal of oil from contaminated sandy soil. *Journal of Chemical Technology and Biotechnology, 82*(7), 687-691.

Sargent, R. G. (2015). Model Verification and Validation *Modeling and Simulation in the Systems Engineering Life Cycle* (pp. 57-65): Springer.

Sarikaya, M. and Güllü, A. (2015). *The Analysis of Process Parameters for Turning Cobalt-Based Super Alloy Haynes 25/L 605 Using Design of Experiment.* Paper presented at the Solid State Phenomena.

Schubert, M., Lehmann, K., and Paschke, A. (2007). Determination of radon partition coefficients between water and organic liquids and their utilization for the assessment of subsurface NAPL contamination. *Science of The Total Environment, 376*(1), 306-316.

Shary, S. P. (2014). Maximum consistency method for data fitting under interval uncertainty. *Journal of Global Optimization*, 1-16.

Shen, Z., Chen, L., and Chen, T. (2012). Analysis of parameter uncertainty in hydrological and sediment modeling using GLUE method: a case study of SWAT model applied to Three Gorges Reservoir Region, China. *Hydrology and Earth System Sciences, 16*(1), 121-132.

Shoeb, E., Akhlaq, F., Badar, U., Akhter, J., and Imtiaz, S. (2013). Classification and industrial applications of biosurfactants. *Academic Research International, 4*(3), 243-252.

Šimůnek, J. and Bradford, S. A. (2008). Vadose zone modeling: Introduction and importance. *Vadose Zone Journal, 7*(2), 581-586.

Sin, G., Gernaey, K. V., Neumann, M. B., van Loosdrecht, M. C., and Gujer, W. (2011). Global sensitivity analysis in wastewater treatment plant model applications: prioritizing sources of uncertainty. *Water Research, 45*(2), 639-651.

Smith, M. B., Koren, V., Reed, S., Zhang, Z., Zhang, Y., Moreda, F., . . . Cosgrove, B. A. (2012). The distributed model intercomparison project–Phase 2: Motivation and design of the Oklahoma experiments. *Journal of Hydrology, 418*, 3-16.

Sobol', I. y. M. (1990). On sensitivity estimation for nonlinear mathematical models. *Matematicheskoe Modelirovanie, 2*(1), 112-118.

Sobol, I. M. (2001). Global sensitivity indices for nonlinear mathematical models and their Monte Carlo estimates. *Mathematics and Computers in Simulation, 55*(1), 271-280.

Solomatine, D., Dibike, Y., and Kukuric, N. (1999). Automatic calibration of groundwater models using global optimization techniques. *Hydrological Sciences Journal, 44*(6), 879-894.

Song, X., Hong, E., and Seagren, E. A. (2014). Laboratory-scale in situ bioremediation in heterogeneous porous media: Biokinetics-limited scenario. *Journal of Contaminant Hydrology, 158*, 78-92.

Song, X. and Seagren, E. A. (2008). In situ bioremediation in heterogeneous porous media: dispersion-limited scenario. *Environmental Science & Technology, 42*(16), 6131-6140.

Sonnenborg, T. O., Christensen, B. S., Nyegaard, P., Henriksen, H. J., and Refsgaard, J. C. (2003). Transient modeling of regional groundwater flow using parameter estimates from steady-state automatic calibration. *Journal of Hydrology, 273*(1), 188-204.

Souto, H. P. A. and Moyne, C. (1997). Dispersion in two-dimensional periodic porous media. Part II. Dispersion tensor. *Physics of Fluids (1994-present), 9*(8), 2253-2263.

Stumpp, C., Lawrence, J. R., Hendry, M. J., and Maloszewski, P. (2011). Transport and bacterial interactions of three bacterial strains in saturated column experiments. *Environmental Science & Technology, 45*(6), 2116-2123.

Suarez, M. P. and Rifai, H. S. (1999). Biodegradation rates for fuel hydrocarbons and chlorinated solvents in groundwater. *Bioremediation Journal, 3*(4), 337-362.

Suk, H., Lee, K., and Lee, C. (2000). Biologically reactive multispecies transport in sanitary landfill. *Journal of Environmental Engineering, 126*(5), 419-427.

Sun, Y., Kang, S., Li, F., and Zhang, L. (2009). Comparison of interpolation methods for depth to groundwater and its temporal and spatial variations in the Minqin oasis of northwest China. *Environmental Modelling & Software, 24*(10), 1163-1170.

Suthar, H., Hingurao, K., Desai, A., and Nerurkar, A. (2008). Evaluation of bioemulsifier mediated microbial enhanced oil recovery using sand pack column. *Journal of Microbiological Methods, 75*(2), 225-230.

Svab, M., Kubal, M., Müllerova, M., and Raschman, R. (2009). Soil flushing by surfactant solution: Pilot-scale demonstration of complete technology. *Journal of Hazardous Materials, 163*(1), 410-417.

Swartjes, F., Rutgers, M., Lijzen, J., Janssen, P., Otte, P., Wintersen, A., . . . Posthuma, L. (2012). State of the art of contaminated site management in The Netherlands: Policy framework and risk assessment tools. *Science of The Total Environment, 427*, 1-10.

Tang, Z., Zhenzhou, L., Zhiwen, L., and Ningcong, X. (2015). Uncertainty analysis and global sensitivity analysis of techno-economic assessments for biodiesel production. *Bioresource Technology, 175*, 502-508.

Thacker, B. H., Doebling, S. W., Hemez, F. M., Anderson, M. C., Pepin, J. E., and Rodriguez, E. A. (2004). Concepts of model verification and validation: Los Alamos National Lab., Los Alamos, NM (US).

Tian, W. (2013). A review of sensitivity analysis methods in building energy analysis. *Renewable and Sustainable Energy Reviews, 20*, 411-419.

Tick, G. R., Harvell, J. R., and Murgulet, D. (2015). Intermediate-Scale Investigation of Enhanced-Solubilization Agents on the Dissolution and Removal of a Multicomponent Dense Nonaqueous Phase Liquid (DNAPL) Source. *Water, Air, & Soil Pollution, 226*(11), 1-21.

Tick, G. R., Lourenso, F., Wood, A. L., and Brusseau, M. L. (2003). Pilot-scale demonstration of cyclodextrin as a solubility-enhancement agent for remediation of a tetrachloroethene-contaminated aquifer. *Environmental Science & Technology, 37*(24), 5829-5834.

Um, J., Lee, G., Song, S., Hong, S., and Lee, M. (2013). Pilot Scale Feasibility Test of In-situ Soil Flushing by using'Tween 80'Solution at Low Concentration for the Xylene Contaminated Site. *Journal of Soil and Groundwater Environment, 18*(6), 38-47.

Van Griensven, A., Meixner, T., Grunwald, S., Bishop, T., Diluzio, M., and Srinivasan, R. (2006). A global sensitivity analysis tool for the parameters of multi-variable catchment models. *Journal of Hydrology, 324*(1), 10-23.

Veličković, A. V., Stamenković, O. S., Todorović, Z. B., and Veljković, V. B. (2013). Application of the full factorial design to optimization of base-catalyzed sunflower oil ethanolysis. *Fuel, 104*, 433-442.

Vijaya, B., Jayalakshmi, N., and Manjunath, K. (2014). Isolation and partial characterization of a biosurfactant produced by Pseudomonas aeruginosa PAVIJ from contaminated soil. *Research Journal of Pharmaceutical, Biological and Chemical Sciences, 5*(2), 881-895.

Volkering, F., Breure, A., and Rulkens, W. (1997). Microbiological aspects of surfactant use for biological soil remediation. *Biodegradation, 8*(6), 401-417.

Voss, C. I. (2011). Editor's message: Groundwater modeling fantasies—part 2, down to earth. *Hydrogeology Journal, 19*(8), 1455-1458.

Wang, J., He, J., and Chen, H. (2012). Assessment of groundwater contamination risk using hazard quantification, a modified DRASTIC model and groundwater value, Beijing Plain, China. *Science of The Total Environment, 432*, 216-226.

Wang, L., Tsang, D. C., and Poon, C.-S. (2015). Green remediation and recycling of contaminated sediment by waste-incorporated stabilization/solidification. *Chemosphere, 122*, 257-264.

Wang, S. and Mulligan, C. N. (2009). Rhamnolipid biosurfactant-enhanced soil flushing for the removal of arsenic and heavy metals from mine tailings. *Process Biochemistry*, *44*(3), 296-301.

Wayt, H. I. and Wilson, D. J. (1989). Soil clean up by in-situ surfactant flushing. II. Theory of micellar solubilization. *Separation Science and Technology, 24*(12-13), 905-937.

Welsch, R. E. (1980). Regression sensitivity analysis and bounded-influence estimation *Evaluation of Econometric Models* (pp. 153-167): Academic Press.

Whitaker, S. (1986). Flow in porous media I: A theoretical derivation of Darcy's law. *Transport in Porous Media*, *1*(1), 3-25.

White, M. D. and Oostrom, M. (1998). Modeling surfactant-enhanced nonaqueous-phase liquid remediation of porous media. *Soil Science, 163*(12), 931-940.

Whittaker, G., Confesor, R., Di Luzio, M., and Arnold, J. (2010). Detection of overparameterization and overfitting in an automatic calibration of SWAT. *Transactions of the ASABE, 53*(5), 1487-1499.

Widdowson, M. A., Molz, F. J., and Benefield, L. D. (1988). A numerical transport model for oxygen-and nitrate-based respiration linked to substrate and nutrient availability in porous media. *Water Resources Research, 24*(9), 1553-1565.

Wilson, D. J. (1989). Soil clean up by in-situ surfactant flushing. I. Mathematical modeling. *Separation Science and Technology, 24*(11), 863-892.

Witek-Krowiak, A., Chojnacka, K., Podstawczyk, D., Dawiec, A., and Pokomeda, K. (2014). Application of response surface methodology and artificial neural network methods in modelling and optimization of biosorption process. *Bioresource Technology, 160*, 150-160.

Wu, H., Lye, L. M., and Chen, B. (2012). A design of experiment aided sensitivity analysis and parameterization for hydrological modeling. *Canadian Journal of Civil Engineering, 39*(4), 460-472.

Wu, Y., Liu, S., Li, Z., Dahal, D., Young, C. J., Schmidt, G. L., . . . Werner, J. M. (2014). Development of a generic auto-calibration package for regional ecological modeling and application in the Central Plains of the United States. *Ecological Informatics, 19*, 35-46.

Xu, D. L., Yang, J. B., and Wang, Y. M. (2006). The evidential reasoning approach for multi-attribute decision analysis under interval uncertainty. *European Journal of Operational Research, 174*(3), 1914-1943.

Xu, Z., Chai, J., Wu, Y., and Qin, R. (2015). Transport and biodegradation modeling of gasoline spills in soil–aquifer system. *Environmental Earth Sciences*, 1-12.

Yadav, B. K., Ansari, F. A., Basu, S., and Mathur, A. (2014). Remediation of LNAPL contaminated groundwater using plant-assisted biostimulation and bioaugmentation methods. *Water, Air, & Soil Pollution, 225*(1), 1-9.

Yang, A., Huang, G., Qin, X., and Fan, Y. (2012). Evaluation of remedial options for a benzene-contaminated site through a simulation-based fuzzy-MCDA approach. *Journal of Hazardous Materials, 213*, 421-433.

Yang, H., Li, Y., and Xue, Y. (2015). Interval uncertainty analysis of elastic bimodular truss structures. *Inverse Problems in Science and Engineering, 23*(4), 578-589.

Yaws, C. L. (1995). *Handbook of transport property data: viscosity, thermal conductivity, and diffusion coefficients of liquids and gases*: Inst of Chemical Engineers.

Yeh, W. W. (2015). Review: Optimization methods for groundwater modeling and management. *Hydrogeology Journal*, 1-15.

Yen, H., Wang, X., Fontane, D. G., Harmel, R. D., and Arabi, M. (2014). A framework for propagation of uncertainty contributed by parameterization, input data, model structure, and calibration/validation data in watershed modeling. *Environmental Modelling & Software, 54*, 211-221.

Yu, H., Huang, G., An, C., and Wei, J. (2011). Combined effects of DOM extracted from site soil/compost and biosurfactant on the sorption and desorption of PAHs in a soil–water system. *Journal of Hazardous Materials, 190*(1), 883-890.

Yu, H., Huang, G., Zhang, B., Zhang, X., and Cai, Y. (2010). Modeling biosurfactant-enhanced bioremediation processes for petroleum-contaminated sites. *Petroleum Science and Technology, 28*(12), 1211-1221.

Zahraee, S. M., Hatami, M., Yusof, N. M., Rohani, J. M., and Ziaei, F. (2013). Combined Use of Design of Experiment and Computer Simulation for Resources Level Determination in Concrete Pouring Process. *Jurnal Teknologi, 64*(1).

Zhang, B., Zhu, Z., Jing, L., Cai, Q., and Li, Z. (2012). Pilot-scale demonstration of biosufactant-enhanced in-situ bioremediation of a contaminated site in Newfoundland and Labrador.

Zhang, C., Wang, R., and Meng, Q. (2015). Calibration of Conceptual Rainfall-Runoff Models Using Global Optimization. *Advances in Meteorology, 2015*, 1-12.

Zhang, H. (2015). *Integrated Nano Zero Valent Iron and Biosurfactant Aided Remediation of PCB-Contaminated Soil.* Memorial University.

Zhang, J., Delshad, M., and Sepehrnoori, K. (2005). *A Framework to Design and Optimize Surfactant-Enhanced Aquifer Remediation.* Paper presented at the SPE/EPA/DOE Exploration and Production Environmental Conference.

Zhang, W., Li, J., Huang, G., Song, W., and Huang, Y. (2011). An experimental study on the bio-surfactant-assisted remediation of crude oil and salt contaminated soils. *Journal of Environmental Science and Health, Part A, 46*(3), 306-313.

Zhao, L., Bi, G., Wang, L., and Zhang, H. (2013). An improved auto-calibration algorithm based on sparse Bayesian learning framework. *Signal Processing Letters, IEEE, 20*(9), 889-892.

Zhao, Y. S., Li, L. L., Su, Y., and Qin, C. Y. (2014). Laboratory evaluation of the use of solvent extraction for separation of hydrophobic organic contaminants from surfactant solutions during surfactant-enhanced aquifer remediation. *Separation and Purification Technology, 127*, 53-60.

Zheng, C. and Bennett, G. D. (2002). *Applied contaminant transport modeling* (Vol. 2): Wiley-Interscience New York.

Zheng, G., Selvam, A., and Wong, J. W. (2012). Enhanced solubilization and desorption of organochlorine pesticides (OCPs) from soil by oil-swollen micelles formed with a nonionic surfactant. *Environmental Science & Technology, 46*(21), 12062-12068.

Zhuo, L., Mekonnen, M., and Hoekstra, A. (2013). *Sensitivity and uncertainty analysis for crop water footprint accounting at a basin level.* Paper presented at the AGU Fall Meeting Abstracts.